Acknowledgment

I would like to thank to those that directly or indirectly contributed to the accomplishment of this work, especially to:

- My supervisor Prof. Abel Oliva, for the permanent supervising, support and advices putted in this thesis, also for being always so attentive.
- My co-supervisor Prof. Pedro Fevereiro for the scientific supervising, knowledge and support along the master; also for being so helpful, dedicated and for his character as a person and investigator, also for his encouraging words during the hard moments.
- My co-supervisor Carlota Vaz Patto for her supervising and sympathy.
- Prof Rui Malhó at FCUL for his precious work, availability and patience in the confocal microscope.
- Sofia Miguel at the Organic Synthesis Lab for being always so attentive and helpful.
- Leonor Tomaz for her precious help and practical tips and also my colleagues at the BCV Lab.
- All my colleagues at BMD Lab, namely, Cláudia Sanchez, Elisa Campos, Haline Victorio and Valério Palmeira for their helpful advices and good mood, always so needed.
- Miguel for being my shelter and for believing in me, making me a stronger person.
- My sister for her tips, attention and for pushing me up when I most needed.
- My family, father, mother and grandmother for their unconditional support and affection.
- All my friends, especially Sónia Neto for our conversations and friendship.

Sumário

O objectivo deste trabalho consistiu no estudo do efeito/interacção de Quantum Dots (QD's) em culturas *in vitro* das leguminosas *Medicago sativa e Medicago truncatula*. Para avaliar a toxicidade foram utilizadas duas amostras de QD's: QD50_MPA usada numa concentração de [160 nM] e QD68_MPA com [40 nM].

A amostra QD50_MPA foi testada na linha embriogénica de *M. truncatula* (M9-10a) com a finalidade de avaliar o efeito dos QD's na diferenciação celular ao nível da embriogénese somática. Os resultados mostraram não haver diferenças quer na morfologia dos embriões quer no tempo de desenvolvimento.

Foi desenvolvida uma cultura fina de células em suspensão de *Medicago sativa* (linha M699) para avaliar o efeito dos QD68_MPA QD's no crescimento celular, viabilidade e stress oxidativo, através da produção de Espécies Reactivas de Oxigénio. Concluiu-se que não são verificadas diferenças significativas numa exposição das células aos QD's até 4 horas, apesar de detectado um stress oxidativo generalizado. Contudo, após 24 horas de exposição das células aos QD's a viabilidade celular começou a decrescer e a produção de Espécies Reactivas de Oxigénio foi intensificada, verificando-se ainda alterações significativas na morfologia das células.

Além disso, foi visualizada a internalização de ambas as amostras de QD's após 72 horas de exposição das culturas em suspensão. A amostra QD50_MPA foi testada nas duas culturas em suspensão, *M. sativa* e *M. truncatula*, sendo visualizados QD's no núcleo e no citosol de ambas as linhas, com excepção dos vacúolos. A amostra QD68_MPA verificou-se ser internalizada pelas células de *M.sativa*, localizando-se sobretudo no hialoplasma e organitos como os plastos e, igualmente como verificado na amostra QD50_MPA, não foi verificada internalização nos vacúolos.

Abstract

The aim of this thesis is a survey of the toxicity of Quantum Dots (QD's) in *in vitro* cultures of the legumes *Medicago sativa* and *Medicago truncatula*. Two samples of QD's were used to assess toxicity: QD50_MPA tested in a concentration of [160 nM] and QD68_MPA with [40 nM].

The QD50_MPA sample was applied in the already available embryogenic cell suspension culture of *M. truncatula* (M9-10a) to evaluate the effect of QD's in plant differentiation at somatic embryogenesis. Results showed no differences in embryo morphology or development time.

A fine suspension culture of *Medicago sativa* (line M699) was established to evaluate the effect of QD68_MPA QD's in cell growth, viability as well in oxidative stress by ROS production. It was concluded that no major differences were seen when cells were exposed to QD's in a period of 4 hours, despite an overall oxidative stress was detected. After 24 hours of exposure of cell suspension cultures to QD's viability of cells started to decrease and ROS production was intensified, also the morphology of cells had significant changes.

Moreover, it was visualized the internalization of both QD´s samples after 72 h of cell suspension cultures exposure to QD's. QD50_MPA sample was used in the two cell suspension cultures used: *M. sativa and M. truncatula*, and in both lines QD's were visualized in the nucleus and in cytosol, with the exception of the vacuoles. QD68_MPA sample was found to be up-taked by *M. sativa* cells and located mainly in the hyaloplasm and organelles such as plasts, and similarly to the other sample, no internalization was observed in the vacuoles.

LIST OF ABBREVIATIONS

QD's – Quantum Dots

NP's – Nanoparticles

ROS – Reactive Oxygen Species

FDA – Fluorescein diacetate

MPA – Mercaptopropionic acid

M&S – Murashige and Skoog

2,4 D – dichlorophenoxyacetic acid

Kin – kinetin

DAB – 3,3'- diaminobenzidine

NBT – Nitrobluetetrazolium

H_2DCFDA – 2',7'- dichlorodihidrofluorescein diacetate

ζ – Zeta potential

μ – specific growth rate

td– time of doubling

LIST OF CONTENTS

LIST OF FIGURES

LIST OF TABLES

1. Introduction

The aim of this work is to assess Quantum Dots (QD's) toxicity in cells of *Medicago sativa* and *Medicago truncatula*, and if they are toxic to cells, what is the extent of the nanotoxicity effect. The outcome will be used to modulate the application of this type of nanoparticles in the precocious detection or in the nano-vaccination of plants susceptible to pathogenic Fusarium spp.

This aim is part of the project: "Development of ultra-sensitive detection methods and plant nano-vaccines for the fungi *Fusarium spp.* using nano-technological devices" (Iberian Capacitation Program in Nanotechnologies). Quantum Dots will be used to conjugate molecules (antibodies) that specifically recognize toxins, proteins and/or DNA sequences of *Fusarium spp..* This will allow the development of a very accurate and sensitive method, to precociously detect the presence of fungi in plants.

Since this technology is to be used in living plants, its potential cytotoxic effects are an important factor to be considered, because it may affect plant physiological status. The size, charge and concentration of the quantum dots, their outer shell bioactivity and oxidative, photolytic or mechanical stress are all factors that, collectively and individually, can determine their cellular toxicity.

The unknown interferences of QDs with physiological processes could lead to misinterpretation of the results, whatever the application is for. Presently it is nearly impossible to draw firm conclusions about the toxicity of QDs in cultured (animal) cells due to (a) the immense variety of QDs and variations of surface coatings used by different labs and (b) a technical disparity in experimental conditions, such as the duration of the nanoparticle exposure to biological material, use of relevant cell lines, media choice, and even the units of concentration (e.g.mg/ml versus nM) (Smith *et al*, 2008).

To date, the literature on toxicity of QDs is a mix of reports of numerous types of QDs with widely varying physicochemical parameters, making comparisons quite difficult. Therefore it is imperative to test QD's in a model plant to evaluate its biotoxicity.

1.1. Nanotecnhology

The definition of nanotechnology is based on the prefix "nano" which means 10^{-9}, or one billionth of something. Nanotechnology is the manipulation or self-assembly of individual atoms, molecules, or molecular clusters into structures to create materials and devices with new or vastly different properties (Joseph and Morrison, 2006).

Nanotechnology is a fast-developing industry, posing substantial impacts on economy, society and environment (Lin and Xing, 2007) and have been predicted to far exceed the Industrial Revolution, generating a $1 trillion market by 2015 (Zhu *et al*, 2008). A diverse array of engineered nanoscale products and processes have emerged [e.g., carbon nanotubes, fullerene derivatives, and quantum dots], with widespread applications in fields such as medicine, plastics, energy, electronics, aerospace (Hardman, 2006) and agriculture (González-Melendi *et al*, 2007).

The range of nanotechnology products is now extensive and can be separated into a number of different compound classes, including carbonaceous nanomaterials; metal oxides; semiconductor materials, including quantum dots; zero-valent metals such as iron, silver, and gold; and nanopolymers, such as dendrimers (Klaine *et al*, 2008).

The questions about the side effects of products of nanotechnologies are pertinent, since the potential for exposure to nanoparticles will increase as the quantity and types of nanoparticles used grow. As the outcome of all these debates and concerns, a new branch in toxicological research has emerged with the aim to investigate possible harmful effects of exposure to nanomaterials.

1.1.1. Nanotoxicology

Nanotoxicology is emerging as an important subdiscipline of nanotechnology. Nanotoxicology refers to the study of the interactions of nanostructures with biological systems with an emphasis on elucidating the relationship between the physical and chemical properties (e.g. size, shape, surface chemistry, composition, and aggregation) of nanostructures with the induction of toxic biological responses (Fischer and Chan, 2007). This data information is important to characterize nanomaterial applications in biotechnology, ecosystems, agri- and aqua-culture, biomedical applications and toxicity screening.

Cell-based assays are currently considered central to toxicity testing. Five main cellular response categories, including reactive oxygen species (ROS) production and accumulation, reduction of cell viability, cell stress, cell morphology phenotyping, and cell–particle uptake, are central themes in such testing (Jones and Grainger, 2009). A brief description of the first two cellular responses will be made as well as the" state of the art" of what is presently known about the effect of nanoparticles in plants.

1.1.1.1. ROS Production

Reactive oxygen species (ROS) is the term used to describe forms of oxygen that are energetically more reactive than molecular oxygen. ROS include the two free radical species, the superoxide anion

O_2^-• and its protonated form the perhydroxyl radical HO_2•, the uncharged, non-radical species hydrogen peroxide (H_2O_2) and the highly reactive hydroxyl radical OH• (Smirnoff, 2005; Rio *et al*, 2003).

Several ROS are continuously produced in plants as byproducts of aerobic metabolism and processes such as respiration and photosynthesis unavoidably lead to the production of ROS in mitochondria, chloroplasts, and peroxisomes (Apel and Hirt, 2004; Bolwell and Wojtaszek, 1997). Under normal growth conditions, the production of ROS in cells is low, while many stresses that disrupt the cellular homeostasis of cells enhance the production of ROS. These include drought and desiccation, salinity, chilling, heat shock, heavy metals, ultraviolet radiation, mechanical injury, nutrient deprivation, pathogen attack and high irradation (Mittler, 2002; Smirnoff, 2005).

ROS are a central component in stress responses and the level of ROS determines the type of response (Shao *et al*, 2008). High ROS concentrations can result in non-controlled oxidation of a variety of cellular structures, including DNA, proteins and membrane lipids (Smirnoff, 2005), thus causing lipid peroxidation, membrane damage, and inactivation of enzymes (Apel and Hirt, 2004) and can cause apoptosis or necrosis depending on the severity of damage (Maysinger *et al*, 2006). Therefore plants have evolved an extensive enzymatic and non-enzymatic antioxidant system to scavenge these ROS (Pfannschmidt, 2009; Gechev *et al*, 2006) and the accumulation of ROS may be the consequence of a disruption in the balance between their production and the antioxidant system activity (Zhang *et al*, 2009).

Cells are sensitive to ROS and once the production of ROS overcomes the antioxidant defense, cellular redox balance is shifted and the cells are then in a state of oxidative stress (Maysinger *et al*, 2007; Halliwell, 2007). Sensitivity of cells to ROS may depend on the cell type, the level and the duration of oxidant production, the species of ROS generated, and the specific site of ROS production (Maysinger *et al*, 2007).

The three reactive oxygen species: O^-_2•, H_2O_2 and OH•, are linked by spontaneous or enzymatic dismutation, therefore the question arises as to which species must be measured (Batandier *et al*, 2002). The first step during O_2 reduction leads to the formation of superoxide (O^-_2•) or hydroperoxide (HO_2•) radicals (Figure 1-1). O^-_2• has a short halflife of 2 to 4 microseconds (Gechev *et al*, 2006; Batandier *et al*, 2002). The second step leads to formation of hydrogen peroxide (H_2O_2), which is a relatively stable molecule with a 1 miliseconds half-life and because of this longer half-life and diffusibility, H_2O_2 can migrate from the subcellular synthesis sites to adjacent compartments and even neighboring cells (Gechev *et al*, 2006). Among the different reactive oxygen species, OH• is probably the most unstable with a half-life of 10^{-9} sec (Batandier *et al*, 2002).

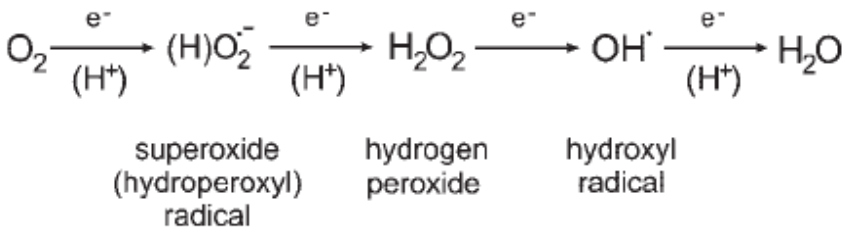

Figure 1-1 Generation of ROS by multistep reduction of molecular oxygen (Gechev *et al*, 2006).

The destructive properties of O^{-}_{2}• and H_2O_2 are more prominent when they interact in the presence of metal ions to form the highly reactive hydroxyl radical (OH•) (Gechev *et al*, 2006). H_2O_2 has been shown to accumulate at the surface of plant cells following recognition of pathogen invasion and plays a central role in the orchestration of the hypersensitive response, as the substrate driving cross-linking of cell wall structural proteins (Brisson *et al.*, 1994; Tenhaken *et al.*, 1995), as a local threshold trigger of programmed cell death in challenged cells and as a diffusible signal for the induction of cellular protectant and defense genes in surrounding cells (Tenhaken *et al.*, 1995).

Chloroplasts and mitochondria are often included among the major sites of intracellular H_2O_2 production. Other compartments in which H_2O_2 could accumulate include the intrathylakoid space, mitochondrial intermembrane space, endomembrane systems, and vacuole (Queval *et al*, 2008).

Probably the most important toxic feature of nanomaterials, the induction of oxidative stress, has repeatedly been reported for a considerable number of nanomaterials, so the phenomenon is probably generic for (almost) all nanomaterials (Hoet and Boczkowsky, 2008).

QDs are redox active nanoparticles (effective electron donors and acceptors) and can generate highly reactive free radicals (Lovrić *et al*, 2005 b)) with or without exposure to light (Green and Howman, 2005).

Various techniques have been used to quantify H_2O_2 contents in plant tissue extracts. In general, light emission as fluorescence or luminescence offers greater sensitivity than absorbance measurements (Queval *et al*, 2008), therefore fluorescence and bright field evaluation under light microscope will be the base of the analysis carried out in this study.

1.1.1.2. Cell viability

A cell is considered viable if it has the ability to grow and develop. Viability assays are based on either the physical properties of viable cells, such as membrane integrity or cytoplasmic streaming, or on their metabolic activity (Loyola-Vargas and Vázquez-Flota, 2006).

Cell viability can be accessed directly through the presence of cytoplasmic esterases that cleave moieties from a lipid-soluble nonfluorescent probe, like fluorescein diacetate, to yield a fluorescent product (Figure 1-2). The product is charged and thus is retained within the cell if membrane function is intact (Coder, 1997). Hence, when excited by blue light (488 nm), nonviable cells are nonfluorescent and viable cells (with fluorescein molecules) give a bright green fluorescence (Spence, 2001; Pollard and Walker, 1990).

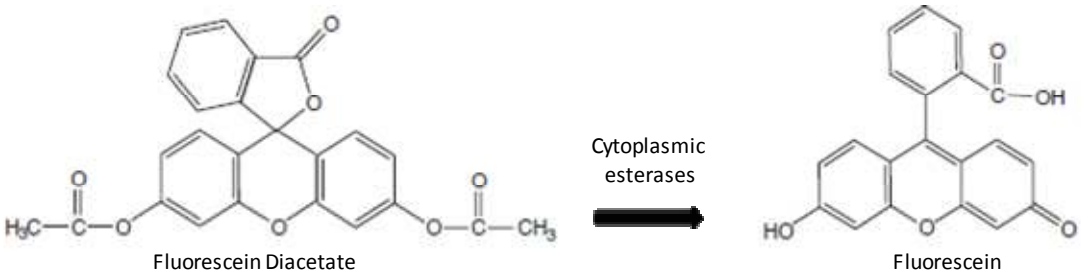

Figure 1-2 Fluorescein diacetate is hydrolysed by cytoplasmic esterases to yield the fluorescent product fluorescein, which is intracellulary accumulated (adapted from Green *et al*, 2006).

1.1.2. Nanotoxicity in plants

Nanotoxicity, an emerging concept, is receiving increasing attention with the fast development of nanotechnology. However, to date, plants, as important ecological receptors, have not received enough nanotoxicity research (Lin and Xing, 2008).

The few studies conducted to date on the effects of NPs on plants have focused mainly on phytotoxicity and how certain plant metabolic functions are affected. The reported effects vary depending on the type of nanoparticle, as well as plant species, and are not always consistent between different studies (Zhu *et al*, 2008).

For example, titanium nanoparticles (TiO_2) were reported to promote photosynthesis (Hong *et al*, 2005) and nitrogen metabolism, and then improve growth of spinach at an optimal concentration (Zheng *et al*, 2005; Yang *et al*, 2006), however Yang and Watts (2005) reported that alumina nanoparticles inhibit root elongation of several plants (corn, cucumber, soybean, cabbage, and carrot).

Lin and Xing (2007) investigated the effects of five types of NPs (multi-walled carbon nanotube, aluminium, alumina, zinc and zinc oxide) on seed germination and root growth of six higher plant species (radish, rape, ryegrass, lettuce, corn, and cucumber) and showed that seed generation was in general not affected in most cases while root elongation was inhibited. A more recent study of these authors (2008)

shows that in the presence of ZnO nanoparticles the ryegrass biomass is significantly reduced, root tips shrank, and root epidermal and cortical cells are highly vacuolated or collapsed, and the toxicity increased with increasing concentration. They also describe that the nanoparticles were able to concentrate in the rhizosphere and enter the root cells.

A recent study demonstrates that pumpkin plants grown in medium containing magnetite (Fe_3O_4) NPs can absorb, translocate and accumulate the nanoparticles in various tissues, predominantly near the roots as well as in leaves (Zhu *et al*, 2008).

So far, the only study of QD's toxicity in suspension cultures was performed by Wang *et al* (2008). They evaluated the toxicity of two types of widely used NMs, Titanium dioxide (TiO_2) and quantum dots (CdTe), using the green microalgae *Chlamydomonas reinhardtii* as a model system, and concluded that growth inhibition occurred as well as an oxidative stress.

All of these studies were performed with a variety of nanoparticles however, there are to date no toxicological studies with QD's in plants.

1.2. Quantum Dots

The term "quantum dot" refers to a crystalline structure whose dimensions are small enough that its electronic states begin to resemble those of an atom or molecule rather than those of the bulk crystal (Borovitskaya and Shur, 2002).

Quantum dots (QDs) are nanocrystals composed of a core of a semiconductor material (2-10 nm, Hild *et al*, 2008), enclosed within a shell of another semiconductor that has a larger spectral band gap. These nanometer-sized crystalline particles, are composed of elements of the periodic groups of II–VI (e.g., CdSe) or III–V (e.g., InP) (Alivisatos *et al*, 2005), while the shell is typically a high bandgap material such as ZnS (Figure 1-3 a) (Azzazy *et al*, 2007). The ZnS layer passivates the core surface, protects it from oxidation, prevents leaching of the Cd/Se into the surrounding solution and also produces a substantial improvement in the quantum yield (Medintz *et al*, 2005; Jaiswal and Simon, 2004; Dabbousi *et al*, 1997), and thus, core–shell nanoparticles are more desirable for biological applications.

1.2.1. Properties

The physical dimensions of QDs are smaller than the exciton Bohr radius (distance in an electron-hole pair, typically about 1 to 10 nm for most semiconductors) and that leads to quantum confinement effect, which is responsible for their unique optical and electronic properties (Vashist *et al*, 2006).

QDs are inorganic fluorophores that have size-tunable emission (i.e. there is a predictable relationship between the size of the QD and its emission wavelength) (Figure 1-5Figure 1-3 b)). They exhibit atom-like size-dependent energy states due to the confinement of the charge carriers (electrons, holes) in three dimensions (Parak *et al*, 2005). As a consequence the energy gap (i.e. the energy difference between the excited and the ground state) of a quantum dot strongly depends on its size and on the nature of the material (Galian and de la Guardia, 2009). Therefore, the smaller the diameter of the quantum dot is, the bigger the energy gap becomes as the Figure 1-4 represents (Hoshino *et al*, 2004).

a) b)

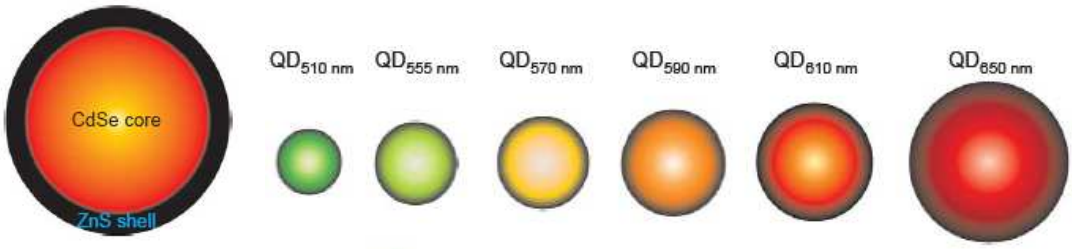

Figure 1-3 a) Structure of a typical CdSe/ZnS QD. b) Small CdSe nanocrystals (about 2 nm core diameter) are fluorescent in the green, whereas bigger ones (about 5 nm core diameter) are fluorescent in the red (adapted from Jaiswal and Simon, 2004).

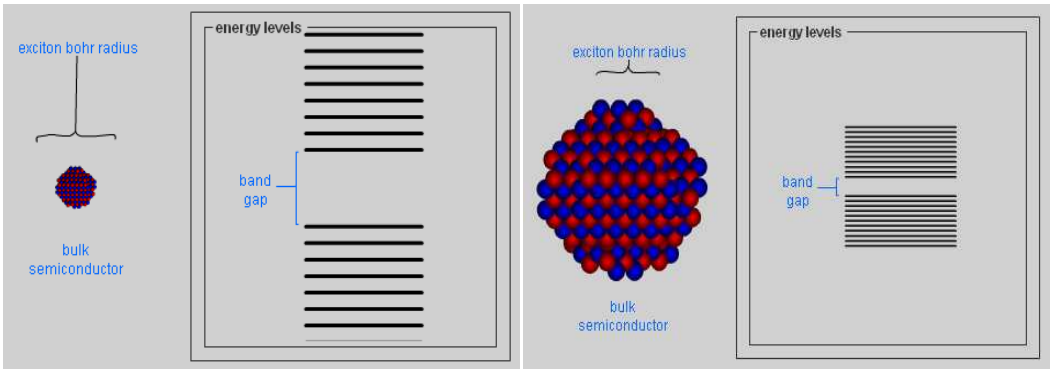

Figure 1-4 Quantum confinement and size dependent control of bandgap in QD's (adapted from www.evidenttech.com)

In semiconductor NPs, after the absorption of energy, the electrons go to the conduction band, leaving a hole in the valence band. The photo-generated electron-hole pair is known as an exciton, which, upon recombination, gives rise to the fluorescence emission of QDs (Galian and de la Guardia, 2009).

The emission spectra of QDs can be tuned across a wide range by changing the size and composition of the QD. The excitation spectra of QDs is very broad, whereas their emission spectra is fairly narrow (Figure 1-5) (Jaiswal and Simon, 2004; Pan *et al*, 2008). A narrow emission spectrum reduces spectral overlap, which improves the possibility of distinguishing multiple fluorophores simultaneously. The broad excitation spectrum of QDs facilitates the use of a single excitation, because the fluorescence can be excited with any wavelength shorter than the wavelength of fluorescence (Parak *et al*, 2005; Jaiswal and Simon, 2004). The large separation between the excitation and emission wavelength of QDs (Stokes shift), enables the whole emission spectra to be collected, resulting in improved sensitivity of detection, a feature that cannot be achieved with conventional fluorophores (Jaiswal and Simon, 2004).

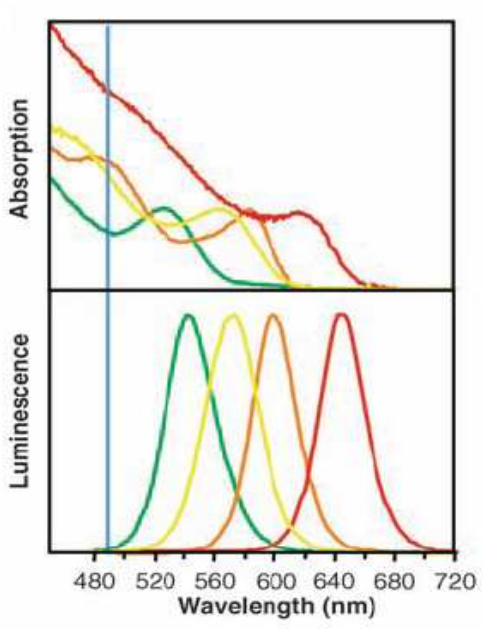

Figure 1-5 Absorption (upper curves) and emission (lower curves) spectra of four CdSe/ZnS qdot samples. The blue vertical line indicates the 488-nm line of an argon-ion laser, which can be used to efficiently excite all four types of QD's simultaneously (adapted from Michalet *et al*, 2005).

One of the biggest advantages of quantum dots is their reduced tendency to photobleach. Photostability is a critical feature in most fluorescence applications, and is an area in which QDs have singular advantage. Unlike organic fluorophores which bleach after only a few minutes on exposure to

light, QDs are extremely stable and can undergo repeated cycles of excitation and fluorescence for hours with a high level of brightness and photobleaching threshold (Jamieson *et al*, 2007).

Organic fluorophores can undergo irreversible light-induced reactions upon optical excitation, which result in loss of fluorescence. Due to their inorganic nature quantum dots suffer much less from photobleaching (Parak *et al*, 2005). Moreover, unlike organic fluorophores, the inorganic nature of QDs makes them resistant to metabolic degradation: QDs have been shown to remain fluorescent and to be retained in live cells and organisms for several weeks to months (Jaiswal and Simon, 2004).

The unusual physicochemical properties of engineered nanomaterials are attributable to their small size (surface area and size distribution), chemical composition (purity, crystallinity, electronic properties, etc.), surface structure (surface reactivity, surface groups, inorganic or organic coatings, etc.), solubility, shape, and aggregation. Particle size and surface area are important material characteristics from a toxicological perspective. As the size of a particle decreases, its surface area increases and also allows a greater proportion of its atoms or molecules to be displayed on the surface, as the Figure 1-6 illustrate (Nel *et al*, 2006). The increase in surface area determines the potential number of reactive groups on the particle surface, thus the contact between particles and cells.

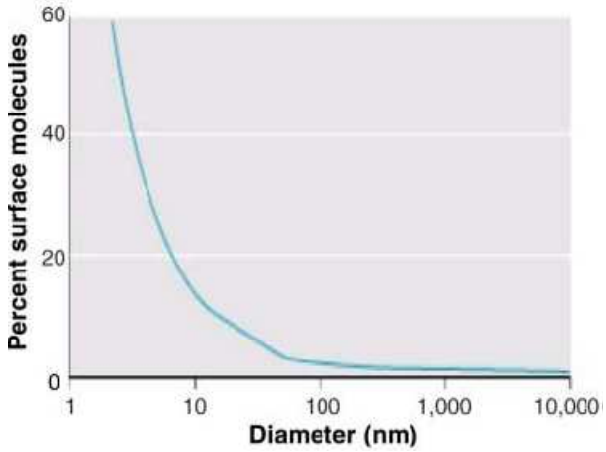

Figure 1-6 Inverse relationship between particle size and number of surface expressed molecules (Nel *et al*, 2006).

1.2.2. Biocompatibility

The use of semiconductor QDs as biological fluorescent probes requires that they: (i) are water soluble; (ii) offer reactive groups on their surface for subsequent bioconjugation; (iii) maintain all their photo physical properties when transferred into aqueous buffers (wide excitation band, narrow emission, long fluorescence lifetime, high quantum yield, high photochemical and photo physical stability); (iv) remain monodispersed; and (v) have a reasonable final small size (Rigler and Vogel, 2008).

High-quality QDs are most commonly synthesized in organic solution and surface-stabilized with hydrophobic organic ligands and thus lack intrinsic aqueous solubility. Biological applications require the further modification of the QD surface with a variety of bifunctional surface ligands to promote solubility in aqueous media (Delehanty *et al*, 2009).

These ligands mediate both the colloid's solubility and serve as a point of chemical attachment for biomolecules. Capping ligands serve another critical role in insulating/passivating/protecting the QD surface from deterioration in biological media (Medintz *et al*, 2005).

The superior photo physical features of semiconductor QDs are usually observed in organic solvents, and their introduction into aqueous media is usually accompanied with a drastic decrease in the luminescence yields of the QDs (Cordero *et al*, 2000), therefore is necessary to use a strategy that render the QDs hydrophilic without losing their fluorescence. Choice of shell and coating are gaining particular importance, as the shell stabilizes the nanocrystal and to some extent alters the photophysical properties, whilst the coating confers properties to the QD which allow its incorporation into a desired application (Jamieson *et al*, 2007).

1.2.3. Applications

Some of the early and most successful uses of QDs have been in immunofluorescence labeling of fixed cells (Kirchner *et al*, 2005) and tissues, immunostaining of membrane proteins (Michalet *et al*, 2005) and fluorescence *in situ* hybridization of chromosomes (Michalet *et al*,2005; Müller *et al*, 2006). Fluorescent QDs can be conjugated with bioactive receptors to target specific biological events and cellular structures, a few examples of bioconjugated QDs and their targets in cells are summarized in Figure 1-7.

They also serve as specific markers for cellular and molecular structures, tracing cell line age, monitoring physiological events in live cells (Pan *et al*, 2008), measuring cell motility (Kirchner *et al*, 2005), and tracking cells in vivo (Alivisatos, 2004; Pan *et al*, 2008).

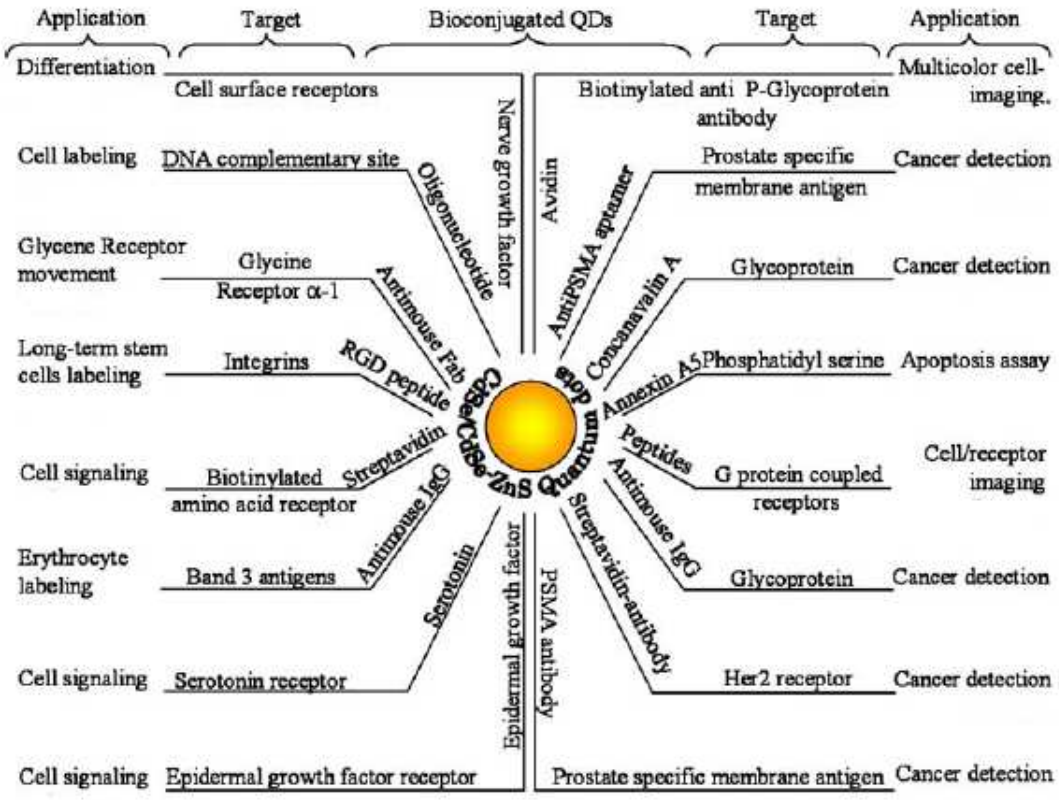

Figure 1-7 Biolabels of CdSe and CdSe–ZnS QDs and their targets in cells (Biju *et al*, 2008).

Quantum dots are anticipated to improve the speed, accuracy, and affordability of clinical diagnostic tests and deliver a specific amount of a drug to a certain type of cell (Müller *et al*, 2006; Male *et al*, 2008). They can also be used to label specific proteins, genes, and biomolecules to visualize such individual molecules (Male *et al*, 2008; Azzazy *et al*, 2007).

QDs, with their unique fluorescence properties and photoelectrochemical functions, are photoactive materials for the development of sensor systems. For example, a CdSe/ZnS dual QD system was used to measure potassium ions in aqueous solutions (Chen *et al*, 2006).

So far CdSe/ZnS QDs have been used mainly in animal systems. Table 1 summarizes the applications in plant systems up to now.

Table 1: CdSe/ZnS QD's applications in plant systems.

QD type	Application	Specie	Reference
CdSe/ZnS covalently linked to oligonucleotides	Detect transcripts in the plant	*Arabidopsis thaliana*	Riegler *et al*, 2008
CdSe/ZnS streptavidin conjugated	Immunolabeling/ *in situ* hybridisation	Zea *mays/Allium fistulosum*	MÜller *et al*, 2006
CdSe/ZnS protein conjugated	Localization of a small plant adhesion protein	*Lilium longiflorum*	Ravindran *et al*, 2005
CdSe/ZnS PEG conjugated	Follow fluid phase endocytic uptake	*Acer pseudoplatanus*	Etxeberria *et al*, 2006
CdSe/ZnS crosslinked to amino acid	Detect binding sites on protoplast membrane	*Nicotiana tabacum/ Arabidopsis*	Yu *et al*, 2006

1.2.4. Toxicity

Although impressive from a physicochemical viewpoint, the novel properties of nanomaterials raise concerns about their possible adverse effects on biological systems (Nel *et al*, 2006) and therefore, a key issue in evaluating the utility of these materials is assessing their potential toxicity, either due to their inherent chemical composition or as a consequence of their nanoscale properties (Derfus *et al*, 2004).

QD toxicity depends on multiple factors derived from both individual QD physicochemical properties and environmental conditions: size, charge, concentration, outer coating bioactivity (capping material, functional groups), and oxidative, photolytic, and mechanical stability. Each of these has shown to be determining factors in QD toxicity (Figure 1-8)(Hardman, 2006; Male *et al*, 2008).

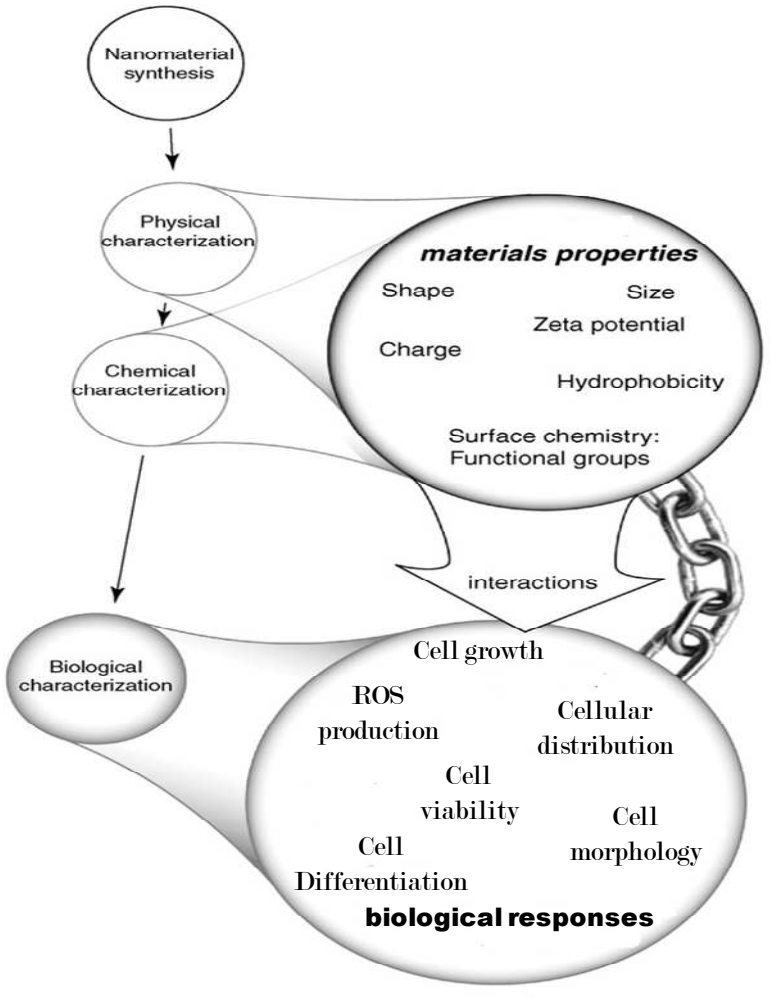

Figure 1-8 The nanomaterial physico-chemical property relationship to *in vivo* responses. Each property of nanomaterials could influence cells response (adapted from Fisher and Chan, 2007).

Quantum dot dosage/exposure concentrations reported in the literature vary widely in units of measurement (e.g., micrograms per milliliter, molarity, milligrams per kilogram body weight, QDs per cell) (Hardman, 2006). It also has been demonstrated that a high concentration of nanoparticles would promote particle aggregation, and therefore reduce toxic effects compared to lower concentrations (Buzea *et al*, 2007).

Further, some QDs were found to be cytotoxic only after degradation of their core coatings both in vivo and/or in vitro (Hardman, 2006). Mahendra *et al* (2008) evaluated the resulting toxicity of weathered QD's in extreme pH conditions (Figure 1-9). This study reports the QD weathering and release of toxic core components following the degradation of surface coatings after exposure to moderate acidic and alkaline conditions.

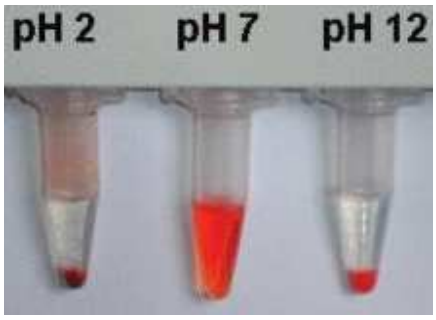

Figure 1-9 Effect of the pH in QDs stability. At pH 7 QD's are well dispersed in solution, at pH 2 and 12 QD's are precipitated (adapted from Mahendra *et al*, 2008).

Based on the evidence from the studies published so far, it is typically proposed that the toxicity of particles increases with the decrease of the particle size, because smaller particles have smaller sizes, larger particle numbers and larger surface area per unit mass (Yang and Watts, 2005; Buzea *et al*, 2007).

A research made by the Lovrić group (2005 a)) demonstrate that CdTe QDs can enter in rats cells and distribute in different subcellular compartments, employing red- and green-emitting cationic QDs in experiments they found that the CdTe QD distribution was in part dependent on nanoparticle size. Also Shiohara *et al* (2004) suggest that the mobility of QD's inside the cells depend on the size of QD's and the difference in cell damage may be explained by that reason. This study was performed in two animal cell lines and one primary cell culture (human).

Maysinger *et al* (2007) propose two possible mechanisms to explain why QDs lead to cell damage or/and death: (i) leaching of metals from the core of nanoparticles with compromised integrity (ions of Cd, Se, Te, Hg, Pb, etc.), and/or (ii) formation of reactive oxygen species (ROS).

Cadmium and selenium, two of the most widely used constituent metals in QD core metalloid complexes, cause acute and chronic toxicities in vertebrates and are of considerable human health and environmental concern (Male *et al*, 2008). Because the toxicity of Cd^{2+} ions is well documented, a significant body of work has focused on the intracellular release of free cadmium from the QDs (Smith et al, 2008)

Derfus *et al* (2004) have shown that CdSe-core quantum dots are cytotoxic under certain conditions. Exposure to air induces oxidation of the quantum dot surface and exposure to UV radiation catalyses oxidation of the quantum dot surface (Figure 1-10), which finally results in the release of Cd^{2+} ions and correlated with cell death. Surface coatings such as ZnS and BSA were shown to significantly reduce,

but not eliminate cytotoxicity (Parak *et al*, 2005), in fact, one of the primary conditions governing cytotoxicity is the degree and stability of the QD surface coating that makes these inorganic nanoparticles water-soluble .

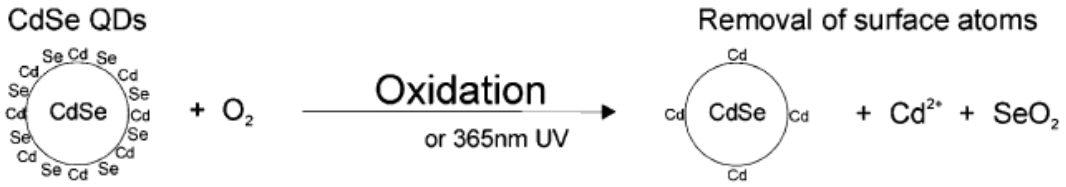

Figure 1-10 Surface oxidation leads to release of cadmium ions (adapted from Derfus *et al*, 2004).

To investigate oxidative stress produced by QDs, Lovrić *et al* (2005b)) used dihydroethidium (DHE). DHE is oxidized by ROS to ethidium, which intercalates with cellular DNA, yielding bright red, fluorescent nuclear staining. Using confocal microscopy, they observed ROS production after 4 hr of QDs exposure in culture medium.

Notwithstanding, Chang *et al* (2006) refers that it is important to distinguish whether cellular toxicity arises from the interaction of QD surface molecules with cell membranes or from the intracellular uptake of endocytosed QDs, which is influenced by surface molecules on these nanoparticles.

Kirchner *et al* (2005) investigated the cytotoxicity of CdSe and CdSe/ZnS nanoparticles for different surface modifications in four different mammalian cell lines, the group concluded that in addition to the release of Cd^{2+} ions from the surface of nanoparticles, cells can also be impaired if nanoparticles precipitate on the cell surface. Furthermore, cytotoxic effects are different in the case that particles are ingested by the cells compared to the case that particles are just present in the medium surrounding the cells. According with another study of Hoshino *et al*. (2004) it is concluded that there is a massive influence of the surface chemistry of the particles on their cytotoxic behavior in addition to the release of toxic molecules.

The fate of cells exposed to nanoparticles depends on their extracellular and intracellular environment. Moreover, the signal duration, location and intensity will determine whether cells will proliferate, die or differentiate, as illustrated in Figure 1-11.

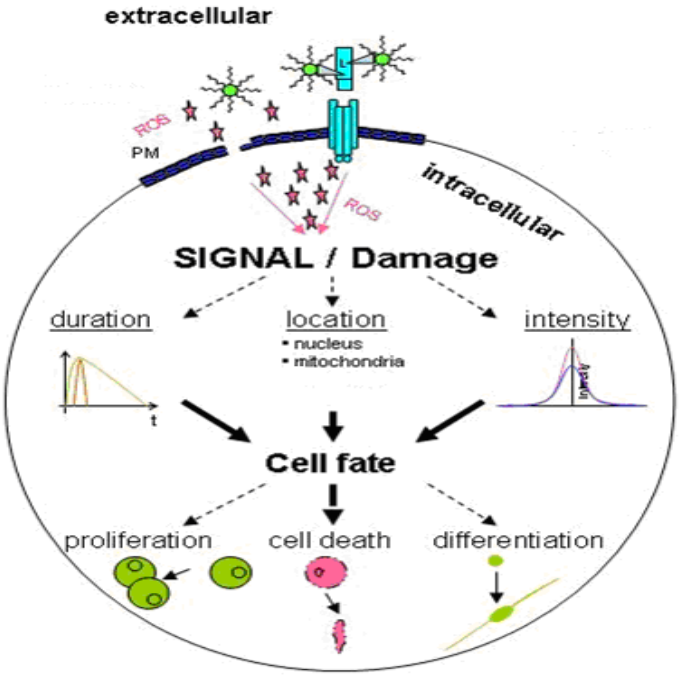

Figure 1-11 Mechanism of cell fate induced by nanoparticles (adated from Maysinger *et al*, 2006).

It is feasible that a significant amount of toxicological data obtained for QDs thus far has been considerably influenced by the colloidal nature of these nanoparticles. The tendency for nanoparticles to aggregate, precipitate on cells in culture, nonspecifically adsorb to biomolecules, and catalyze the formation of reactive oxygen species (ROS) may be just as important as heavy metal toxicity contributions to toxicity (Smith *et al*, 2008).

Because of the diversity of their synthesis, not all QDs are alike and QDs conjugated with biomolecules cannot be considered a uniform group of nanomaterials (Male *et al*, 2008). Obtaining a straight answer about QD cytotoxicity is difficult due to the lack of standardized QD synthesis protocols, coatings, solubilization ligands, and cell systems employed in different studies.

However, from this diversity it can be concluded that protection of the QD surface plays a crucial role. Particles with surfaces well protected by polymers or proteins are mostly not harmful to cells (Maysinger *et al*, 2007), nevertheless, further research is needed before we move forward toward widespread use of quantum dots in biological systems.

1.3. *Medicago sativa* and *Medicago truncatula*

Model species are valuable not only because they lead to discoveries about basic biology, but also because they provide resources that facilitate improvements in crops of economic importance. The plants used in this work were the legumes *Medicago sativa* and *Medicago truncatula*.

Legumes comprise one of the most important agricultural taxa worldwide, providing a major source of protein and oil for humans and animals, and nitrogen for soil improvement, besides they also offer unique research opportunities in areas of basic and applied plant biology (Cook, 1999).

1.3.1. Medicago sativa

Alfalfa or Lucerne (*Medicago sativa* L., Figure 1-12) known as the "Queen of Forages", is the world's economically most important and widely grown forage legume (May and Dixon, 2004; Yang *et al*, 2008), distributed in temperate zones of the world: USA, southern Canada, Europe, China, southern Latin America, South Africa (www.fao.org).

M. sativa is a tetraploid, perennial and allogamous (i.e. non self-fertile) plant (www.grainlegumes.com) and has a higher tolerance of saline soils than many other forage species (www.fao.org). Many genes in *M. truncatula* have over 98% sequence identity with their orthologs in alfalfa (May and Dixon, 2004). The high degree of sequence identity and remarkably conserved genome structure and function between the two species enables *M. truncatula* genes to be used directly in alfalfa improvement (Yang *et al*, 2008).

Alfalfa has spread and become popular because of its productivity and high feed value. With its high protein content, it complements corn silage and grains in formulating livestock feeds. Alfalfa is a versatile crop and can be used for pasture, hay, silage, green-chop, soil improvement, and soil conservation (Lacefield *et al,* 1997).

1.3.2. Medicago truncatula

Medicago truncatula, commonly known as 'barrel medic' because of the shape of its seed pods (May and Dixon, 2004; Figure 1-12), belongs to the phylogenetic group of legumes, the Galogoid (www.grainlegumes.com). *Medicago truncatula* is a diploid (2n=16), autogamous species and among many reasons, is chosen as a model legume because of its modest genome size of 500–550 million base

pair (1.8×109 bp for the Jemalong cultivar), short seed-to seed generation time, workable levels of transformation, excellent mutant populations, and large collections of diverse ecotypes (Young and Udvardi, 2009).

The Jemalong cultivar is one of the most used in agricultural practices and pastures for animals (Araújo *et al*, 2004). *M. truncatula* is an omni-Mediterranean species grown as an annual forage legume and it is a near relative of alfalfa (May and Dixon, 2004).

Of crop legumes, alfalfa has become an immediate beneficiary from the study of the *M. truncatula* genomics, not only because alfalfa is a close relative of *M. truncatula*, but also because alfalfa itself is not amenable to genetic analysis. In addition to a focus on symbiotic plant- microbe interactions, significant efforts have taken advantage of *M. truncatula* as a model system to characterize legume pathogen interactions. Importantly, most alfalfa pathogens also are pathogens of *M. truncatula* (Yang *et al*, 2008).

Figure 1-12 *M. truncatula* plant, the shape seed pods lead to its common name "barrel medic" (left image, Cook, 1999). Plant of *M. sativa* (right image, www.fao.org).

1.4. Detection of fungal diseases in *Medicago spp.*.

Among the principal diseases of *Medicado spp*. is the *Fusarium* root rot and *Fusarium* wilt, both caused by *Fusarium spp* .(www.fao.org), an ascomycota fungi.

Fusaria are among the most common and widespread fungi and are of great economic importance. *Fusarium* species are serious pathogens on a wide range of major food and fiber crops such as wheat, corn, rice, bananas, potatoes, cotton and flax to mention only a few. They are also important as spoilage

organisms of stored products and producers of mycotoxins, and can cause disease of humans, animals, and insects. Yet *Fusarium* diseases continue to be among the most important plant diseases (Nelson *et al*, 1985).

Due to the non-specific symptoms, the isolation and identification of the agents is the essential step in the diagnostic of the disease. Most disease-control decisions for alfalfa are made before diseases are visibly apparent. For several alfalfa diseases, once the symptoms appear, little can be done to control the disease. Therefore, careful planning is necessary to keep alfalfa diseases from building up to damaging levels. Like most crop diseases, alfalfa diseases are most effectively managed by integrating as many control methods as practical. With the exception of seed treatment, alfalfa diseases cannot be controlled economically using commercial fungicides (Vincelli *et al*, 1997).

A recurrent challenge to alfalfa production is the significant yield loss caused by disease (Yang *et al*, 2008). Lucerne wilt diseases, e.g. *Fusarium* wilt, invade through the roots but the adverse effects are expressed in the shoots. In some cases, fungicidal control is possible and economic but in other cases it is neither possible nor economic (www.fao.org). Therefore, nanotechnology opens new ways in detect precociously the fungi in the plant and in the control of the infection.

1.5. Plant cell suspension cultures

Unorganized plant cells can be grown as callus in aggregated tissue masses, or they can be freely dispersed in agitated liquid medium. Cell suspension cultures are usually started by placing an inoculum of friable callus in liquid medium. Under agitation single cells and small clumps of cells are released into the medium that soon start to divide. Because the walls of plant cells have a natural tendency to adhere, it is not possible to obtain suspensions that consist only of dispersed single cells (George *et al*, 2008). Plant cell cultures present growth kinetics similar to microorganisms except for the time span which is in the range of days.

Cell suspension cultures are widely used, especially in research as one of the plant tissue culture techniques. It has the advantages of giving homogeneity and a higher efficiency of propagation of cultured cells compared with callus culture on solidified media (Ibaraki and Kenji, 2001).

1.6. Objectives

Within the aim of this thesis the following objectives were pursued:

- to evaluate the effect of QD's in plant differentiation using an already available embryogenic cell suspension culture of *M. truncatula*.
- to establish a fine suspension culture of *M. sativa* in order to evaluate the effect of QD's:
  - in cell growth parameters
  - in cell viability
  - in oxidative stress by ROS production
- to verify if QD's are up-taked by cells of both *M. truncatula* and *M. sativa*, and if yes what is the extent of internalization.

2. Materials

2.1. Quantum dots samples

The QD samples used in this work, and also all the characterization information, were kindly supplied by Sofia Miguel (Organic Synthesis Laboratory, ITQB, Oeiras).

Two different samples were employed in this work: the first one is identified as QD50_MPA sample and the latter is identified as QD68_MPA sample. Both are CdSe/ZnS (core/shell) QD's and mercaptopropionic acid (MPA) functionalized. As it was discussed above, diameter, charge and surface coatings were shown to be correlated with cytotoxicity and this way, is of extremely importance to characterize them.

All samples were stored in the dark at 4-7 ºC in basified MiliQ water.

2.1.1. QD50_MPA

This first sample was synthesized by the method described in Wang *et al* (2007), with modifications of reagents used. This procedure allows simultaneous *in situ* functionalization of CdSe QDs by MPA and surface passivation by a thin ZnS shell (Figure 2-1). Furthermore, avoids the second-step ligand exchange after the core shell formation and yet preserves high QY and stability of the QDs.

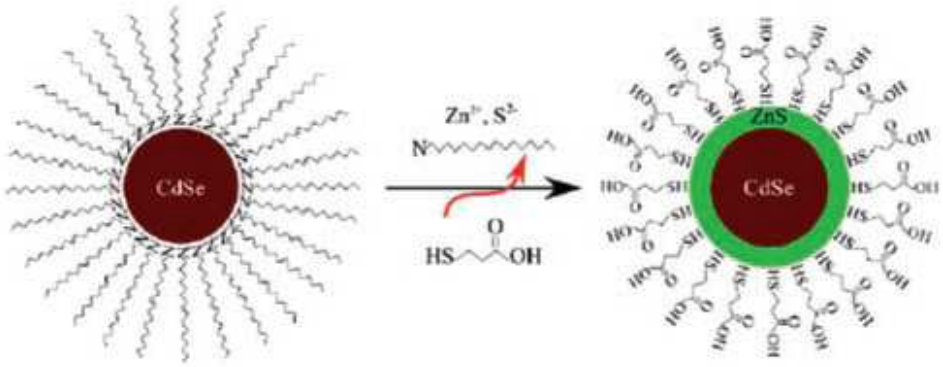

Figure 2-1 Preparation of MPA-Capped CdSe/ZnS Core-Shell QDs through One-Step *in situ* Surface Functionalization Method (adapted from Wang *et al*, 2007).

These samples were the first to be done by the group that supplied the material, and therefore, they were test samples. For that reason, they were not very well characterized. The information given is that they had an MPA excess residue, and had absorbance maximum at λ=475-480 nm. Concerning the size, it

was obtained by AFM (atomic force microscopy) and, despite the results were not very precise, the obtained average size was 30 nm.

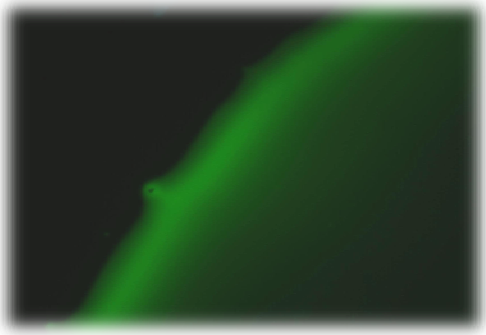

Figure 2-2 QD's in MiliQ water under UV light of inverted microscope. Magnification 200x.

2.1.2. QD68-MPA

In this sample, the MPA-coated nanocrystals were synthesized by the phase transfer method. When reacted with ZnS-capped CdSe QDs in chloroform, the mercapto group binds to Zn atom and the polar carboxylic acid group renders the QDs water-soluble. The free carboxyl group is also available for covalent coupling to various biomolecules (such as proteins, peptides, and nucleic acids) by cross-linking to reactive amine groups.

UV-Vis absorption spectra were taken with a Beckman DU-70 spectrometer and photoluminescence (PL) spectra were taken with a SPEX-Fluorolog fluorometer (Figure 2-3 and Figure 2-4). Quantum yield (QY) was measured relative to Rhodamine 123 (standard) with excitation at 511 nm. Fluorescence spectra of QD and dye were taken under identical spectrometer conditions. The results are presented in Table 2.

Table 2: Emission wavelength and Quantum Yield of QD68_MPA.

Sample	*Emission*	*QY %*
QD68-MPA	Exc=530nm Em=603nm	7.0

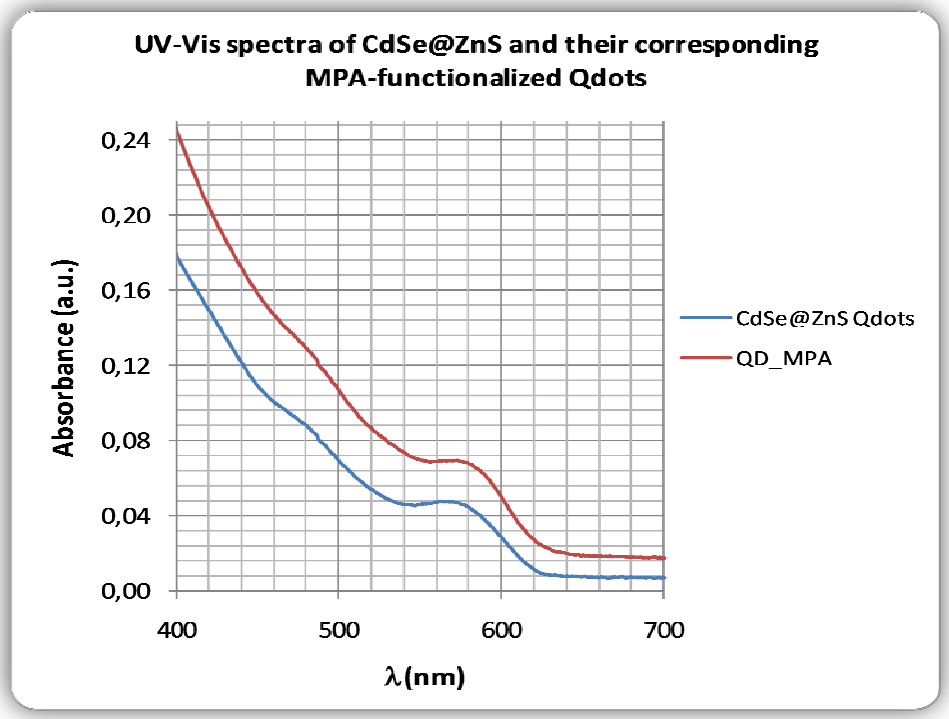

Figure 2-3 UV-Vis Spectra of CdSe/ZnS and their MPA-functionalized QDs.

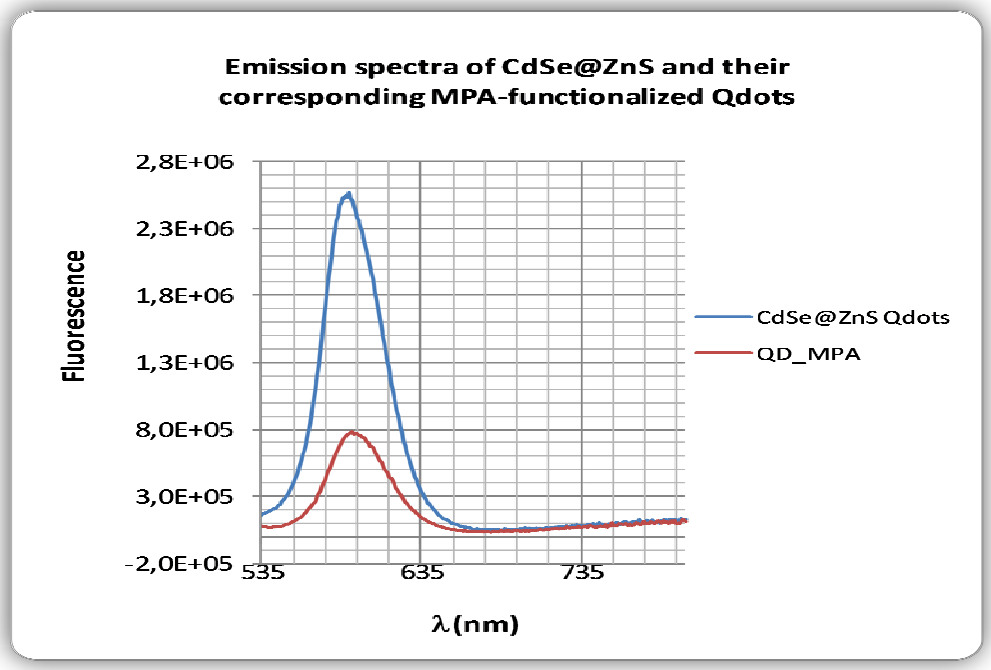

Figure 2-4 Emission Spectra of CdSe/ZnS and their MPA-functionalized QDs when excited at 530 nm.

Light scattering analysis (Figure 2-5) was performed using a Nano series dynamic light scatterer from Malvern, which analyzes the hydrodynamic diameter and zeta potential (ξ) of CdSe@ZnS hydrophilic Qdots, which are summarized in Table 3. Hydrodynamic diameter assumes a spherical symmetric density distribution of the colloidal particles and Zeta potential gives an indication of the potential stability of the colloidal system, large negative or positive ξ tend to repel each other. Particles with Zeta potential more than -30 mV are considered stable (www.nbtc.cornell.edu/facilities/downloads/Zeta potencial - An introduction in 30 minutes.pdf).

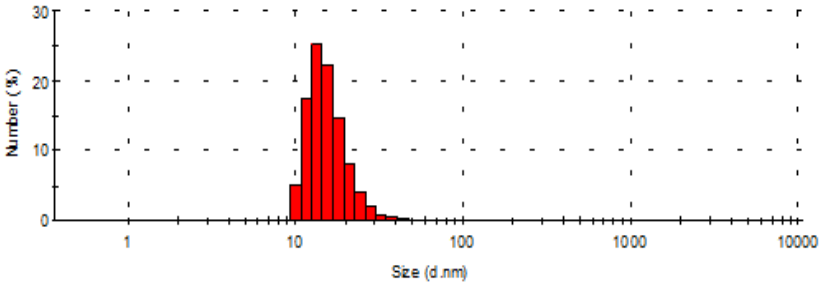

Figure 2-5 Representative dynamic light scattering histogram of the hydrodynamic diameter obtained of the MPA-functionalized Qdots in H_2O.

Table 3: Hydrodynamic diameter and zeta potential of samples

Sample	*Hydrodynamic diameter (nm)*	*ξ-Potential (mV)*
QD68_MPA (H_2O)	13,5	-45,6
QD68 – CdSe@ZnS ($CHCl_3$)	9,3	-

In Figure 2-6 are images of this sample of QD´s, at this time the microscope only had the B-2E/C filter, which has a low band pass that blocks the emission of QD's, so the images were taken in UV and Green filters.

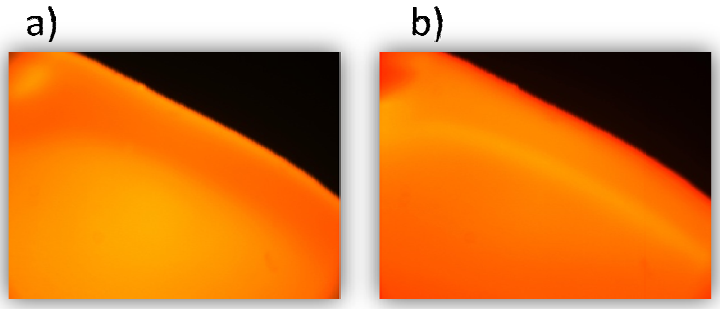

Figure 2-6 QD's [2.45 µM] solution in H_2O pH=12 under UV and Green filter, respectively a) and b) of the inverted microscope. Magnification 200x.

2.2. Optical and fluorescence microscopes

Almost all of the work was performed using fluorescence microscopy, unless stated otherwise. An inverted microscope model TE2000-S from Nikon equipped with a Nikon HMX-4 100 W Mercury lamp as a light source. The microscope was equipped with four different filter sets (

Table 4). Microscope images were acquired with an Evolution MP 5.1 megapixel digital CCD Color Camera (Media Cybernetics), and image capture and exposure times were controlled using Image Pro Plus 5.0 software (Media Cybernetics).

Table 4: Filter Sets specifications.

Filter set	Excitation filter (nm)	Barrier filter
UV-2A	330-380	420 (LP)
B-2E/C	465-495	515-555 (BP)
G-2E/C	528-553	590-650 (BP)
B-2A*	450-490	515 (LP)

Also a stereomicroscope was used: a Leica MZ8 with a Plan 1X objective lens, equipped with a projector light bulb lamp CLS 100 Leitz/Leica and a digital imaging system with resolution of 1.3 megapixels (Leica DC 200; Leica Microscopy Systems), connected to a computerized image analysis system (IM 50; Leica Microsystems A/S) was used.

The confocal images were acquired using a Leica SP-E confocal laser scanning microscope (Leica DMI 4000b) equipped with the Leica Application Suite (LAS) software. A X20 Plan Apo dry objective

(Numerical Aperture= 0.75) (Leica) was used. For quantification purposes, gain and offset settings were kept constant.

2.3. Plant cell cultures

The first part of the work was performed with a long term embryogenic cell suspension culture of *M. truncatula* cv. Jemalong line M9-10a, established by the Plant Cell Biotechnology Laboratory, and maintained as described by Iantcheva *et al* (2006). Suspension cultures were sub-cultured at the end of the exponential growth phase (every 9/10 days) to fresh Murashige & Skoog basal salts and vitamins, 3 % (w/v) sucrose and supplemented with 1 mg/L 2,4-D (dichlorophenoxyacetic acid) and 0,2 mg/L kinetin. Suspension cultures were kept in an orbital shaker at 110 rpm (Innova 4900, New Brunswick Scientific, Germany) in the dark, at 24 ºC.

Also a fine suspension culture of *M. sativa* line M699 was developed, as described in point 3.1 of methods.

3. Methods

3.1. Establishment of a cell suspension culture of *Medicago sativa* line M-699

3.1.1. Seed material

The seeds of line M699 were kindly provided by Diego Rubiales at the Instituto de Agricultura Sostenible (IAS) of the CSIC (Consejo Superior de Investigaciones Científicas) in Córdoba, Spain, and it was collected in Palomares, Cuenca, Spain.

The seeds were surface sterilized with 97% solution of sulfuric acid (H_2SO_4) or a 50% Domestos 3 (commercial detergent) as follows: they were placed in H_2SO_4 or Domestos 3 for 8 minutes, then after removing all the possible acid or Domestos, washed five times with sterile distilled water. After being rinsed with ethanol 70% for about two minutes they were washed again with sterile distilled water and germinated in a sterile Petri dish with wet paper in dark at room temperature.

After three days germinated seeds were transferred to growth-regulator-free medium (MS0G) – M&S (Murashige and Skoog, 1962) basal salts and vitamins, 3 % (w/v) sucrose (Duchefa Biochemie), 0.2 % (w/v) gelrite (Duchefa). Plant material is maintained under a 16 hours photoperiod applied as cool white fluorescent light and a day/night temperature of 24º/22ºC (Phytotron Edpa 700, Aralab, Portugal).

The pH of medium is always adjusted to 5.8 with 1 M NaOH solution before autoclaving (121ºC, 20 min.).

3.1.2. Callus induction from plant explants and maintenance

Well-developed leaflets, roots and petioles from 25 day in vitro cultured M699 plants were used as explants for callus induction. Leaflets, roots and petioles were cutted and transferred (in the case of petioles with the abaxial side-down) to Petri-dishes containing callus induction medium: M&S basal salts and vitamins, 3 % (w/v) sucrose, 0.2% (w/v) gelrite supplemented with 5 mg/L of dithiothreitol (DTT) and growth regulators in two concentrations: 0.1 mg/L of 2,4-D and Kin, and 0.5 mg/L of 2,4-D and Kin.

Calli were maintained under a 16 hours photoperiod of 100 $\mu mol.m^{-2}.s^{-1}$ applied as cool white fluorescent light and a day/night temperature of 24º/22ºC (Phytotron Edpa 700, Aralab, Portugal). Every 4 weeks the calli were sub-cultured into fresh media.

Growth regulators were always filter sterilized through 0.2 µm Orange Scientific filters and added to autoclaved medium.

3.1.3. Initiation of suspension culture

To initiate cell suspension cultures, two friable portions of 8 week grown callus derived from roots maintained in solid M&S medium supplemented with 0.1 mg/L 2,4-D and kin, and two compact portions of 8 week grown callus derived from petioles maintained in solid M&S medium supplemented with 0.5 mg/L 2,4-D and kin were placed in 250 mL Erlenmeyer flask with 50 mL of liquid M&S medium, supplemented with the same growth hormone composition used for callus phase. After 10 days 100 ml of fresh medium was added to each flask.

After 10 days, 20 mL of cell suspension culture from each line was placed in 100 mL of fresh medium. To separate a fine fraction from a calli fraction of the petiole cell suspension culture they were decanted. 25 mL of fresh medium was added to the calli fraction and 10 mL of it was taken to 100 mL of fresh medium, a new settlement was made with the fine fraction and 20 mL was removed to 100 mL of fresh medium. Until an adequate cell density is obtained for both cultures, the cells are pellet and medium substituted every 9, 10 days.

Sub-cultures of both cultures are carried out by transferring 20 mL of the cell suspension every 8 days to 100 ml of fresh medium (in 250 ml Erlenmeyer flasks). Both cell suspension cultures are maintained in an orbital shaker at 110 rpm (Innova 4900, New Brunswick Scientific, Germany) in the dark, at 24 ºC.

3.2. Growth kinetic parameters determination

There are several techniques available for measuring culture growth: determination of cell number, fresh and dry weights, packed cell volume, cell counting, and optical density among others. The method that gives the most accurate picture of cell growth is the determination of cell numbers (Pollard and Walker, 1990). Cell density is obtained by direct counting of cells under the microscope, using a cell counting chamber, such as the Neubauer chamber.

3.2.1. M. truncatula line M910-a

Plant cell suspensions rarely contain a high percentage of single cells. Instead, they consist mostly of cell clumps of varying sizes, like *M. truncatula*, and therefore was necessary to employ other technique to measure culture growth. The most widely used method of growth determination is the measurement dry weight of cells.

The determination of growth kinetics of *M. truncatula* was carried out as described by Zottini *et al* (2006). One Erlenmeyer flask with 200 mL of M. truncatula suspension culture with 9 days old, was randomly taken from the stock and 20 mL aliquots were inoculated in three Erlenmeyer flaks containing 100 mL of fresh MS medium. Then every day, 5 mL of each of the replicates (in triplicate) were vacuum filtrated in filter paper disks (70 mm, Macherey- Nagel). The filter paper disks were previously dried at 70 °C in a oven (Binder, Germany) for two days before use, and then they were cooled down in a dessicator containing silica gel (Merck) for 20 min (in order to stabilize them) and their weight was registered. The collected cells (3 disks/sample) were dried for two days at 70 °C, and then their weight was registered. Fresh weight was determined by subtraction of the weight corresponding to the filter paper. This experiment was repeated two times.

3.2.2. *M.sativa* line M699

To determine the growth parameters of the fine *M.sativa* cell suspension culture, which is mainly consisted by individualized cells, a Bright Line Counting chamber (Improved Neubauer, Hausser Scientific, U.S.A) was used to determine cell concentration.

A 500 mL Erlenmeyer flask with 200 mL of *M. sativa* suspension culture with 8 days old was randomly taken from the stock and 20 mL aliquots were inoculated in three Erlenmeyer flaks containing 100 mL of fresh medium. Then every day, small aliquots (about 1 mL) of the three replicates were taken and cells were counted in the Neubauer Chamber. Two counts by replicate were performed, and from the total counts the three most concordant were selected to represent the growth curve.

To calculate cell concentration the following equations were applied, and then the average was calculated:

$$\frac{\text{Nº of cells counted in 5 squares}}{0.5\ (mm3)} = cells/mm3 \quad \textbf{(Equation 1)}$$

$$Equation\ 1 \times 1000 = cells/mL \quad \textbf{(Equation 2)}$$

The values obtained in the exponential growth phase and semi-logarithmic plots were used to determine parameters that describe growth efficiency, namely, specific growth rate (μ) and time of doubling. The doubling time (Td) was determined according to the formula:

$$\frac{\mathcal{LN}(2)}{\mu} = Td \textbf{ (Equation 3)}$$

3.3. Cytotoxicity assays

3.3.1. Cell differentiation (somatic embryogenesis)

One Erlenmeyer flask with 200 mL of *M. truncatula* suspension culture with 9 days old was randomly taken from the stock and 4 mL aliquots were inoculated in nine Erlenmeyer flasks containing 20 mL of fresh M&S medium. In day 9 of sub-culture, in three Erlenmeyer flasks [160 nM= 84.5 µL] of QD50_MPA were added, and also in another three Erlenmeyer flasks the same volume (84.5 µL) of sterilized MiliQ water was added (these and the three undisturbed cultures were controls).

In the following day (24 hours after the addition of QD's), 1mL of each Erlenmeyer flask (in triplicate) was transferred into Petri dishes with M&S0G free-regulators medium and gently distributed over the solidified medium. Then, they were putted under a 16 hours photoperiod of 100 $\mu mol.m^{-2}.s^{-1}$ applied as cool white fluorescent light and a day/night temperature of 24º/22ºC (Phytotron Edpa 700, Aralab, Portugal). After 8 days, Petri dishes were visualized in the stereomicroscope and photographed.

3.3.2. Growth parameters

To evaluate the effect of the QD's in the growth cycle a similar protocol to the growth curve determination was performed.

A 250 mL Erlenmeyer flask with 120 mL of *M. sativa* suspension culture with 8 days old was randomly taken from the stock and 4 mL aliquots were inoculated in five 100 mL Erlenmeyer flaks containing 20 mL of fresh medium. In day 3 of sub-culture, [40nM] of QD68_MPA was added in two Erlenmeyer flasks. At the day of the inoculation, at day 3 and at day 8 small aliquots (about 0.5 mL) of the five erlenmeyers were taken and cells were counted in the Neubauer Chamber. At day 8 of culture they were sub-cultured by gentle setting and addition of fresh medium. Then, every day small aliquots (about 0.5 mL) of the five erlenmeyers were taken and cells were counted in the Neubauer Chamber. Eight counts per Erlenmeyer were executed, and from the total counts the four most concordant were selected to represent the growth curve. The growth parameters were determined as referred in point 3.2.2..

3.3.3. Cell viability

To check the viability of cells in the presence of QD's the following set up was carried out: a 250 mL Erlenmeyer flask with 120 mL of *M. sativa* suspension culture with 8 days old was randomly taken from the stock and 2 mL aliquots were inoculated in five 50 mL Erlenmeyer flaks containing 10 mL of fresh medium. In day 3 of culture [40nM] of QD60_MPA was added in two erlenmeyers. Before adding the QD's and after that, every day, viability of the cultures was checked using Fluorescein Diacetate (FDA) method described by Pollard and Walker (1990).

A stock solution of FDA was prepared by adding 10 mg of FDA and 2 mL of acetone and kept at -20 ºC. A diluted solution of FDA was then freshly prepared at the time of the assay, adding 20 µL of the stock solution to 1 mL of MS medium. At last, a drop of both suspension culture and diluted FDA was placed in a microscope slide and covered with a cover slip. The counts were performed in the inverted microscope, with excitation at about 488 nm. Two preparations were made to each Erlenmeyer and counted five random spots per microscope slide. Eight counts were selected to calculate the percentage of viability and then the average. The percentage of cell viability is calculated using the formula:

$$\%\ \boldsymbol{viability} = \frac{\boldsymbol{Number\ of\ Viable\ cells}}{\boldsymbol{Total\ Number\ of\ cells}} \times \mathbf{100} \quad \textbf{(Equation 4)}$$

3.3.4. Oxidative stress

To investigate the oxidative stress eventually produced by the presence/interaction of the QD's it were used three widely employed probes: 3,3- Diaminobenzidine (DAB), nitroblue tetrazolium (NBT) and 2',7'-Dichlorodihydrofluorescein diacetate (H_2DCFDA). The assays were performed with different times of exposure of the cultures with QD's (QD68_MPA)

which will be designated as: **(1)** QD's introduced at the time of the assay and **(2)** QD's introduced at day three of culture. Except for the DAB assay which was performed only in case **(1)**.

3.3.4.1. 3,3'- Diaminobezidine (DAB)

Production of H_2O_2 at the cellular level was examined by applying the DAB staining technique described by Thordal-Christensen et al, (1997), with a few modifications.

A 250 ml flask with 120 mL of a seven day old cell suspension culture of *M. sativa* was randomly taken to establish the following experimental setup:

- 2 mL of suspension culture,

- 2 mL of suspension culture plus 20 µL DAB to final concentration of 0,1 mg/ml,

-2 mL of suspension culture treated 35 ºC for 10 minutes plus 20 µL DAB to final concentration of 0,1 mg/ml,

-2 mL of suspension culture plus 40 µL H_2O_2 to final concentration 10 mM plus 20 µL DAB to final concentration of 0,1 mg/ml,

-2 mL of suspension culture plus 32.6 µL QD's to a final concentration 40nM plus 20 µL DAB to final concentration of 0,1 mg/ml,

all samples were placed in sterilized 6 well plate (Orange Scientific) in triplicate, in the orbital shaker at 110 rpm in the dark at 24 ºC. After 1.30 hour and 3 hours a drop (about 20 µL) was taken from each assay and placed in a microscope slide, covered with a cover slip and observed in the inverted microscope in bright field.

Stock solutions:

- ✓ 20 mg DAB in 2mL dimethyl sulfoxide (final concentration 12 mM) vortexed, centrifuged and sterilized with a 0.2 µm filter (Orange Scientific) kept in dark at 4ºC.
- ✓ 102 µL of H_2O_2 (AnalaR BDH) in 2 ml of distilled water (final concentration 0,5 M) and sterilized with a 0.2 µm filter (Orange Scientific) kept in dark at 4ºC.

3.3.4.2. Nitroblue tetrazolium (NBT)

The detection of superoxide anion (O_2^- •) was carried out as described by Fryer *et al.* (2002) with slight modifications.

(1) A 250 ml flask with 120 mL of a seven day old cell suspension culture of *M. sativa* was randomly taken to establish the following experimental setup:

- 2 mL of suspension culture,

- 2 mL of suspension culture plus 10 µL NBT to final concentration of 60 nM,

-2 mL of suspension culture treated 45 ºC for 20 minutes plus 10 µL NBT to final concentration of 0.06mM,

- 2 mL of suspension culture plus 32.6 µL QD's to a final concentration of 40nM plus 10 µL NBT to final concentration of 60 nM,

all samples were placed in sterilized 6 well plate (Orange Scientific) in triplicate, in the orbital shaker at 110 rpm in the dark at 24 ºC. After 4 hours a drop (about 20 µL) was taken from each assay and placed in a microscope slide, covered with a cover slip and observed in the inverted microscope in bright field.

Stock solutions:

- ✓ 20 mg NBT in 2 mL distilled water (final concentration 12 mM) vortexed and sterilized with a 0.2 µm filter (Orange Scientific) kept in dark 4ºC.

(2) A 250 ml flask with 120 mL of a eight day old cell suspension culture was randomly taken from the stock, 4 mL and 20 mL aliquots were inoculated in a 100 mL and 250 mL Erlenmeyer flasks containing 20 mL and 100 mL (control) of fresh medium, respectively. At day 3 of culture [40nM] of QD60_MPA was added in the Erlenmeyer flask with 24 mL of cell suspension culture. Then at day 5 and 6 of culture the same set up applied above was performed:

- 2 mL of suspension culture of the control,

- 2 mL of suspension culture of the control plus 10 µL NBT to final concentration of 60 nM,

-2 mL of suspension culture of the control treated 45 ºC for 20 minutes plus 10 µL NBT to final concentration of 60 nM,

- 2 mL of suspension culture with the QD's plus 10 µL NBT to final concentration of 60 nM,

all samples were placed in sterilized 6 well plate (Orange Scientific) in triplicate, in the orbital shaker at 110 rpm in the dark at 24 ºC. After 4 hours a drop (about 20 µL) was taken from each assay and placed in a microscope slide, covered with a cover slip and observed in the inverted microscope in bright field.

3.3.4.3. 2',7'-Dichlorodihydrofluorescein diacetate (H_2DCFDA)

H_2DCFDA was used to determine cellular oxidative stress as described by Ortega-Villasante *et al*. (2005), with minor modifications.

(1) A 250 ml flask with 120 mL of a seven day old cell suspension culture of *M. sativa* was randomly taken to establish the following experimental setup:

- 2 mL of suspension culture,

- 2 mL of suspension culture plus 1 µL H_2DCFDA to final concentration of 5 µM,

-2 mL of suspension culture treated 45 ºC for 20 minutes plus 1 µL H_2DCFDA to final concentration of 5 µM,

- two ml of suspension culture plus 32.6 µL QD's to a final concentration 40nM plus 1 µL H_2DCFDA to final concentration of 5 µM,

all samples were placed in sterilized 6 well plate (Orange Scientific) in triplicate, in the orbital shaker at 110 rpm in the dark at 24 ºC. 1.30 hour after, a drop (about 20 µL) was taken from each assay and placed in a microscope slide, covered with a cover slip and observed in the inverted microscope.

Stock solutions:

- ✓ 9.7 mg H_2DCFDA in 2mL dimethyl sulfoxide (final concentration 10 mM) vortexed and sterilized with a 0.2 µm filter (Orange Scientific) kept in dark -20 ºC.

(2) A 250 ml flask with 120 Ml of eight days old cell suspension culture was randomly taken from the stock, 4 mL and 20 mL aliquots were inoculated in a 100 ml and 250 mL Erlenmeyer flasks containing 20 mL and 100 mL (control) of fresh medium, respectively. At day 3 of culture [40nM] of QD60_MPA was added in the Erlenmeyer flask with 24 mL of suspension culture. Then, at day 5 and 6 of culture the same experimental set up described above was applied:

- 2 mL of suspension culture of the control,

- 2 mL of suspension culture of the control plus 1 µL H_2DCFDA to final concentration of 5 µM,

-2 mL of suspension culture of the control treated 45 ºC for 20 minutes plus 1 µL H_2DCFDA to final concentration of 5 µM,

- 2 mL of suspension culture with QD's plus 1 µL H_2DCFDA to final concentration of 5 µM,

all samples were placed in sterilized 6 well plate (Orange Scientific) in triplicate, in the orbital shaker at 110 rpm in the dark at 24 ºC. 10 minutes and one hour after, a drop (about 20 µL) was taken from each assay and placed in a microscope slide, covered with a cover slip and observed in the inverted microscope.

3.3.5. Quantum dots up-take by cells

The QD50_MPA up-take by cells was monitored using both suspension cultures: *M. truncatula* and *M. sativa*. In the case of QD68_MPA only *M. sativa* cell suspension cultures were used.

3.3.5.1. QD50_MPA

A 500 mL Erlenmeyer flask with 200 mL of a 7 days old *M. truncatula* cell suspension culture was randomly taken from the stock and 10 mL were pippeted into a 50 mL Erlenmeyer flask and 160 nM of QD50_MPA was added. After three days samples were visualized in the confocal microscope referred in point 2.2 of the Materials .

One Erlenmeyer flask with 120 mL of a 6 days old *M. sativa* cell suspension culture was randomly taken from the stock and 10 mL were pippeted into a 50 mL Erlenmeyer flask and 160 nM of QD50_MPA was added. After three days samples were visualized in the confocal microscope.

3.3.5.2. QD68_MPA

A 250 mL Erlenmeyer flask with 120 mL of *M. sativa* suspension culture was randomly taken from the stock and 2 mL aliquots were inoculated in two 50 mL Erlenmeyer flaks containing 10 mL of fresh MS medium. After 4 days of culture [40 nM] of QD568_MPA was added. At day 7 samples were visualized in a confocal microscope.

A specific marker of cell wall was selected, Diphenyl Brilliant Flavine 7GFF (Direct Yellow 96), to visualize the internalization of the QD's. A 0,15 % (v/v) stock solution of Direct Yellow 96 in distilled water was prepared as described by Hoch *et al* (2005), and applied as 0,4 (v/v) in suspension culture as follows: 1 µL of stock solution was added to 250 µL of suspension culture into a eppendorf, and after 5-10 minutes a sample was visualized in the confocal microscope.

4. Results and Discussion

4.1. Obtaining *M. sativa* suspension culture

After transfer to M&S liquid medium, *callus* started to dissociate into small cell clumps and single cells. Within 20 days of culture, the cell suspension cultures obtained from petioles callus consisted of single cells and small aggregates of 2-10 cells (Figure 4-1). Typically, two months are needed before cell suspension cultures become stable. After that time, cell suspension culture had a heterogeneous cell population with respect to cellular morphology, with elongated and spherical cells ranging between 40-100 nm in size, but was essentially composed of individualized cells as the Figure 4-3 a) shows. Because it was the more friable line, it was selected to perform the assays.

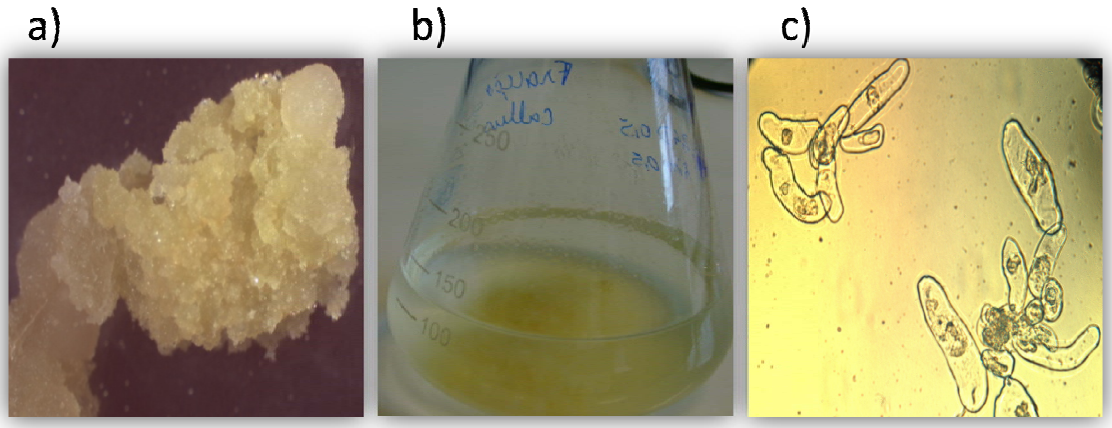

Figure 4-1 Different stages of development of *M.sativa* cell suspension culture from callus derived from petioles, induced in 0.5 mg/L 2,4-D and kin. a) friable callus from petiole in M&S solid medium. b) cell suspension culture with 20 days. c) cell suspension culture observation in microscope in bright field, magnification 200x.

Initially, the cell suspension culture obtained from callus derived roots was uniform and with individual cells (Figure 4-2), however, and contrary to the cell suspension culture of petioles, after two months the suspension culture was essentially composed of cell clusters (Figure 4-3 b)).

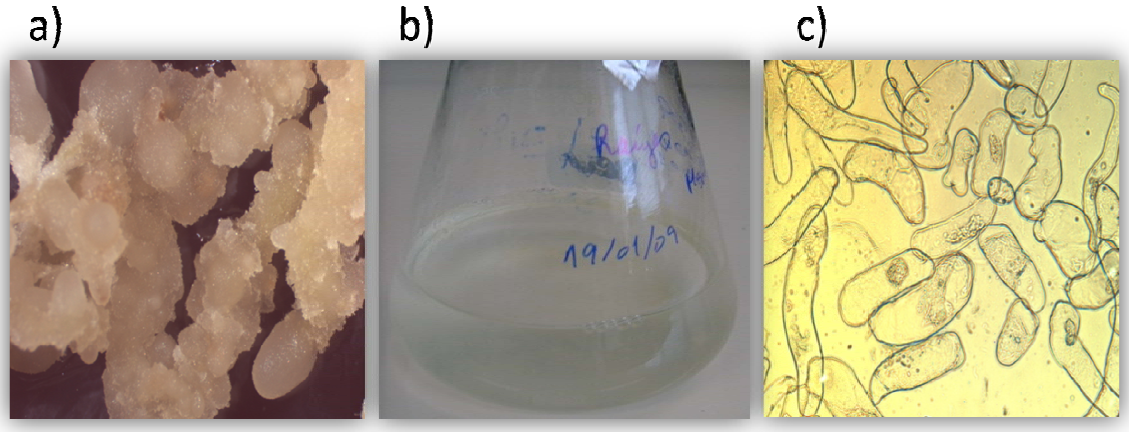

Figure 4-2 Different stages of development of *M.sativa* cell suspension culture from callus derived from roots, induced in 0.1 mg/L 2,4-D and kin. a) friable callus from root in M&S solid medium. b) suspension culture with 20 days. c) suspension culture observation in microscope in bright field, magnification 200x.

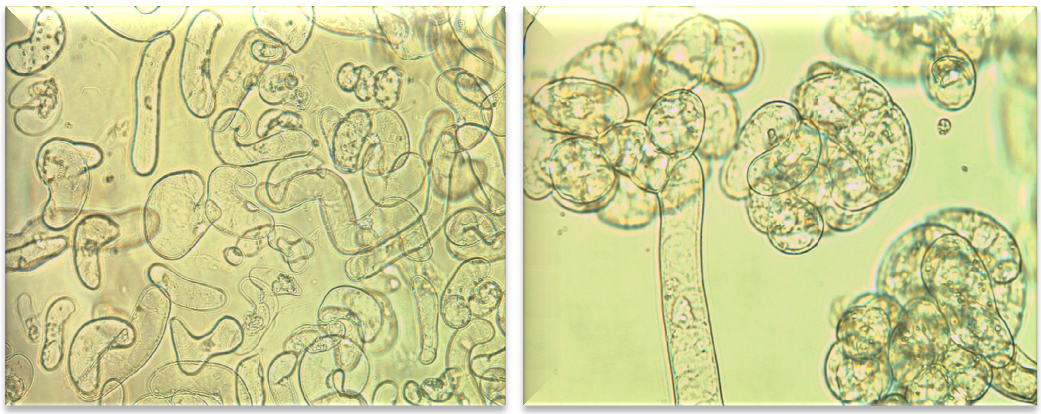

Figure 4-3 Cell suspension culture of *M.sativa* from petioles (left) and from root (right) *calli* after two months, in bright field. Magnification 200x.

The success on the establishment of a cell suspension culture depends, in a great extent, on the availability of "friable" callus tissue (i.e., a tissue that, when stirred in liquid medium, rapidly disaggregate into single cells and small clusters) (Loyola-Vargas and Vázquez-Flota, 2006), but also on the concentration of growth regulators used, as well as the technique used during the sub-culturing process.

4.2. Growth parameters determination

4.2.1. *M. truncatula* line M910-a

The determination of the growth curve of *M. truncatula* by the dry weight technique presented several drawbacks: requires large volumes of sample to be filtrated, which means to increase the final volumes of the cultures, and therefore large quantities of QD's; also because this culture is very heterogeneous and makes the sampling quite difficult, particularly in pippeting; despite the stabilization of the filters in dessicator, the weighing required about 20 minutes to stabilize.

To obtain the growth curve only two samples were considered, since standard deviations were significant (relative standard deviation ≥10), perhaps due to the reasons described ago. The growth curve obtained is quite atypical possibly because it is an embryogenic culture. However it can be concluded from Figure 4-4 that until day 8 the culture slowly grew up, and between day 9/10 the growth is more pronounced, where the biomass production almost doubled.

The growth kinetic parameters were not calculated since the exponential phase only presents two points.

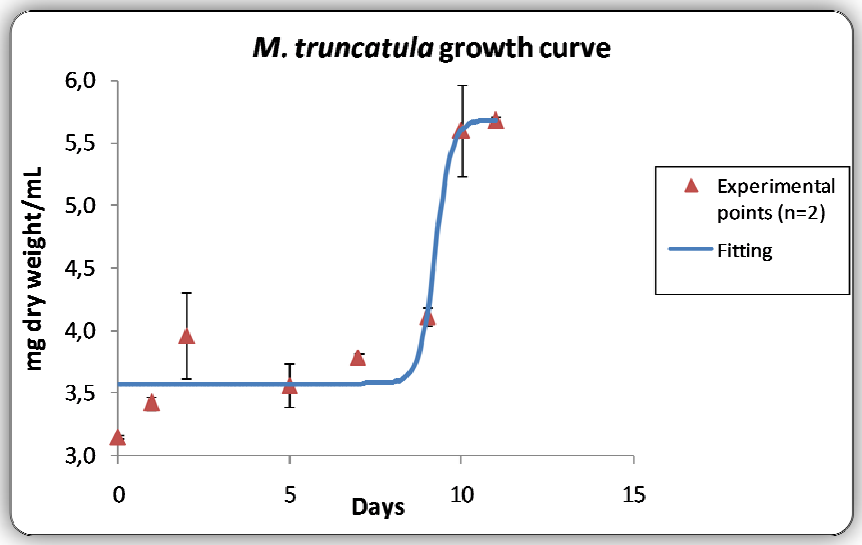

Figure 4-4 *M. truncatula* growth curve. Triangles represent the acquired experimental points and the line represents the fitting obtained by a curve fitting software: TableCurve 2D. Bars represent the standard deviation.

4.2.2. *M.sativa* line M699

The growth curve obtained presents a typical profile, with an initial lag phase during the first two days after which it enters in the exponential phase until day five, and then follows a stationary phase.

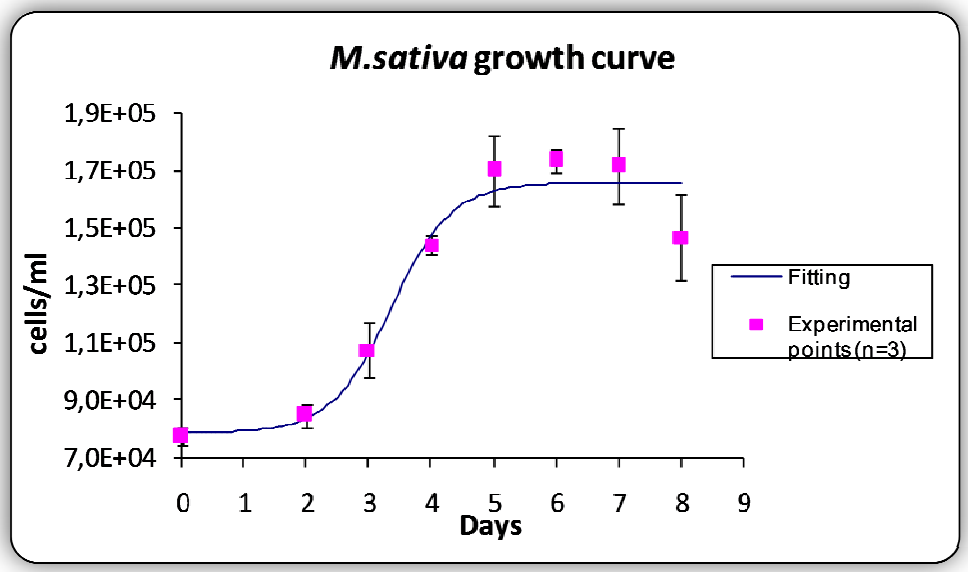

Figure 4-5 *M.sativa* growth curve. The squares represents the acquired experimental points and the line represents the fitting obtained by a curve fitting software (TableCurve 2D). Bars represent the standard deviation.

The specific growth rate (μ) is defined as the rate of increase of biomass of a cell population per unit of biomass concentration in time (Loyola-Vargas and Vázquez-Flota, 2006), and this cell suspension culture presents a specific growth rate of 5,7 h^{-1}(Table 5).

Duplication time (Td) is the time required for the concentration of biomass of a population of cells to double, and to this system it takes 2,9 days, as we can see in Table 5.

Table 5: Specific growth rate and duplication time for the *M.sativa* cell suspension culture

μ	**0,238 ($days^{-1}$)**	**5,7 ($hours^{-1}$)**
Td	**2,9 (days)**	**69,6 (hours)**

4.3. Cytotoxicity assays

The concentration of QD's used in the toxicity studies were of: [160 nM] QD50_MPA and [40 nM] QD68_MPA. This values results from a literature search, where it was found that a wide-range has been applied from 2 nM to 2500 nM in toxicity studies (Hild *et al*, 2008), and the typical concentrations of most molecular-imaging experiments is around 5–20 nM.

4.3.1. M. truncatula

4.3.1.1. Cell differentiation (somatic embryogenesis)

Somatic embryogenesis is the direct way to regenerate plants from single somatic cells, and opens up the possibility of understanding the process of cell cycle reprogramming from somatic to embryogenic type, cloning and characterization of genes involved in wounding, hormone activation, cell division, differentiation and developmental processes (Mujib and Samaj, 2005). Therefore, to evaluate the toxicity of the QD's in cell differentiation the highly embryogenic line M910-a of *M. truncatula* was used.

Cell suspension cultures with three different treatments, one not "disturbed" since the sub-culturing process, other "disturbed" by addition of sterile MiliQ water and another one which [160 nM] of QD50_MPA were introduced at day 9 of culture. 24 hours latter (day 10) 1mL of each of the three cultures was platted in M&S free-regulator solid medium. After 8 days, embryos derived from the yellow proembryogenic masses of the suspension cultures could already been seen in the Petri dishes as Figure 4-6 shows.

The several stages of embryo development can be observed simultaneously in Figure 4-6. The initial globular stage showed in (1), then the heart (3) and torpedo (2) embryo stages, (4) indicates the later-torpedo/dicotyledonar stage.

There are no significant differences observed among the three treatments. It is possible to presume that the contact of the QD's, during 24 hours with the cells in suspension culture does not induce changes in embryo differentiation. In fact, the morphology of the embryos obtained from suspension culture with QD's and the time required to their development was similar to both controls.

One must stress the fact that the QD's used in this assay have a relative big size (≈30 nm), and also the fact that this suspension culture is mainly composed of large cell clumps, could reduce the availability and the contact of the cells with the QD's.

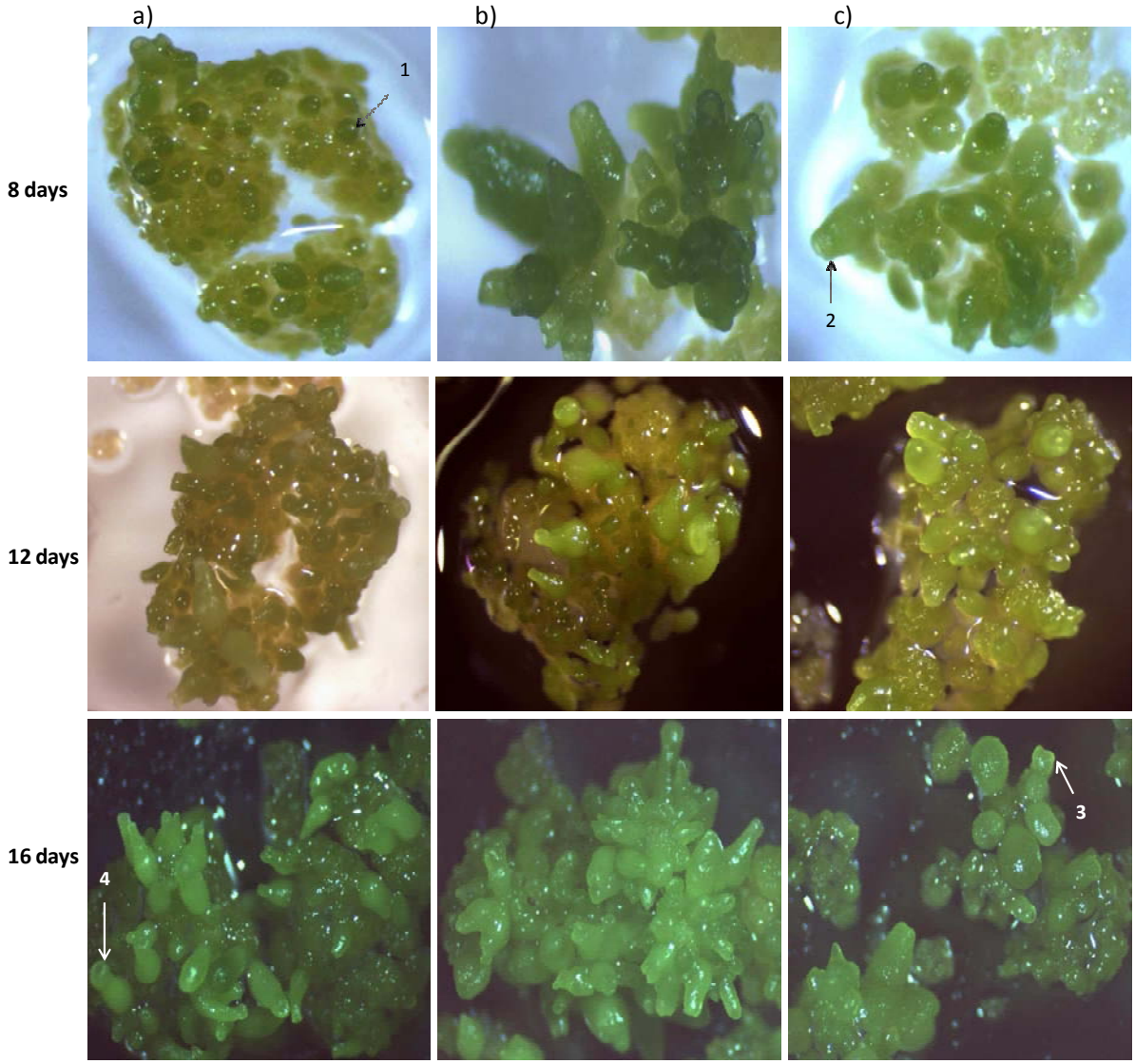

Figure 4-6 Somatic embryos obtained from plated suspension culture of *M. truncatula* in M&S solid medium, after 8, 12 and 16 days. a) Embryos from plated non disturbed suspension culture (control). b) Embryos from plated disturbed suspension culture (addition of MiliQ water). c) Embryos from plated suspension culture with Qd's. (1) globular embryo, (2) torpedo embryo, (3) heart stage embryo and (4) late-torpedo/dicotyledonar embryo. Photos acquired in the stereomicroscope.

4.3.2. M.sativa

In *M. sativa* cell suspension cultures four main cytotoxicity assays were performed, including the effect in cell cycle and cell viability, reactive oxygen species (ROS) production and cell–particle uptake.

4.3.2.1. Cell Cycle

To evaluate the effect of QD's in the growth cycle, exponentially growing cells (day 3 of culture) were exposed to [40 nM] of QD68_MPA. As we can see in Figure 4-7, from day 0 to day 3 when the QD's were added, both cultures grew in parallel. Then, at day 8 a significant difference can be observed, while control culture continued to grow and doubled the biomass, cultures with QD's slowed their growth and the final biomass production was almost the same as at day 3.

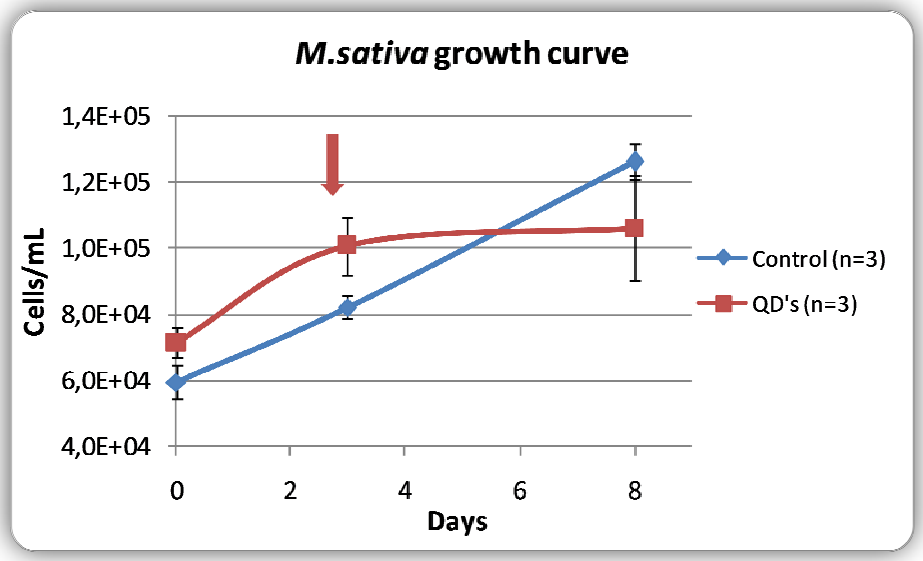

Figure 4-7 Growth curve of *M.sativa*. Blue line refers to control culture and red line to culture with the QD's added at day 3, represented by the arrow. The count at day 3 was done before the addition of the QD's.

This can be understood as the first impact of the QD's in the growth of the suspension cultures. At day 8 the cultures were sub-cultured and the respective new growth curves were followed (Figure 4-8).

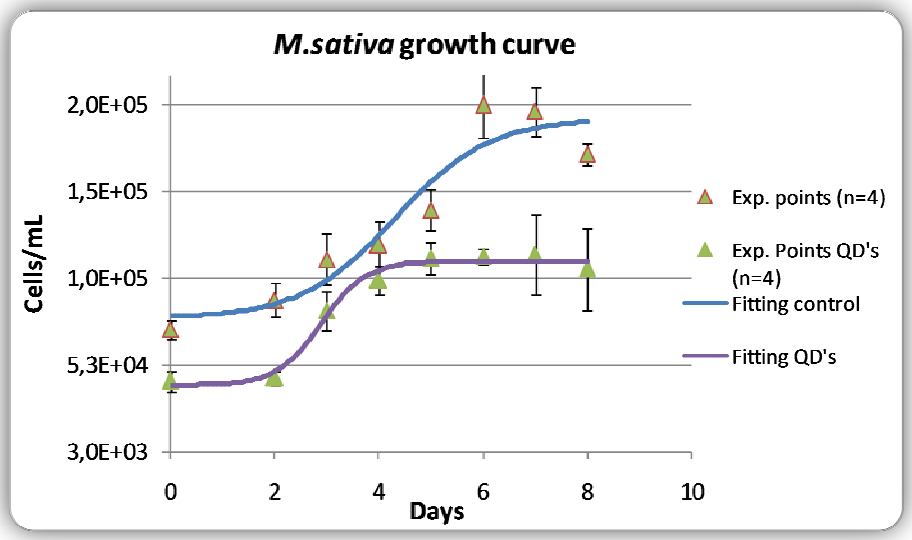

Figure 4-8 Growth curve of *M.sativa*. Blue line refers to control culture and violet line to culture with the QD's. The fitting was obtained by the software TableCurve 2D.

Control culture started with a larger quantity of biomass because it also presented a superior final biomass production in the previous culture. As expected, the growth curve obtained presents a lag phase until day 2 and is followed by an exponential phase that lasted four days before the cell numbers started to decrease.

The QD's culture, similarly to the control culture, underwent a lag phase until day 2, and then entered into the exponential phase that lasted three days, but after day five the culture enters into a stationary phase until the end of culture.

In terms of cells numbers, the control suspension cultures had an increased in $1{,}29*10^5$ cells/mL, while QD's suspension cultures had an increase of $7{,}3*10^4$ cells/mL, which is almost half of control cell number. Observing the growth kinetic parameters of the cultures in

Table 6 we can see that values of specific growth are very similar. Despite, in the case of QD's culture it presents a slightly lower time of duplication, which can be seen by the differences in the growth profile of both cultures, especially by the shorter exponential phase of the QD's culture.

Table 6: Growth kinetic parameters

	Control	QD's
μ (h^{-1})	3,4	3,7
td (h^{-1})	116,40	108

An important observation is the cell aggregation after the QD's addition, as well as QD's aggregation (Figure 4-9) was visible, which makes the cell counting technique quite difficult. Other reports also mention cell aggregation in the presence of nanoparticles (CdTe and TiO_2) (Wang *et al*, 2008).

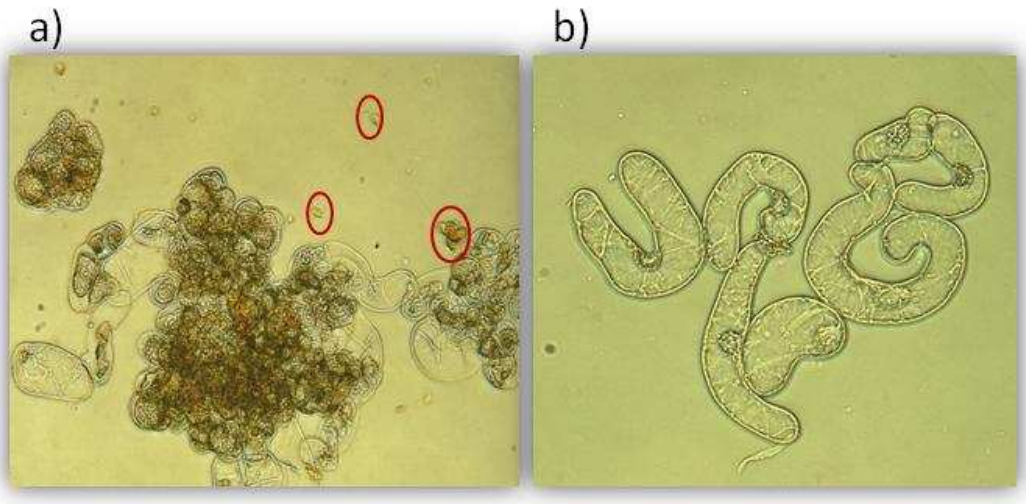

Figure 4-9 *M.sativa* cells a) in the presence of QD's and b) absence of QD's (control) at day 5 of culture. Bright field observation and magnification 200x. Red circles are QD's aggregates.

Koeneman *et al* (2009) demonstrated that non- aggregated QD's were toxic to a human cell line but not toxic when QD's were aggregated in cell culture media, suggesting that the aggregation of QD's may reduce their toxicity.

Surface coating of the QD's has been established as a critical factor for determining the extent and time scale of cytotoxicity. MPA is known to be one of the smallest ligands among deprotonated thiols (thiolates) that are most often used to stabilize QDs in solution. Because of that, the surface of MPA-QD might be easily photodegraded and subject to the aggregation and precipitation processes. This phenomenon would render MPA_QD less available (Lee *et al*, 2009).

However, if this aggregation and precipitation process derives from the culture conditions, namely pH of medium, weathering of QD's may occur when exposed to moderate acidic or alkaline environment, as already referred in point 1.2.4.

After the first experiments, when aggregation was noticed, pH of the medium in suspension cultures, with and without QD's, was followed. The pH of medium culture was adjusted to 5,75-5,80 before autoclaving, after two days in suspension culture, the pH of the medium was measured and was around pH= 4,3. This is an acidic medium for QD's, since the samples came in basified water at pH=12. To solve this problem, an attempt to rise the pH values of the culture was made, so a suspension culture was sub-cultured with medium at pH= 6,0, after two days of culture the medium registered a pH= 4,42 meaning that pH is associated with the characteristics of this type of suspension culture and the specific cell metabolism.

Although it is not known, in this case, if the precipitation is caused by the low pH values of the medium, it is important to stress that despite the aggregation of the QD's could minimize the toxicity, the weathering of QD's and subsequent release of their heavy metal toxic constituents is also a possibility.

Assessment of nanoparticle aggregation and stability under exposure conditions is necessary to correctly interpret biological effects. Nanoparticle aggregation influences uptake by cells, and variables such as the surface ligands and the solution composition influence nanoparticle suspension stability (King-Heiden *et al*, 2009).

QD68_MPA were given as a stable solution (-45,6 mV) in water, but introduction in biological medium may have decreased zeta potential (ζ)and therefore particles tend to aggregate. Therefore, zeta potential of QD's in M&S medium at pH=4.4 was measured using Nano series dynamic light scatterer, and ζ=-12,5 mV which according to literature, is no longer considered a stable solution.

During this experiment it was also verified that cell morphology changed in contact with QD's. Cells in the control suspension culture were elongated with perfectly distinct cell walls and showing proeminent nucleus and cytoplasmic streams. When exposed to UV light they reveal a blue autofluorescence, which could be associated to well viable cells (Figure 4-10).

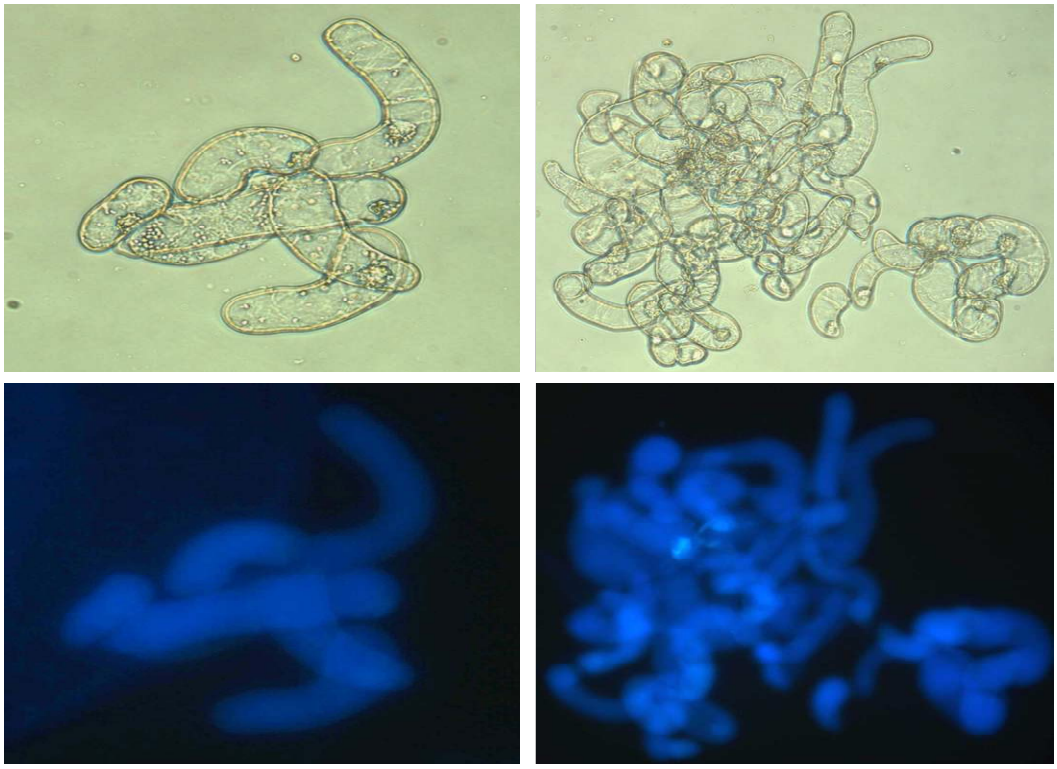

Figure 4-10 Cells of *M.sativa* suspension culture (control) in day 6 in bright field and in UV light. Magnification 200x.

Cells in contact with QD's were more round shaped, somewhat plasmolysed and with signs of cytoplasmic oxidation (Figure 4-11 a)). Plasmolysis occurs when a plant cell's membrane shrinks away from its cell wall, due to the loss of water through osmosis. Even the cells that weren't plasmolysed had a different morphology (Figure 4-11 b)), however the same blue autofluorescense is shown. Figure 4-11 c) shows that cells more isolated do not present the blue autofluorescence, since they are more exposed to QD's as it can be seen by the adsorbed QD's at the surface. In this image it is also visible the cell aggregates essentially composed of small round shaped cells.

To determine if these cells are in fact viable, another assay to determine cell viability in the presence of QD's was carried out.

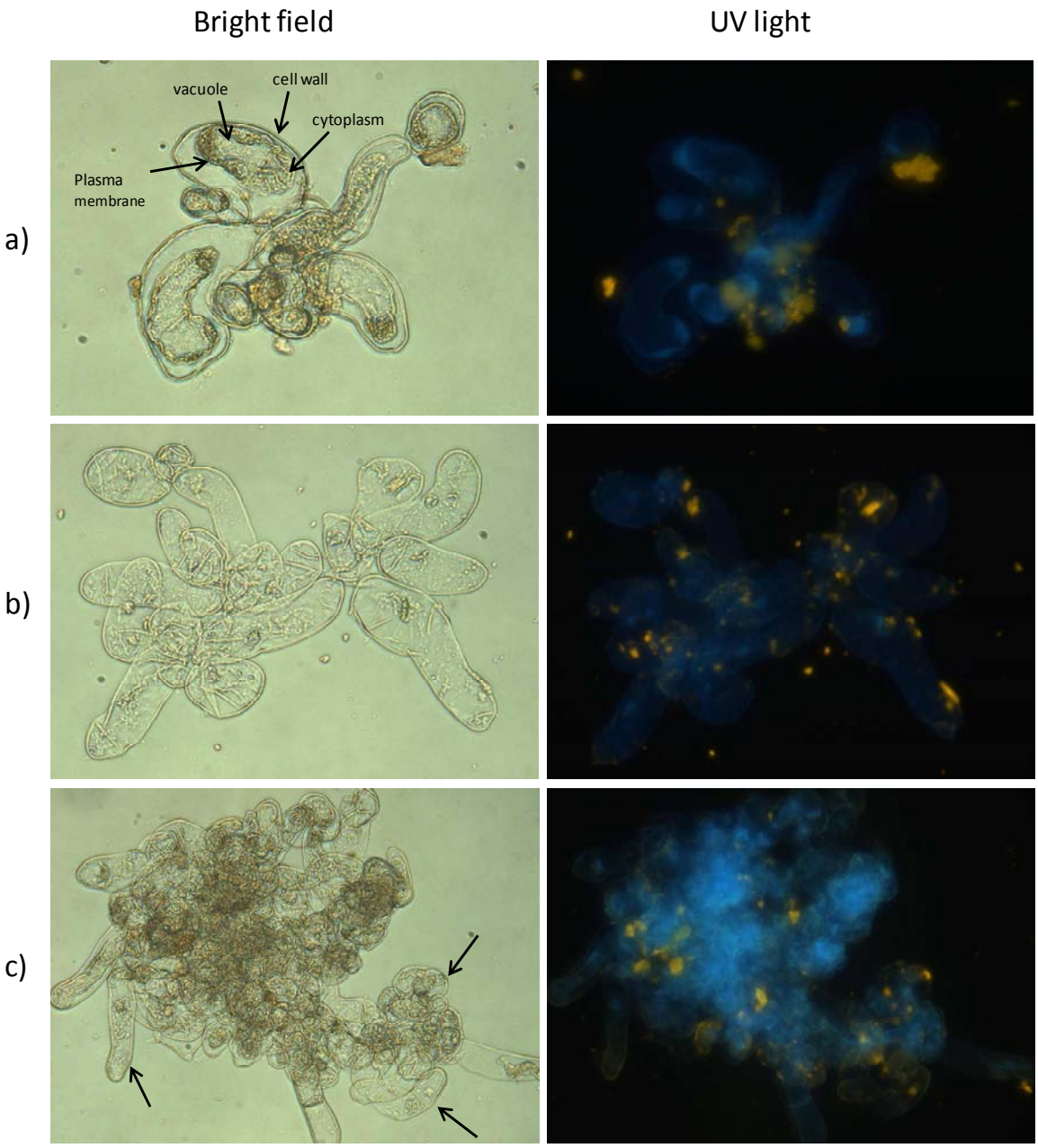

Figure 4-11 Cells of *M.sativa* suspension culture with QD's in day 6. in bright field and UV light. a) cells presenting plasmolysis and signs of cytoplasmic oxidation. b) cells showing altered morphology. c) cells aggregate with arrows pointing to cells that don't present the blue fluorescence. Magnification 200x.

4.3.2.2. Cell viability

To understand the previous results, another set of experiments aiming to evaluate cell viability was performed. At day 3 of culture, [40 nM] of QD68_MPA were introduced and after staining with FDA, cells were counted. Once more, the cell count at day 3 was done before the addition of the QD's.

Figure 4-12 shows the results obtained. As it can be seen, at day 3 (before the addition of QD's) both cultures present similar viabilities (≈85 %); then at day 4/5 cell viability of QD's cell suspension culture decreases to ≈ 66%, but then at day 6 the viability decreases to 29%. Cell viability of control suspension cultures maintained practically the same until day 6.

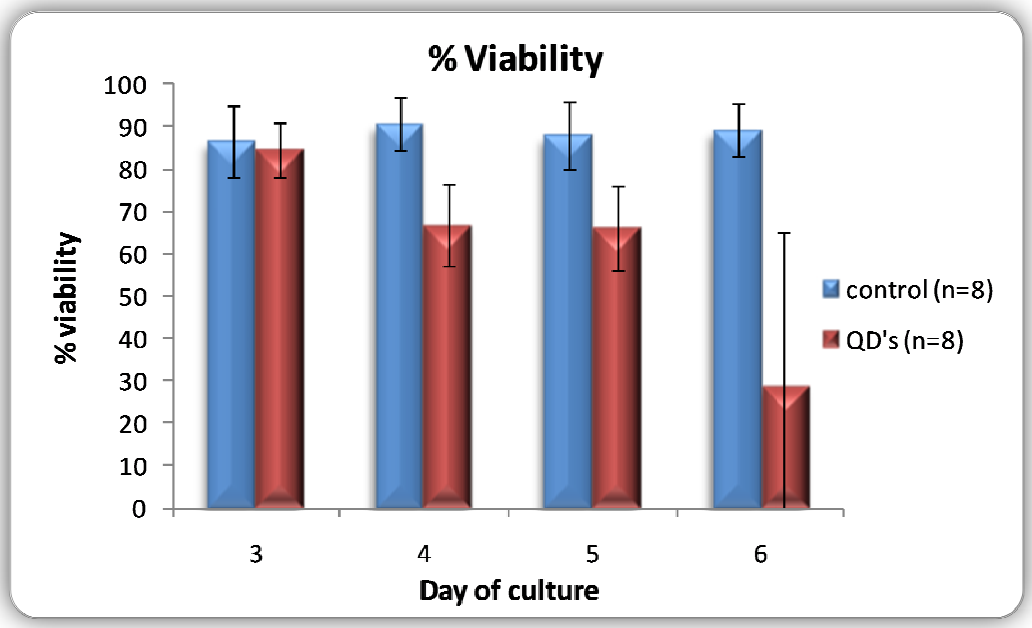

Figure 4-12 Viability of cell cultures with (red) and without QD's (blue) determined with FDA method. Bars represent standard deviation.

In Figure 4-13 it is shown cells of suspension cultures with and without QD's stained with FDA. As it can be seen control cells present the green fluorescence from fluorescein confirming their viability. On the other hand, single cells or small aggregates (3-8 cells) of suspension cultures exposed to QD's were not viable. However, and as already showed in the previous experiment, the presence of QD's promote the aggregation of cells and it was observed that the large clusters with very small cells presented the green fluorescence (bottom image).

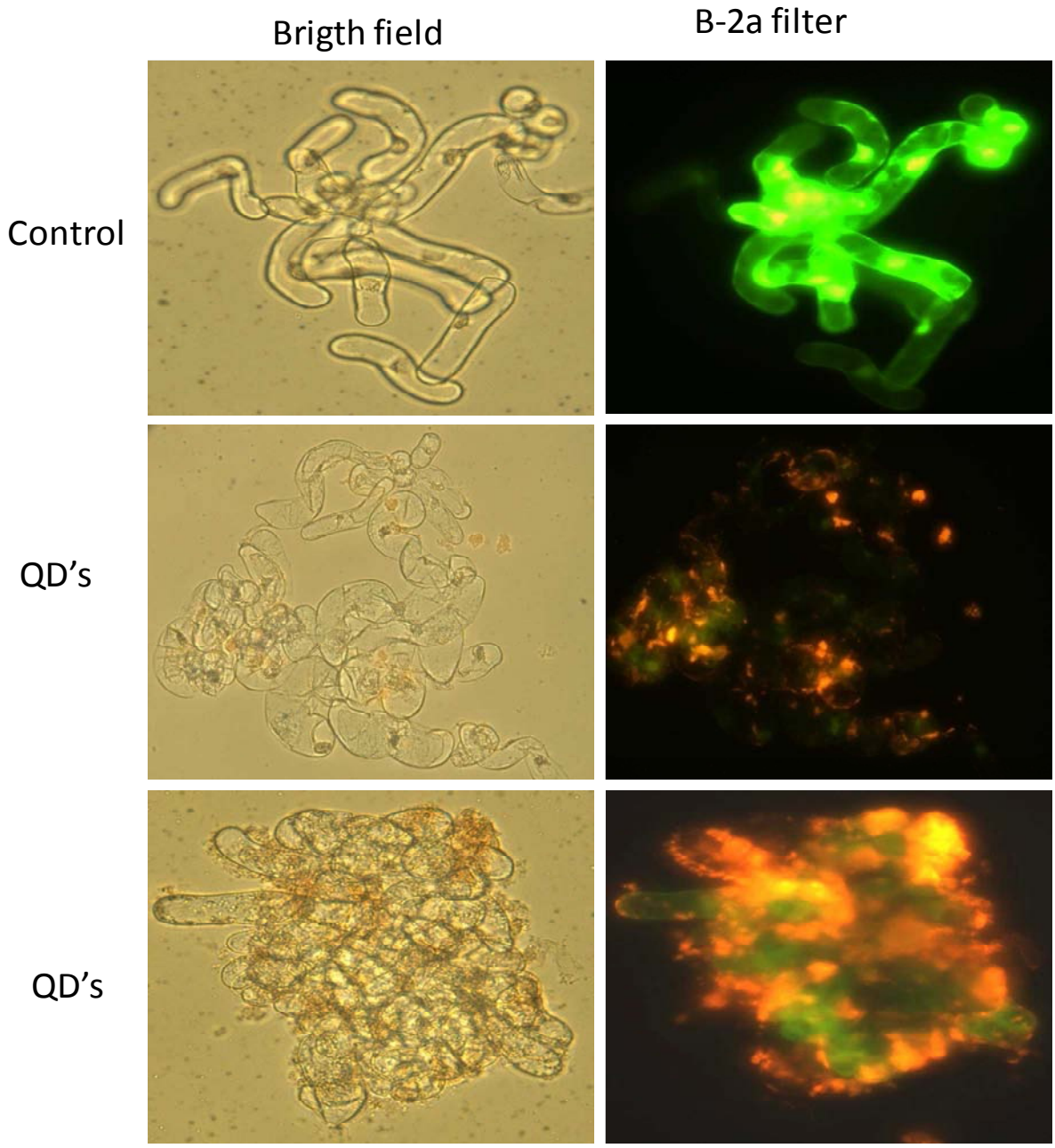

Figure 4-13 Cell cultures with (40 nM) and without QD's at day 6, stained with FDA. Cells that present green fluorescence are viable. Images were acquired with the same settings and exposure times, in bright field and blue filter (B-2a).

Counts were performed only until day 6 because the great number of cells in aggregates combined with the fact that these cells were spherical and very small, prevented an accurate cell counting.

Nevertheless, it is observed from Figure 4-13 that there is a difference in fluorescence intensity between cells exposed to QD's and the control ones. In fact, with the same exposure time, the fluorescence intensity in cells treated with QD's is quite lower comparing to the control cells. This fact has two possible explanations: first the Qd's fluorescence is so strong that "blocks" or makes it difficult to see the green fluorescence of the FDA, second the esterase activity of these cells may be in a "low activity" state, converting fluorescein diacetate to fluorescein but at a low rate.

In fact, several studies report that the metabolism of FDA to fluorescein is a reliably method to measure the esterase activity, and that also reflects the short-term metabolic response of organisms when exposed to toxicants, furthermore, the degree of fluorescence depends on the physical and metabolical state of the cell (Gilbert *et al*, 1992; Regel *et al*, 2002).

In resume, it was found that isolated or small cell aggregates presented themselves frequently plasmolysed and were not viable at day 6 of culture. However, the majority of cells were gathered in large clusters, and these cells revealed viable despite the significant difference in fluorescence intensity.

4.3.2.3. Oxidative stress

QDs may raise the ROS level through a couple of pathways: (i) upon excitation, QDs can form electron-hole pairs to transfer electron to oxygen, (ii) intracellular antioxidant system may be directly damaged via interaction with QDs, and/or (iii) Cd2+ released from QDs causes intracellular ROS elevation (Li *et al*, 2009).

As already referred, to evaluate oxidative stress three different probes were used: DAB, NBT and H_2DCFDA.

4.3.2.3.1. 3,3'- Diaminobezidine (DAB)

Diaminobenzidine (DAB) infiltration of tissues is a common technique used to localize H_2O_2 in plants. DAB reacts rapidly with H_2O_2 in the presence of peroxidase, forming a brown polymerization product (Thordal-Christensen *et al*, 1997).

The assays were carried out in 6 well plates because it makes possible the volume reduction of cell suspension cultures and therefore, QD's volume required. Also it allows performing the assays in a standard and randomized approach.

Figure 4-14 show the results obtained in cell suspension cultures submitted to different treatments in order to compare them with the results of suspension cultures treated with [40 nM] of QD's. It can be concluded that cells treated with DAB, in the absence of an oxidative stress, didn't present the brown coloration typical of the presence of H_2O_2. Cells treated for 10 min at 35 ºC, and subsequent addition of DAB, present somewhere a light brown color which means that this temperature/time heat treatment it not enough to induce a visible oxidative stress. Cells previously treated with 10 mM of H_2O_2 and subsequent addition of DAB, confirms the peroxidase activity and that concentration of H_2O_2 is enough to produce a strong response as it can be seen by the brown precipitates around cells.

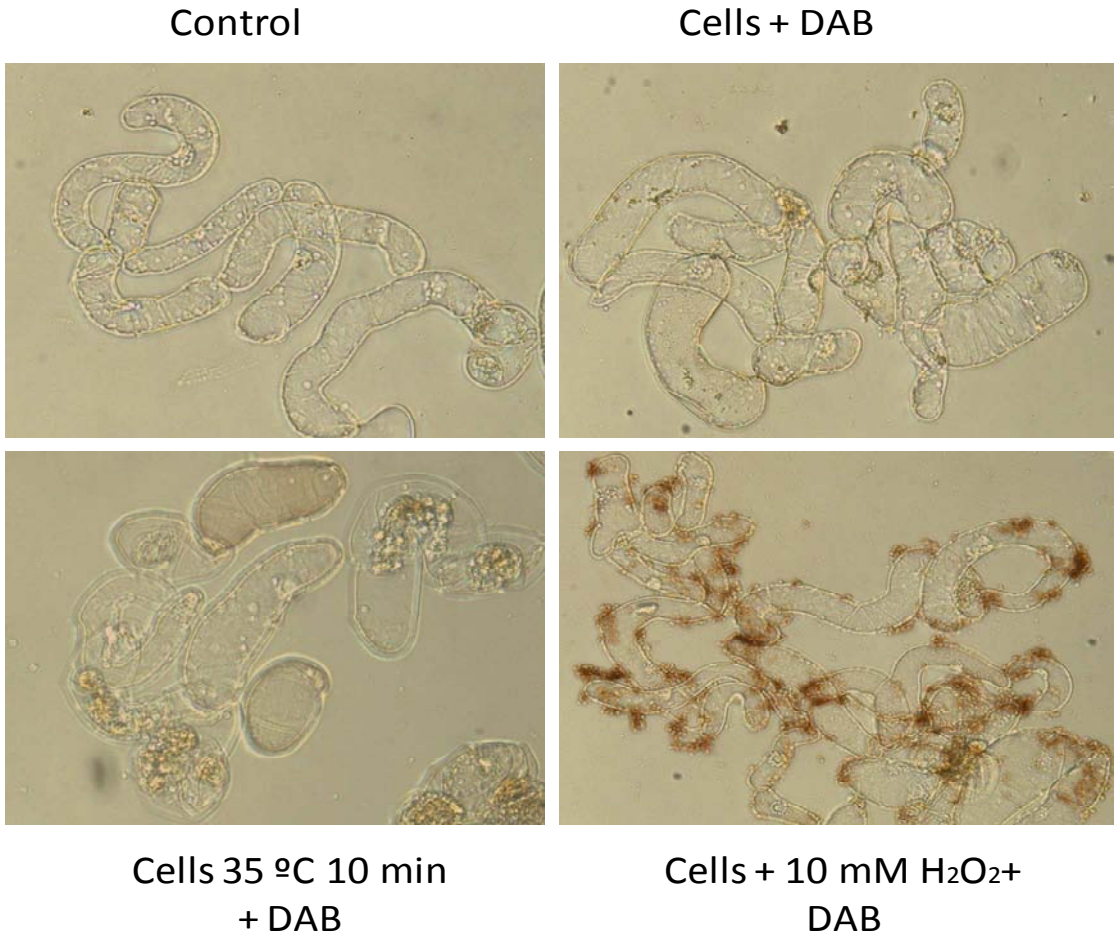

Figure 4-14 Different controls used in the experiment. (control) is the cell suspension culture without treatment. (Cells+DAB) is a cell suspension culture treated with DAB. (Cells 35 º C 10 min+ DAB) is a cell suspension culture heat-treated to induce the production of H_2O_2. (Cells + 10 mM H_2O_2+ DAB) is a suspension culture treated with H_2O_2 and DAB to visualize the peroxidase activity. All experiments were visualized 1.30 hour after the addition of DAB, in bright field.

The presence of QD's does not seem to induce H_2O_2 production as it can be seen in Figure 4-14 . Although the results pointed to the brownish coloration, in fact those orange/brownish precipitates around cells are QD's precipitates, as comproved by the picture in UV filter in comparison with the UV image of control cells with DAB, that don't present the red/orange color.

Comparing the results obtained for the cell suspension cultures with QD's with those obtained in cells+ 10 mM H_2O_2+ DAB, it can be assumed that the probable production of H_2O_2, induced by the addition of QD's to the cell suspension culture, is far less than 10 mM.

Due to the uncertainty of the results obtained with this assay, it was not repeated with exposure of cells to QD's for longer time.

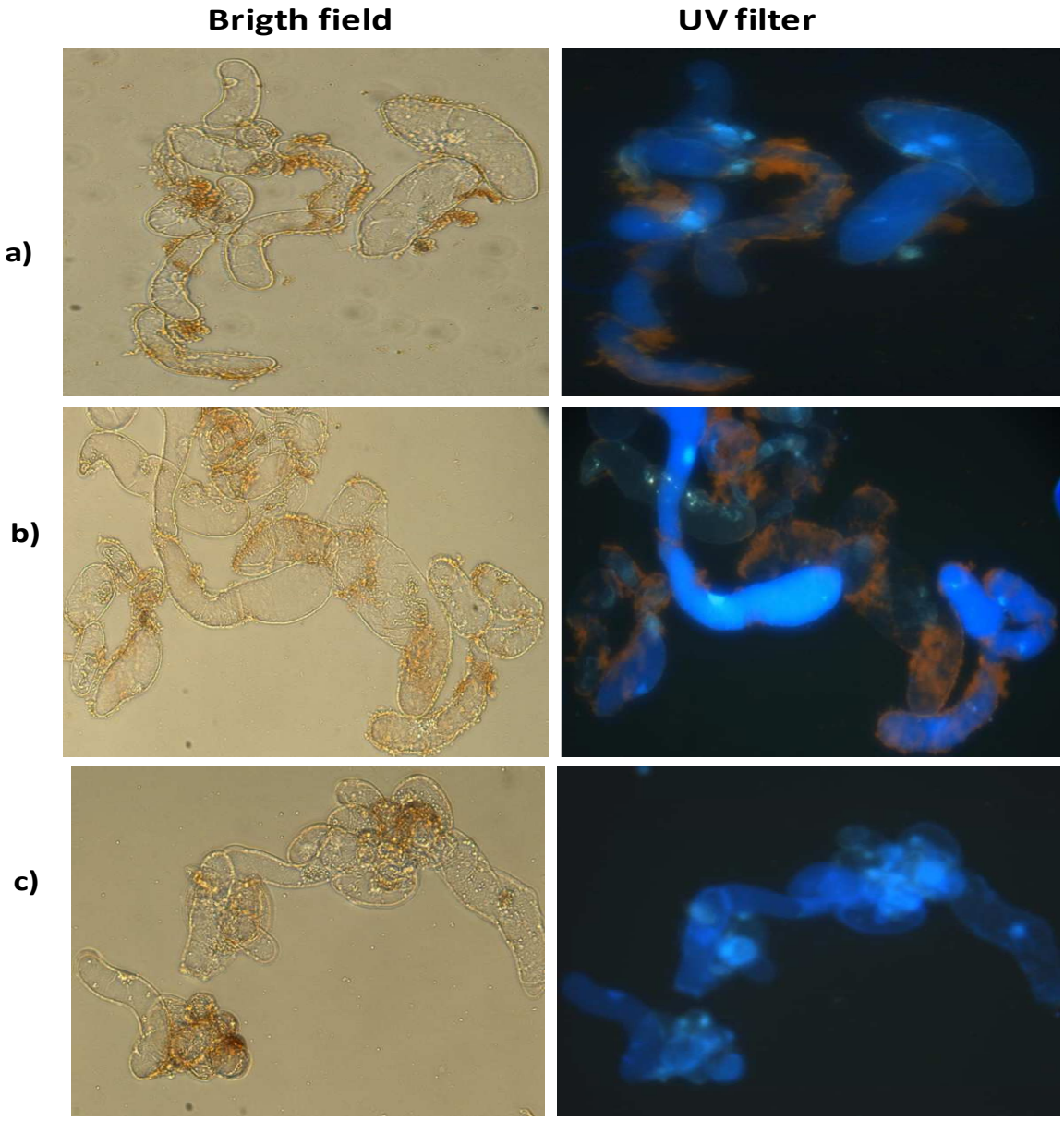

Figure 4-15 a) Cells of suspension cultures with [40 nM] of QD's 1.30 hour after addition of DAB. b)) Cells of suspension cultures with QD's 3 hours after addition of DAB. c) Cells of suspension cultures without QD's 3 hours after addition of DAB. Images were taken with the same settings and exposure time in bright field and UV filter.

4.3.2.3.2. Nitroblue Tetrazolium (NBT)

The NBT assay as described by Fryer *et al* (2002) was used to verify if O_2^- •is produced upon addition of QD's to the cell suspension culture of *M. sativa*. Nitro-substituted aromatics, such as nitroblue tetrazolium, can be reduced by O_2^- • to the monoformazan (NBT^+) (Tarpey and Fridovich, 2001; Armstrong and Whiteman, 2007), giving rise to dark spots of blue formazan (Romero-Puertas *et al*, 2004).

Cell suspension cultures heated at 45 ºC for 20 minutes exhibits dark blue formazan spots (Figure 4-16 b)). These deposits indicate that O_2^- • is produced by the cells in response to heat stress, since no spots are seen when controls are subjected to the same assay (Figure 4-16 a)). The presence of formazan deposits indicate that in those cells the rate of O_2^- • production has become significantly greater than the rate of detoxification (Fryer *et al*, 2002).

Studies that applied the NBT technique are almost focused in evaluating responses in plant tissues rather than in single cells. The few reports in cell suspension cultures that used this technique quantified the response spectrophotometrically, rather than study the precise location of the formazan deposits.

In cell suspension cultures treated with QD's no blue formazan spots could be detected as Figure 4-16 c) shows, and therefore it can be concluded that the presence/interaction of [40 nM]of QD's with cells does not induce the formation of O_2^- •, at least not with this time of exposure (4hours).

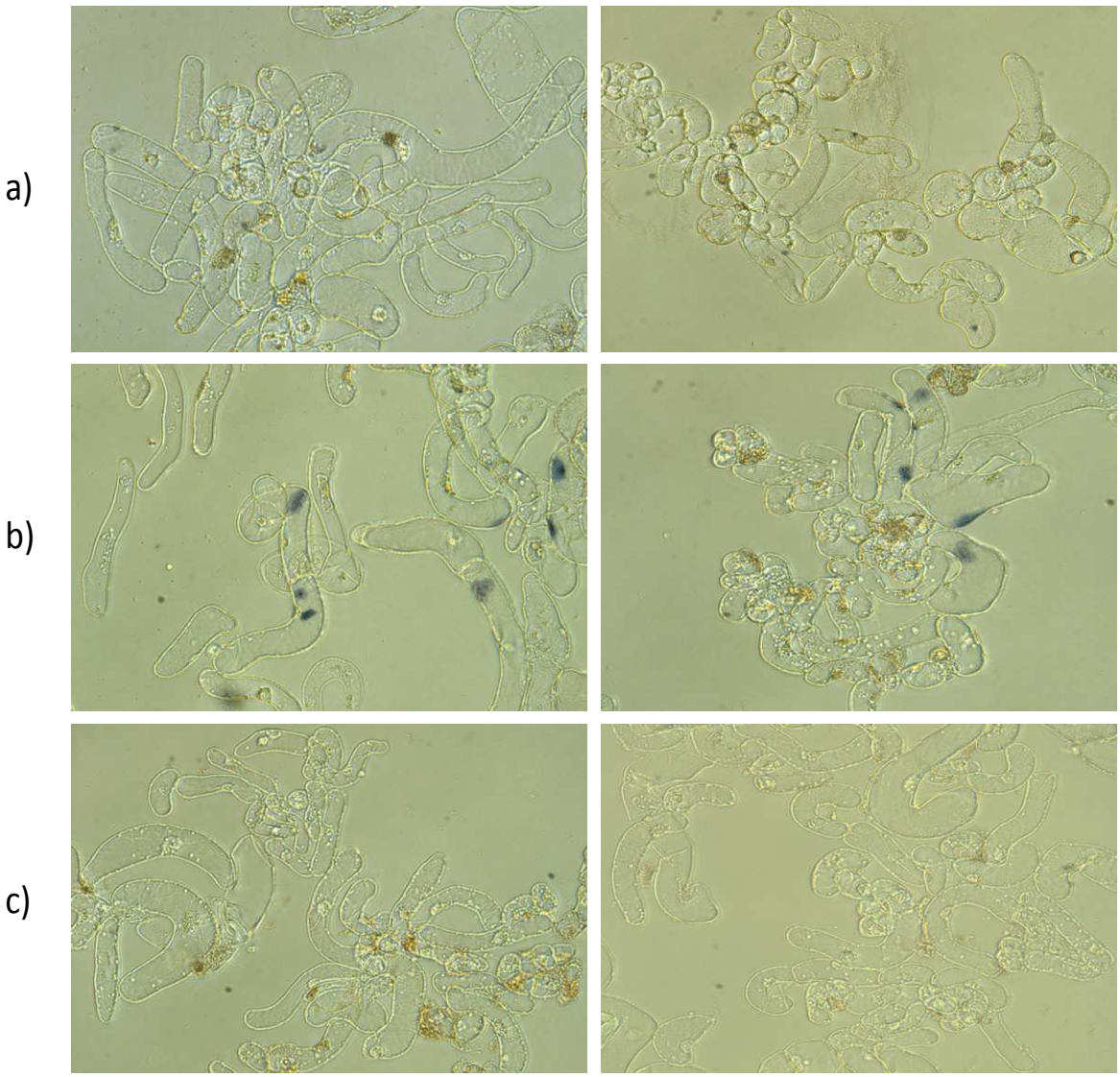

Figure 4-16 Images from cell suspension cultures with the following treatments: a) cell suspension culture without treatment (control); b) cell suspension culture treated with NBT; c) suspension culture heat-treated, to induce the production of $O^{-}_{2}\bullet$, plus NBT; d) cell suspension culture treated with QD's and NBT. All experiments were visualized 4 hours after the addition of NBT, in bright field with the same settings and exposure time. Magnification 200x.

To see if 4 hours of exposure of QD's to cells was not enough to induce the production of $O_2^{-}\bullet$, another assay was carried out, but this time QD's were added to cell suspension cultures at day 3 of culture, and after 48 h (day 5)and 72 h (day 6) the same set up was performed.

The addition of QD's to cell suspension cultures for 48 hours and 72 hours still does not induce a stress response in terms of O_2^- • production. The results obtained for QD's exposure for 48 hours and 72 hours are presented in Figure 4-17 and Figure 4-18, respectively. Once more, cell suspension cultures heat-treated presented the dark blue spots of formazan due to the O_2^- • production, but not the cell suspension cultures with QD's, which allows to conclude that there is no O_2^- • radical production.

Ipe *et al*. (2005) performed a study about the generation of free radicals by three types of QD's and they found that while CdS QDs apparently had sufficient redox power to generate both hydroxyl and superoxide radicals, CdSe QDs exclusively generated hydroxyl radicals. In contrast, the irradiation of CdSe/ZnS core/shell QDs did not produce free radicals under those conditions (with mercaptoacetic ligands and under Hg lamp photoirradiation).

Chloroplasts are a major site of ROS generation in plants due to the photosynthesis processes. Peroxisomes and glyoxysomes are other major sites of ROS generation during photorespiration and fatty acid oxidation, respectively (Gechev *et al*, 2006), however plant cell cultures used in this work are dark grown and therefore do not have chloroplasts. For this reason O_2^-•, that is mainly produced in the photosynthetic electron transfer chains, can be significantly reduced.

Mitochondrial respiration is another process leading to O_2^-• and H_2O_2 formation, although production is much lower compared to chloroplasts (Gechev *et al*, 2006).

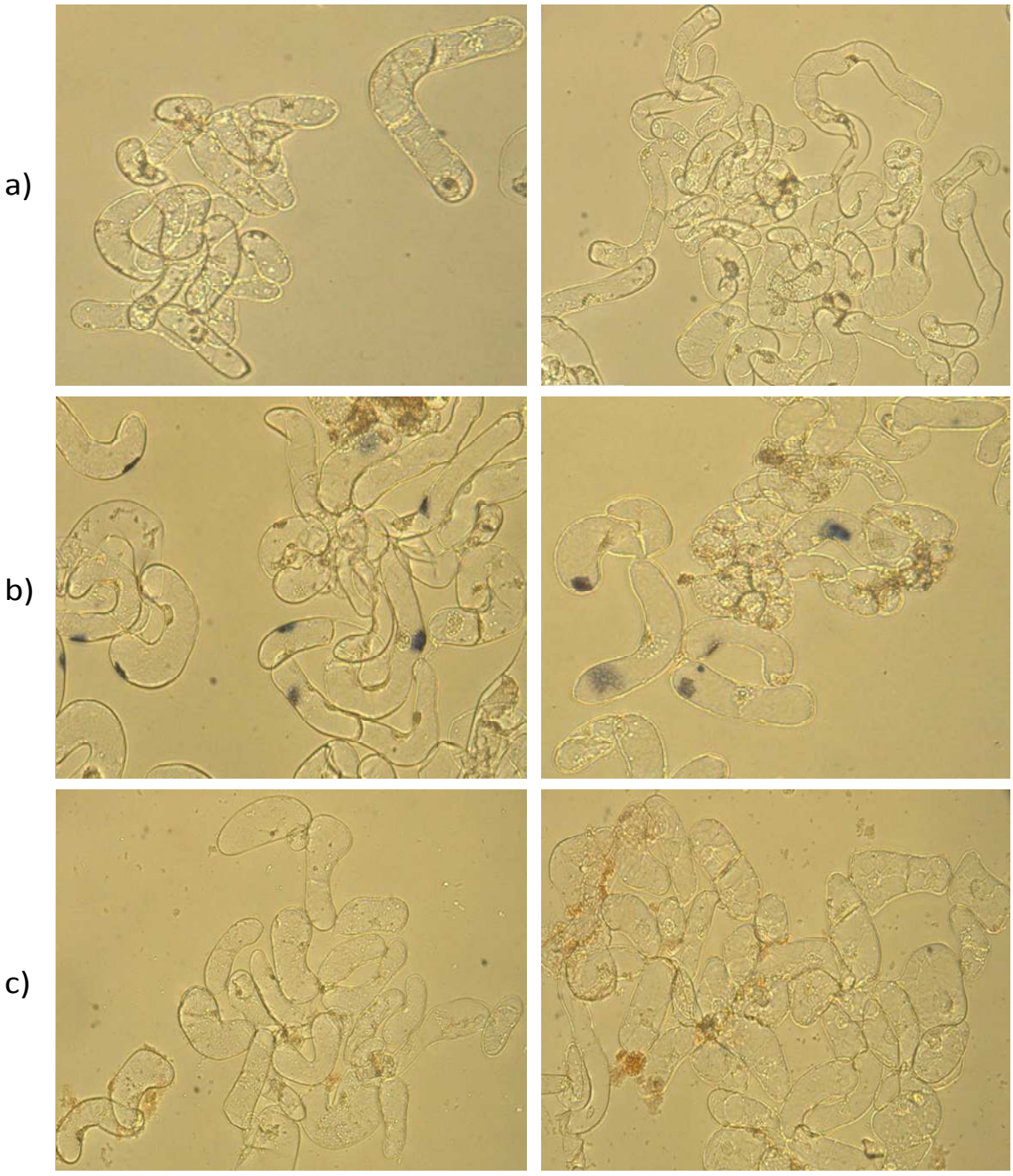

Figure 4-17 Block of two images from cell suspension with the following treatments: a) cell suspension culture treated with NBT; b) cell suspension culture heat-treated plus NBT; c) cell suspension culture treated with QD's for 48 h and NBT. All experiments were visualized 4 hours after the addition of NBT, in bright field with the same settings and exposure time. Magnification 200x.

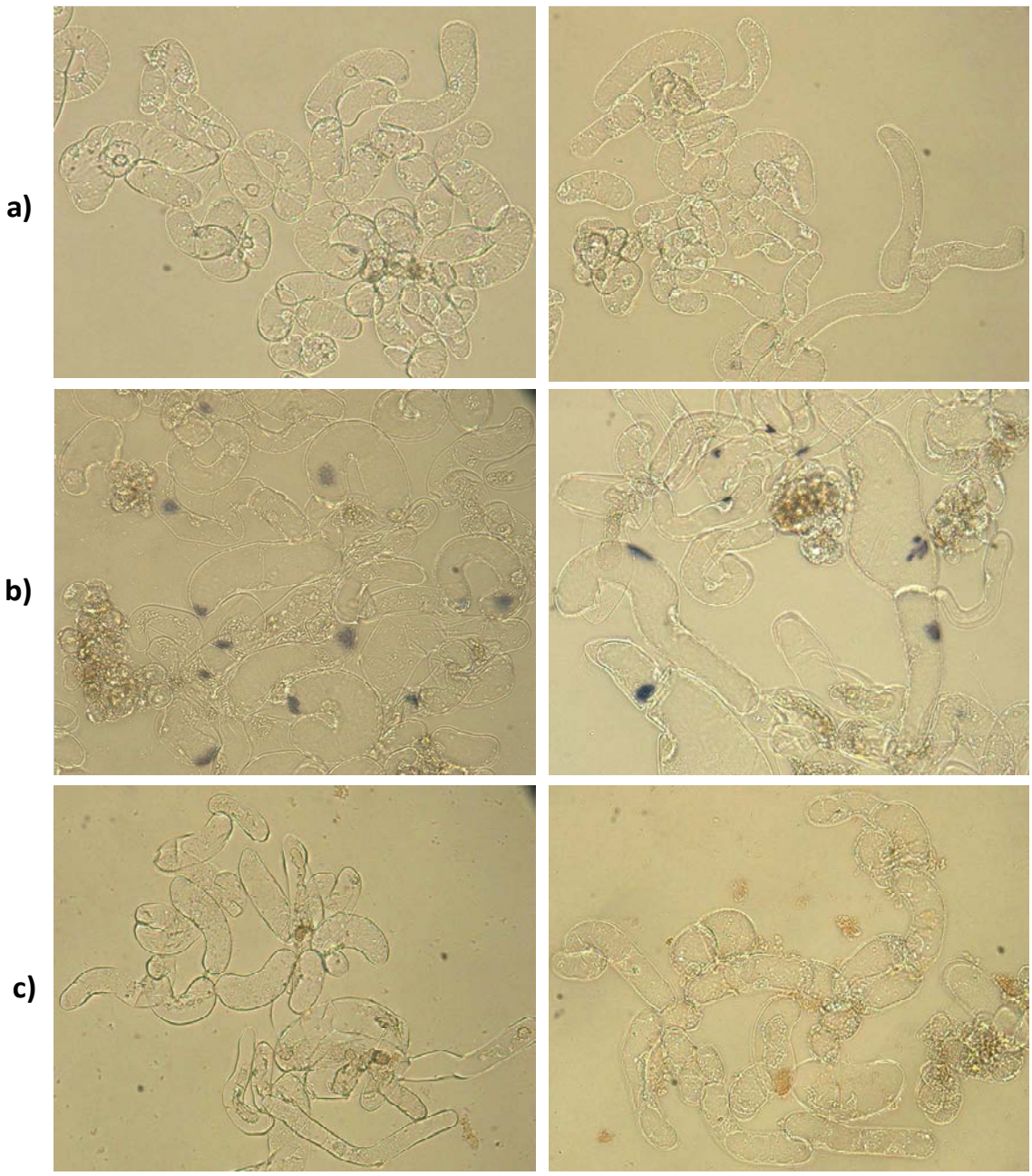

Figure 4-18 Images from cell suspension cultures with the following treatments: a) suspension culture treated with NBT; b) suspension culture heat-treated plus NBT; c) suspension culture treated with QD's for 72 h plus NBT. All experiments were visualized 4 hours after the addition of NBT, in bright field with the same settings and exposure time. Magnification 200x.

4.3.2.3.3. 2, 7'- Dichlorodihydrofluorescein diacetate

H_2DCFDA diffuses passively through the cellular membrane and then is enzymatically hydrolysed by intracellular esterases to 2',7'-dichlorodihydrofluorescein (DCFH). This nonfluorescent product is converted by reactive species into DCF (2',7'-dichlorofluorescein), which can easily be visualized by strong fluorescence at around 525nm when excited at around 488 nm (Figure 4-19) (Gerber and Dubery, 2003; Myhrea *et al*, 2003).

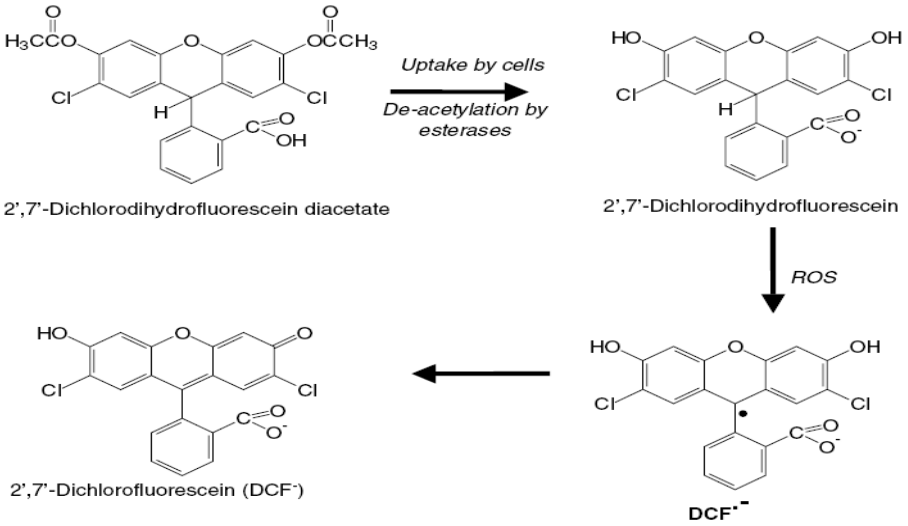

Figure 4-19 Conversion of 2',7'-dichlorodihydrofluorescein diacetate (H_2DCFDA). H_2DCFDA it's hydrolyzed by cellular esterases to dichlorofluorescin (2',7'-dichlorodihydrofluorescein), whose oxidation by several reactive species yields florescent DCF (2',7'-dichlorofluorescein) via an intermediate radial, $DCF^{\bullet -}$ (adapted from Halliwell and Whiteman, 2004).

H_2DCFDA enters cells and accumulates mostly in the cytosol. To avoid any cytotoxicity, cells should be loaded with H_2DCFDA at low concentrations. With a variety of cell types, it was found that loading at 1–10 mM for 45 min–1 h is adequate (Halliwell and Whiteman, 2004).

H_2DCFDA has been widely used to measure the formation of reactive species in cells. It is not clear however, which oxidative species are responsible for oxidation of DCFH to DCF in cells. To determine the cellular oxidative stress of cell cultures with QD's the same controls were used as in the previous experiments. H_2DCFDA treated cells (Figure 4-20 a)) showed a basal-level signal that accumulated in all cytoplasmic areas uniformly, as also reported by Ashtamker *et al*. (2007). In the heat treated cell

suspension culture the DCF signal was significantly elevated in specific locations (Figure 4-20 b)), as well as in the QD's treated cell suspension cultures (Figure 4-20 c)).

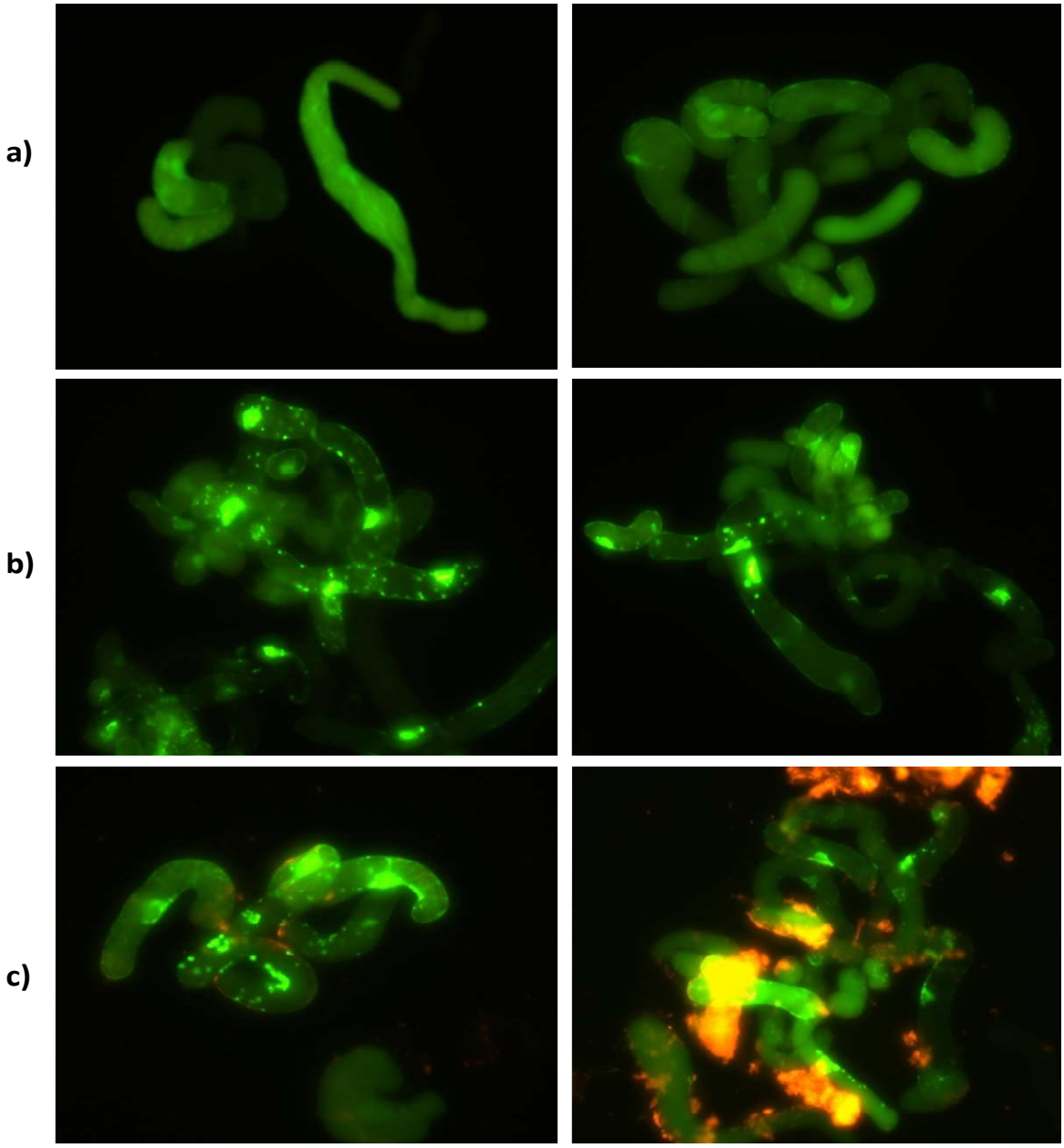

Figure 4-20 Determination of cellular oxidative stress. a) suspension culture treated with H_2DCFDA. b) suspension culture heat-treated to induce an oxidative stress plus H_2DCFDA. c) suspension culture treated with [40 nM] QD's plus H_2DCFDA. All experiments were visualized 1.30 hours after the addition of H_2DCFDA in B-2A filter with the same settings and exposure time. Magnification 200x.

The DCF accumulation can be identified specifically in the nuclear region as well as in organelles and cytosol, all possible sources for intracellular ROS production (Ashtamker *et al*, 2007). These specific locations are also seen in cells heat-treated as well as in cells treated with QD's as Figure 4-21 shows. In this picture is also possible to observe that Qd's are attached at the cell wall surface (indicated by red arrows), suggesting a internalization just 1.30 hour after the exposure.

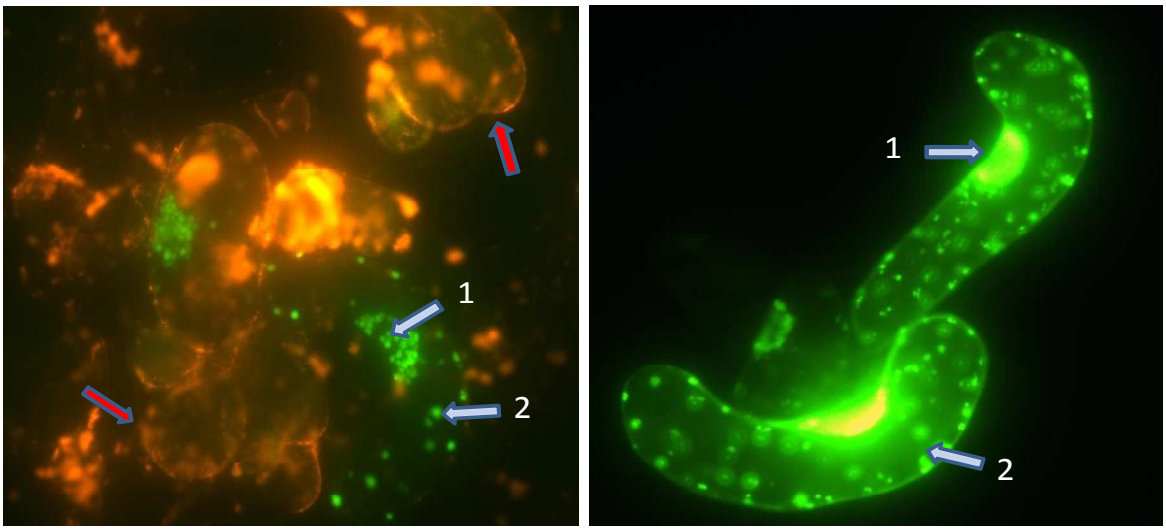

Figure 4-21 Cellular oxidative stress in cell suspension culture with QD's (left image) and in suspension culture heat- treated (right image) 1.3 hour after staining with H_2DCFDA. Arrow 1 indicates the nuclear compartment and arrow 2 organelles such as mitochondria. Images acquired with blue filter (B-2A) and the same settings and exposure time. Magnification 400X.

From this assay it can be assessed that QD's presence/interaction with cell suspension cultures induce a cellular oxidative stress, in a matter of 1.30 hour of exposure with a concentration of [40 nM] QD68_MPA.

To evaluate the response of suspension cultures when exposed to QD's for a larger period of time, QD's were added at day 3 of culture and the same experiment was performed after 48 and 72 hours, day 5 and 6 respectively. The results obtained after 48 hours of exposure are presented in Figure 4-22. The DCF signal is much stronger for both, heat and QD's treated cell suspension cultures. In the case of heat treated cells (Figure 4-22b)), this increase in the response may be due to the small differences in temperature during the treatment, i.e., the temperature of bath water was 2 or 3 ºC above the 45 ºC, which may triggered the response.

Relatively to the QD's cell suspension cultures the DCF signal became more intense, than the one obtained in the previous experiment, in fact the intensity was so strong that the specific localization could not be observed, instead the signal was uniformly distributed in the whole cell (Figure 4-22c)).

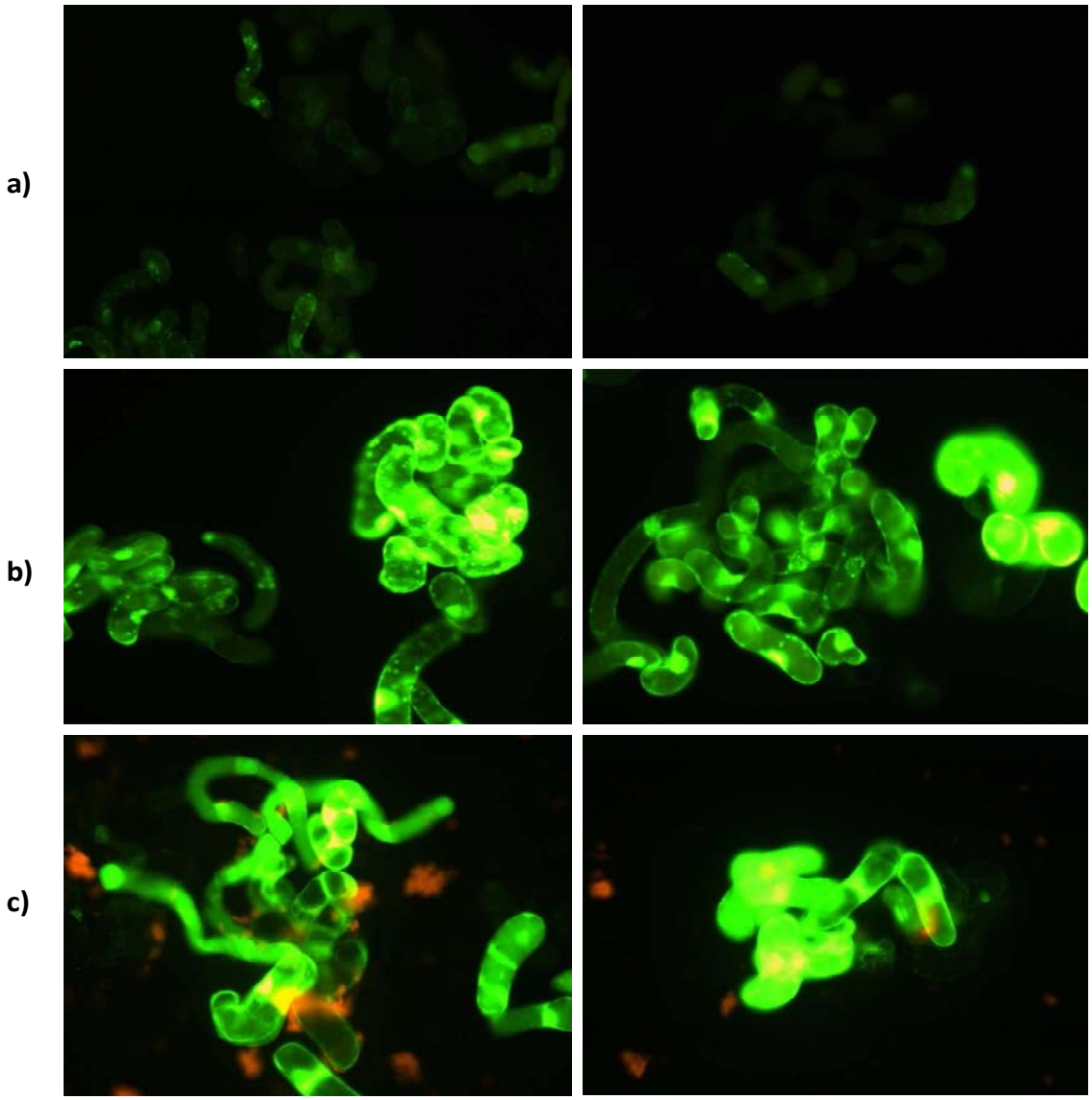

Figure 4-22 Determination of cellular oxidative stress. a) cell suspension culture treated with H_2DCFDA. b) cell suspension culture heat-treated to induce an oxidative stress plus H_2DCFDA. c) cell suspension culture treated with QD's for 48 hours plus H_2DCFDA. All experiments were visualized 1.30 hours after the addition of H_2DCFDA in B-2A filter with the same settings and exposure time. Magnification 200x.

The results obtained in day 6 (after 72 hours) show that the exposure of cultures to QD's induce an oxidative stress in cells (Figure 4-23 c)). Similarly, the intensity is distributed along the cells that no

specific location can be distinguished. Also the heat-treated cells may have suffered an increase in the response due to a slight augmentation in the bath temperature (Figure 4-23 b)).

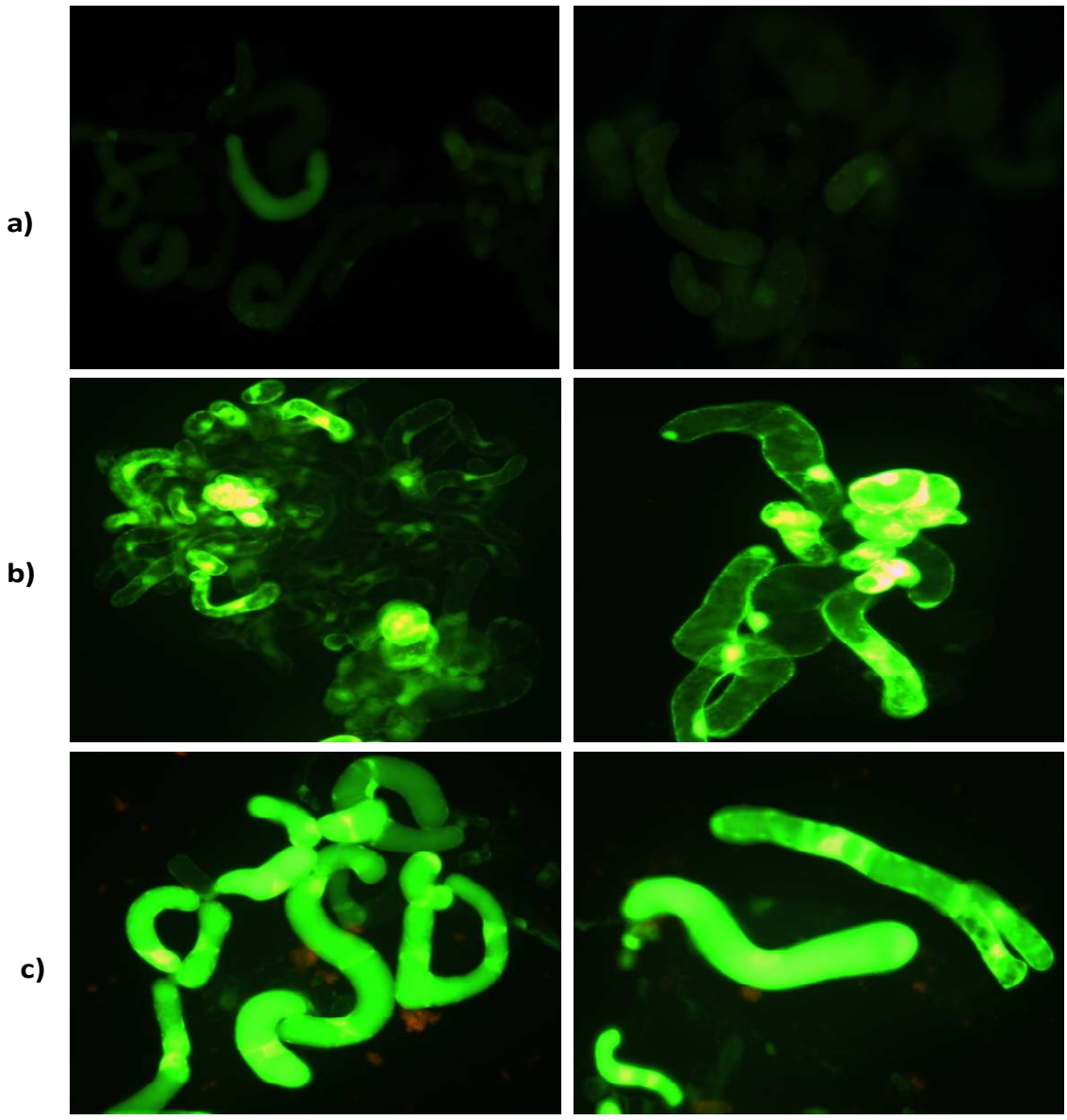

Figure 4-23 Determination of cellular oxidative stress. a) cell suspension culture treated with H_2DCFDA. b) cell suspension culture heat-treated to induce an oxidative stress plus H_2DCFDA. c) cell suspension culture treated with QD's for 72 hours plus H_2DCFDA. All experiments were visualized 1.30 hours after the addition of H_2DCFDA in B-2A filter with the same settings and exposure time. Magnification 200x.

To further clarify the results in terms of the mean fluorescence intensity of DCF signal, a normalized graphic representation was obtained. Using a commercial image processing program (Image J), after

subtracting the background, the channels of the pictures were split (red, blue and green) and using the green channel histogram values, the number of pixels were multiplied with their respective intensity value (0 to 255), and then dividing it for the total number of pixels of the image.

Figure 4-24 shows the graphic representation of the mean fluorescence intensity of pictures from cells +H_2DCFDA, cells 45 ºC 20 min + H_2DCFDA and cells+ QD's+ H_2DCFDA. The exposure times refers to the time that cells have been in contact with QD's. It can be seen that both, heat-treated and QD's treated cell suspension cultures, present higher values of pixel intensity compared to the control ones.

Heat treated cell suspension cultures present a variation in fluorescence intensity in the three experiments, as already referred above, due to differences in bath temperature.

Comparing the results of the three intensity values obtained over time, it can be easily concluded that while the control (cell+ H_2DCFDA) maintained a value bellow 8 a.u. of intensity, cell suspension cultures treated with QD's increased the fluorescence intensity with larger times of exposure of cells to QD's, which means that ROS production is intensified.

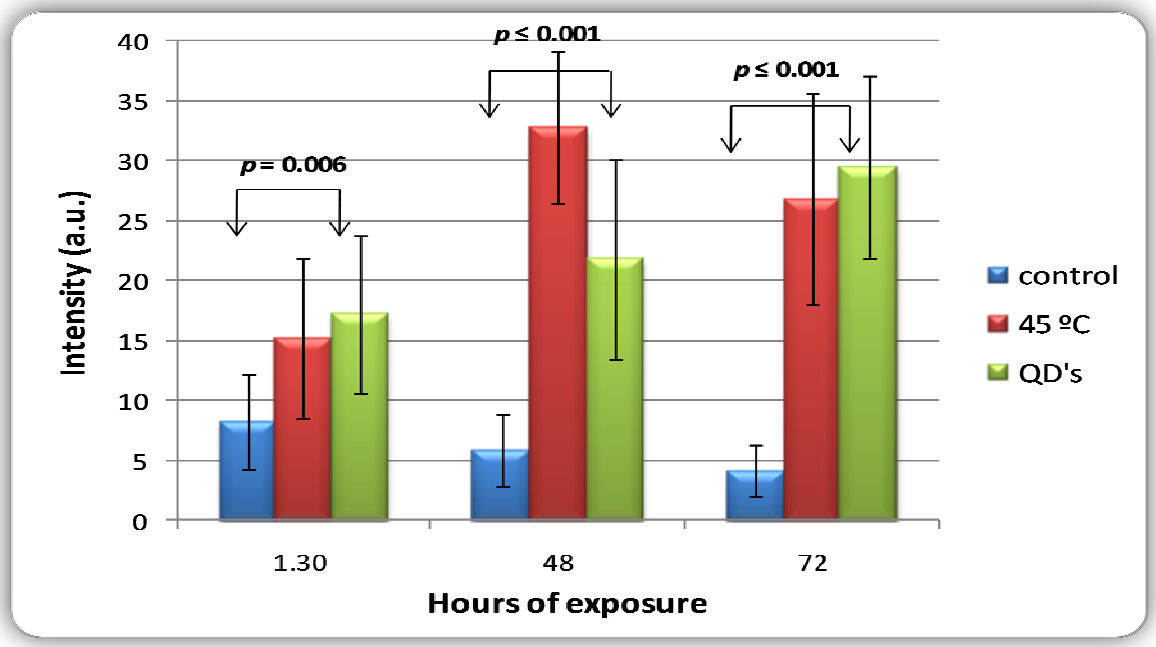

Figure 4-24 Graphic representation of the mean fluorescence intensity of pictures from cells +H_2DCFDA, cells 45 ºC 20 min + H_2DCFDA and cells+ QD's+ H_2DCFDA in the three exposure times performed: 1.30 (n=5), 48 (n=5) and 72 (n=6) hours. Fluorescence was quantified in terms of average pixel intensity, using the commercial program ImageJ. Statistically significant difference determined with 1-way ANOVA.

Although it can be concluded that there is an oxidative stress imposed by the exposure of cells to QD's, it is not possible to conclude with this assay, which reactive species is being produced. Several reports described the use of H_2DCFDA to detect H_2O_2, therefore, another control assay was carried out in order to clarify the type of response by cells when oxidative stress is caused by over production of H_2O_2.

Cell suspension cultures were heat-treated to induce an oxidative stress and 1 mM of H_2O_2 was added to another cell culture following H_2DCFDA.

Figure 4-25 b) shows, as already observed in the previous experiments, that the DCF signal is located in specific compartments. The addition of 1 mM of H_2O_2 was enough to trigger the intensity of the signal (Figure 4-25 c)) and in certain cells it was possible to observe the same type compartmentalization of the DCF (Figure 4-25 c) right image). It is possible that this assay is more sensitive than the DAB assay and, in fact, the ROS being produced is H_2O_2.

However, conclusions drawn of the specificity of H_2DCFDA are contradictory. Hoek *et al* (1997) performed a study were they concluded that DCFH oxidation to DCF can occur as a result of interaction with either H_2O_2 or $\bullet OH^-$. Myhrea *et al* (2003) in a review about the specificity of H_2DCFDA suggest that it is sensitive towards oxidation by $ONOO^-$ (peroxynitrite, often included as ROS), H_2O_2 (in combination with cellular peroxidases), peroxidases alone, and $\bullet OH^-$, while it is not suitable for measurement of NO, HOCl, or $O_2^- \bullet$ in biological systems. Importantly, $\bullet OH^-$, and $ONOO^-$ may be the only oxidants that oxidize DCFH within seconds or a few minutes. Small quantities of these oxidants will rapidly increase DCF formation, whereas other oxidants may need higher concentrations and more time. Also, the simultaneous presence of cellular peroxidases is necessary for DCFH oxidation by H_2O_2; H_2O_2 alone does not oxidize DCFH into DCF.

Wang and Joseph (1999) claim that due to the indiscriminate nature of DCFH, which can be oxidized by various ROS and not just H_2O_2, the increase of intracellular DCF fluorescence does not necessarily reflect the levels of ROS directly, but rather an overall oxidative stress index in cells. Also the review by Halliwell and Whiteman (2004) refers that because of the multiple pathways that can lead to DCF fluorescence and the inherent uncertainty relating to endogenous versus artifactual oxidant generation, this assay may best be applied as a qualitative marker of cellular oxidant stress rather than a precise indicator of rates of H_2O_2 formation (Gomes *et al*, 2005).

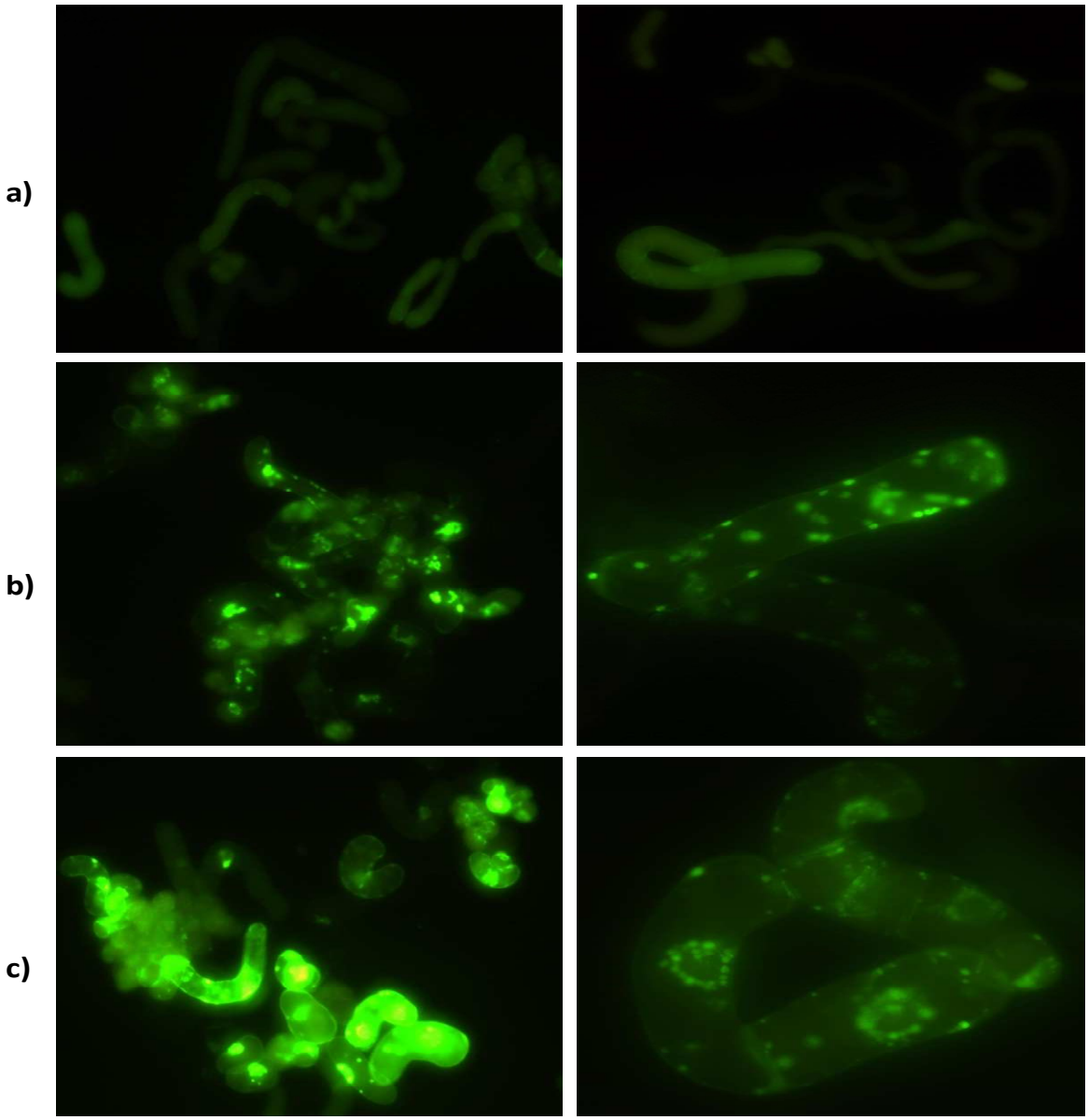

Figure 4-25 Oxidative stress in cells. a) suspension culture + H_2DCFDA. b) suspension culture 45 ºC 20 min + H_2DCFDA. c) suspension culture + 1mM H_2O_2+H2DCFDA. All experiments were visualized 1.30 hour after the addition of H_2DCFDA in B-2A filter with the same settings and exposure time. Magnification 200X, except the right images of b) and c) which are in 400X.

4.3.3. Quantum dot up-take by cells

The observations made to evaluate the cellular stress responses towards QD´s suggested that they could be up-taked by cells besides being attached to the cell wall surface. According to Kirchner *et al*, (2005), this is an important factor to take in consideration as cells can also be impaired if nanoparticles precipitate on the cell surface. Furthermore, cytotoxic effects are different in the case that particles are taken by the cells compared to the case that particles are just present in the medium surrounding the cells.

The tendency for nanoparticles to aggregate, to precipitate and nonspecifically adsorb on cells in culture may be just as important as heavy metal toxicity contribution (Smith *et al*, 2008). To verify this possible internalization both cell suspension cultures were incubated with QD's for a period of time of 72 hours and observed in a confocal microscope.

4.3.3.1. *QD50_MPA*

Confocal images of cell suspension cultures of both, *M.truncatula* and *M.sativa*, present internalization of QD's in cytoplasmic areas and in the nucleus.

Figure 4-26 shows that the nucleus and the cytoplasm present the green fluorescence from QD's. The vacuole occupying the majority of the cell volume is the exception. The same can be seen in cells of the *M. sativa* line(Figure 4-27).

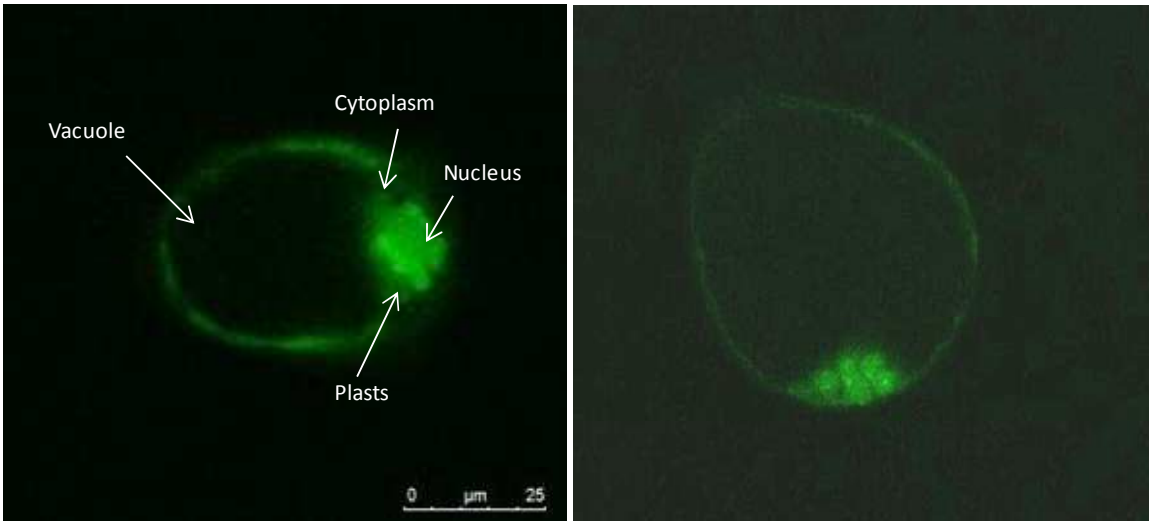

Figure 4-26 Confocal images of *M. truncatula* cell suspension culture with [160 nM] for 72 hours.

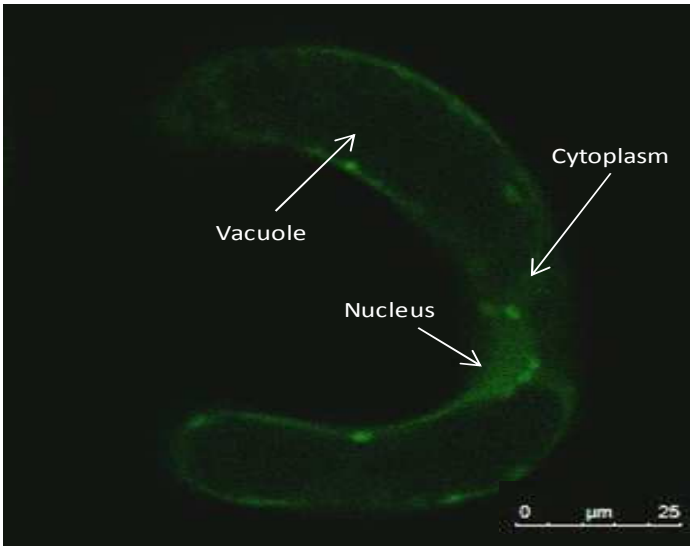

Figure 4-27 Confocal images of *M. sativa* cell suspension culture with [160 nM] for 72 hours.

4.3.3.2. *QD68_MPA*

Figure 4-28 shows a series of confocal images from cell suspension cultures exposed to QD68_MPA for 72 hours. It can be seen that QD fluorescence is located in the cytosol and never in the vacuoles, as already observed with QD50_MPA. The arrow in picture 2 indicates the presence of QD's around cell membrane and/or cell wall.

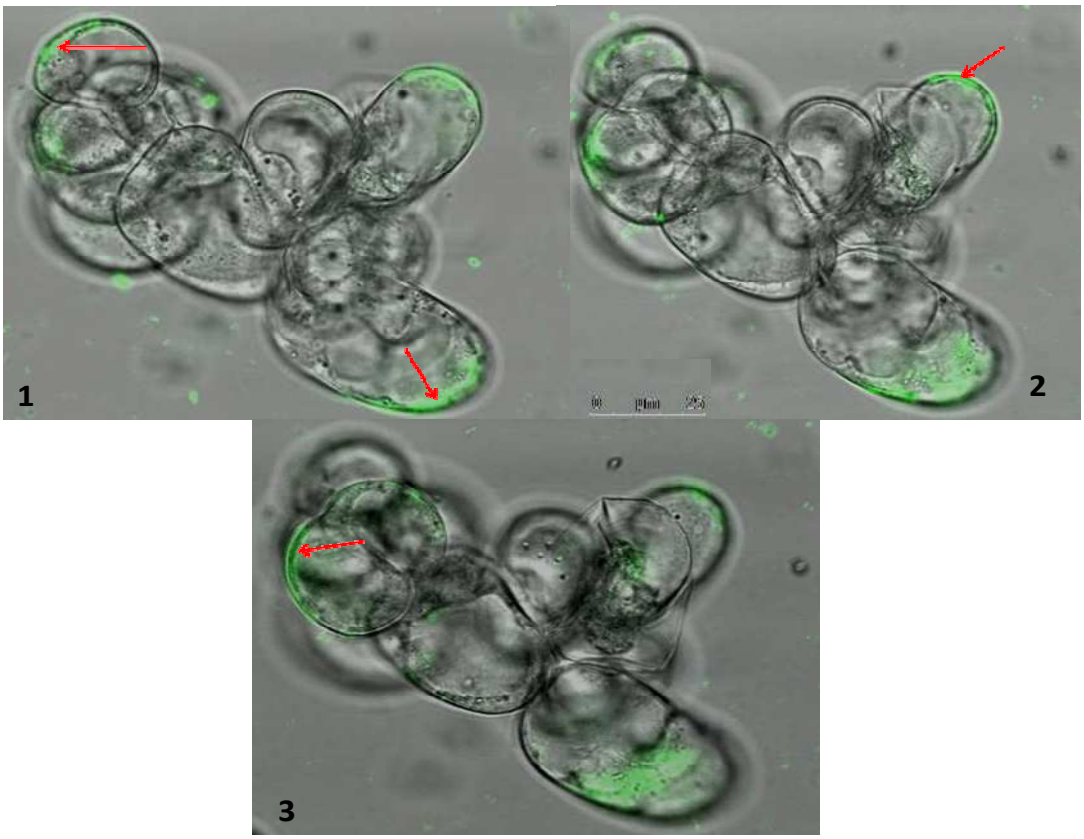

Figure 4-28 Sequence of confocal images of a suspension culture with QD's for 72 hours. Arrows indicate the internalization.

Figure 4-29 and Figure 4-30 shows confocal images of cells exposed to QD68_MPA for 72 hours and stained with Direct Yellow 96. Both image 2 of Figure 4-29 and Figure 4-30 only shows the fluorescence from the QD's, and it can be seen that QD's entered to the cell wall and apparently extended indiscriminately thru the hyaloplasm. The zoom in picture 2 of Figure 4-30 exposes in detail that (CdS/ZnS) QD's do not enter the vacuole, which already has been reported in plant cells (Etxeberria *et al*, 2006).

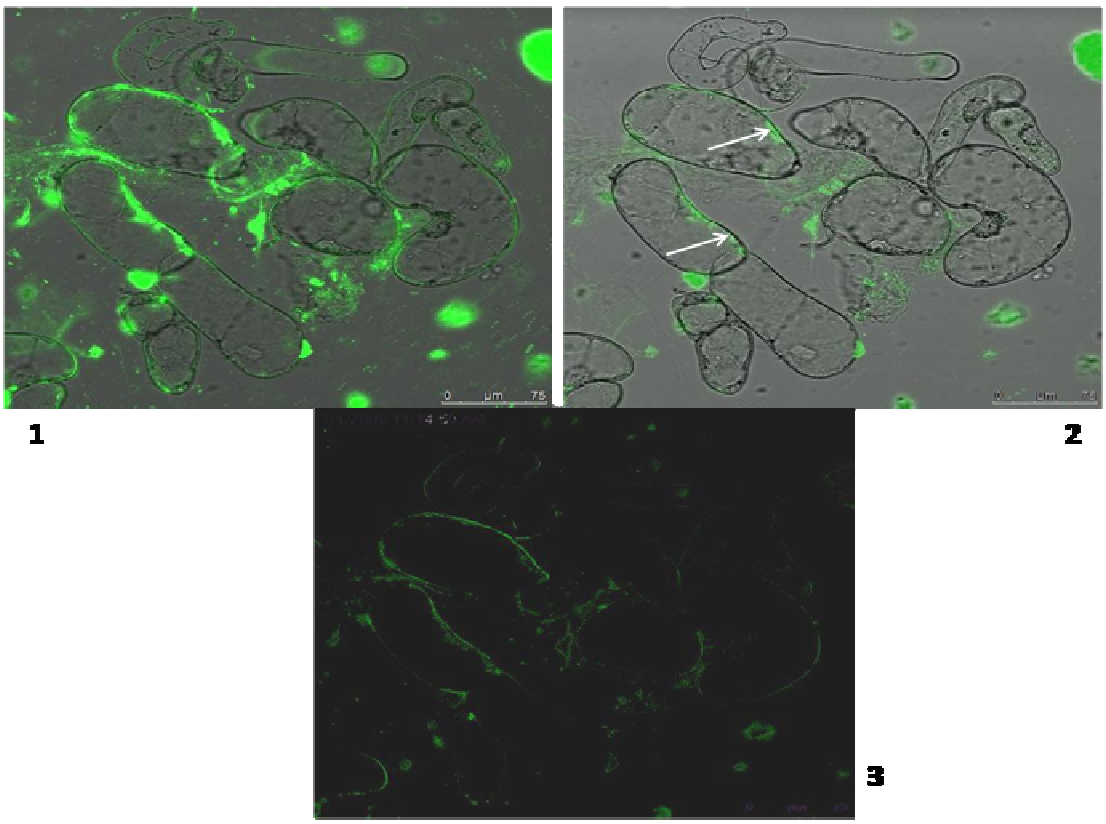

Figure 4-29 Confocal images of cell suspension cultures with QD's for 72 hours and stained with Direct Yellow 96. 1) cells showing fluorescence from the cell wall marker and QD's. 2) cells with fluorescence only from QD's. 3) Difference between image 1 and 2 (fluorescence from the cell wall marker). Arrows indicate some points were the internalization is observed.

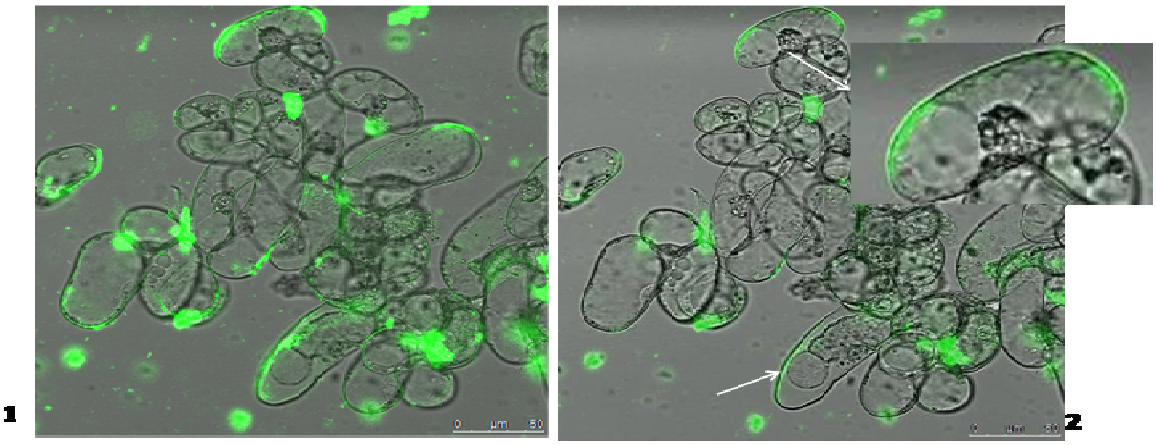

Figure 4-30 Confocal images of cell suspension cultures with QD's for 72 hours and stained with Direct Yellow 96. 1) cells showing fluorescence from the cell wall marker and QD's. 2) cells with fluorescence only from QD's and detail of a cell showing internalization.

Figure 4-31 shows cell suspension cultures exposed to QD's for 4 hours and stained with Direct Yellow 96, and visualized in the inverted microscope with blue and green filters. With the blue filter the green fluorescence observed is from the cell wall marker and the orange fluorescence is from QD's, with the green filter only fluorescence from the QD's is visible. As already seen in oxidative stress experiments, QD's adsorb on cell wall surface and in this case, just in 4 hours of exposure, cells present themselves covered with a fine layer of QD's. Some of these QD's are adsorbed to cell surface but some particles seem to have entered the cell, as previously demonstrated.

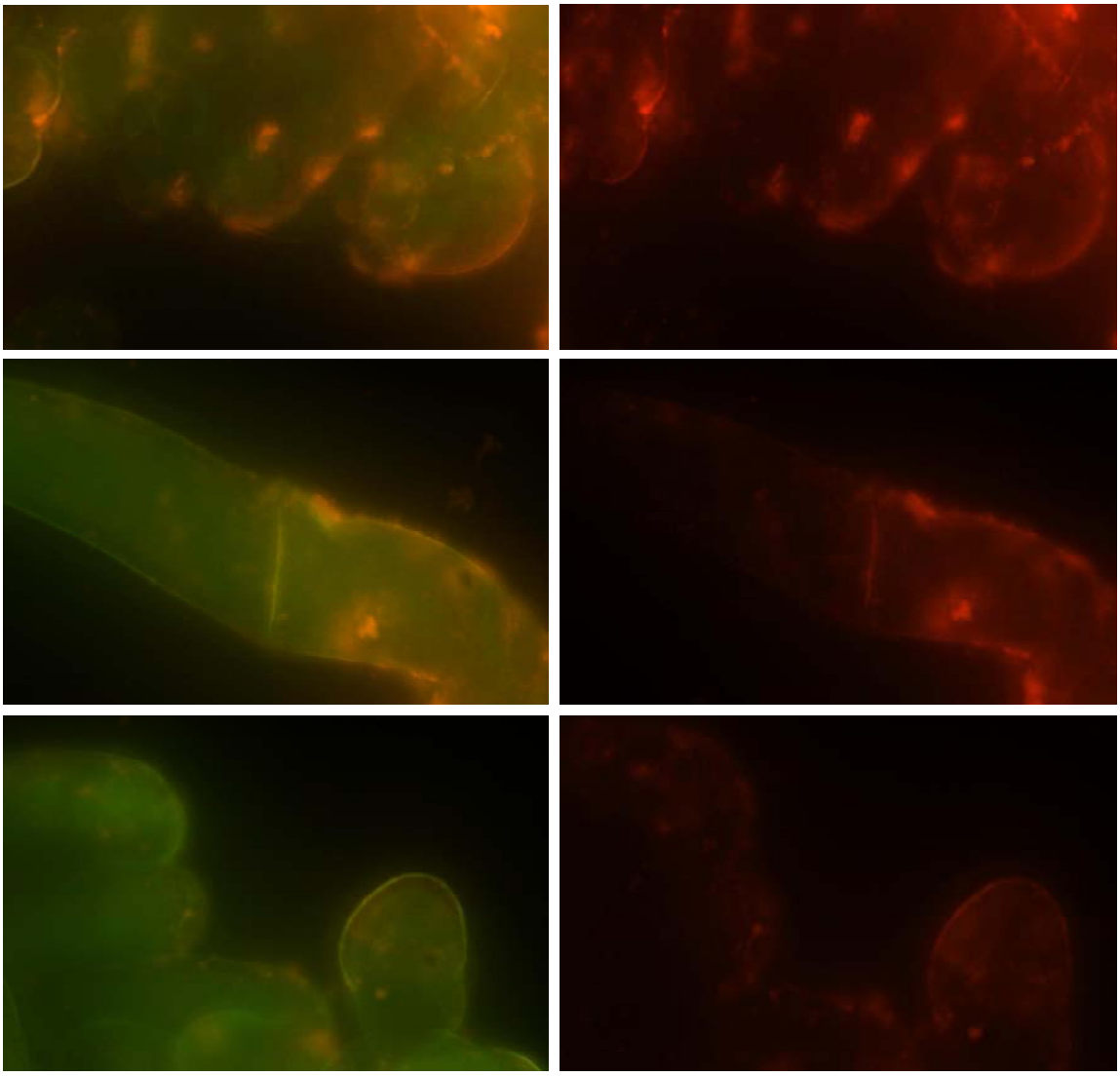

B-2A filter **Green filter**

Figure 4-31 Cell suspension culture exposed to QD's for 4 hours and stained with Direct Yellow 96. Images acquired in inverted microscope with magnification 600X, in blue and green filter.

It was seen that QD´s adhere at the cell wall surface after just 4 hours of exposure, thus to verify if that was observed in a shorter time, cell suspension cultures were exposed to QD's for 30 minutes. In Figure 4-32 are pictures of cell suspension culture in bright field and UV filter acquired in the inverted microscope, and as we can see, only 30 minutes after being in contact with cells, QD's attached to them and, despite it has not been confirmed in the confocal microscope, it seems that probably some of them had already been up-take by cells.

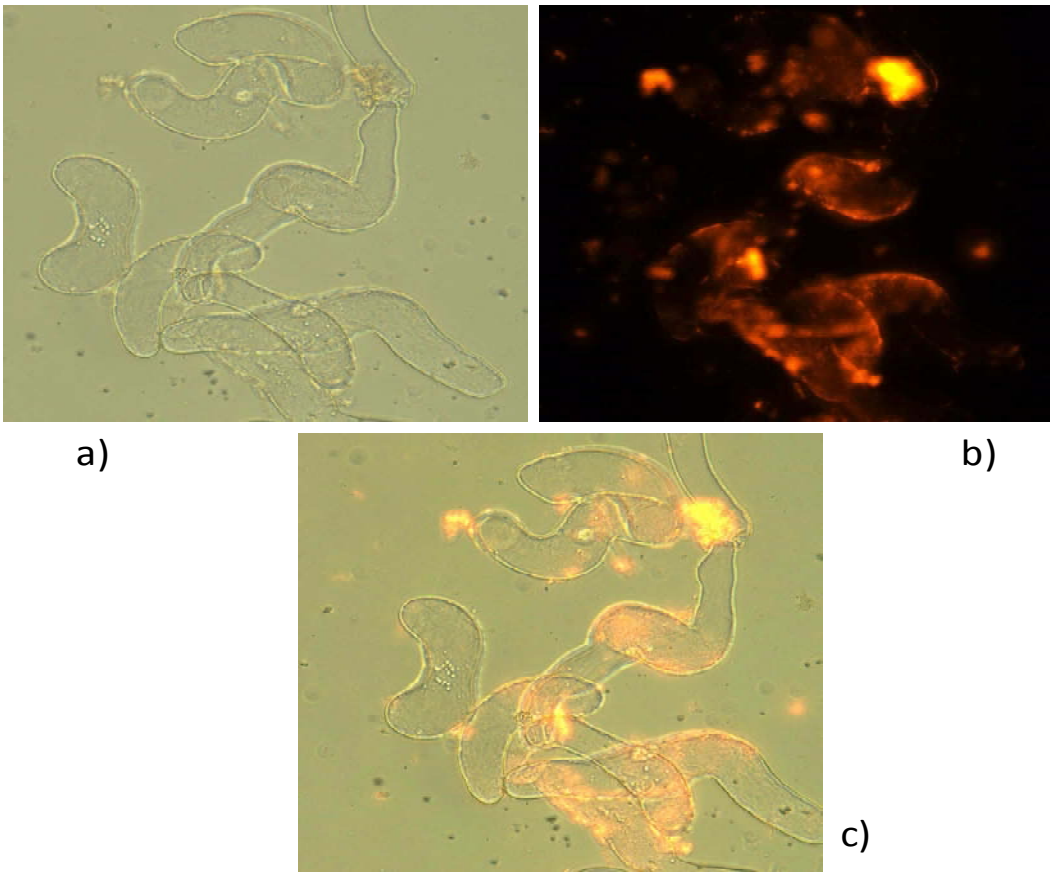

Figure 4-32 Cell suspension cultures with 30 min of exposure to QD's. a) bright field. b) green filter. c) overlay of a) and b). Magnification 200X.

For both QD50_MPA and QD68_MPA QD's no internalization was observed in vacuoles. The difference encountered between the samples is that the first ones were observed in the nucleus, and in the second case QD's were only found in the hyaloplasm and cytoplasmic organelles, probably mitochondria and plasts. The capping material is the same in both QD's but in the case of QD50_MPA the technique used to determine the size was not very precise and it could be that some particles have smaller sizes than 30 nm, and in that way entered in cells up to the nucleus. Moreover, the QD50_MPA

sample at the time of the experiments had already been in stock solution for three months at the time of the experiments and may occurred an oxidation of the outer layers reducing the size of the QD's.

The efficacy of QD's uptake as well as the exact uptake mechanisms (receptor specific versus adsorptive/unspecific) certainly depend on a variety of parameters including particle size, surface chemistry, and also importantly, the cell type under consideration (Parak *et al*, 2004).

In conclusion, several reports indicate that MPA coated particles are taken by cells (Alberola and Rädler, 2009; Lóvric *et al*, 2005 a); Chang *et al*, 2006; Etxeberria *et al*, 2006). The physicochemical characteristics of QDs influence their sub- cellular location, namely the size and the capping material, and also the stability in medium. It seems that smaller particles can easily enter the nucleus while the bigger ones distribute mainly in the cytoplasm. Red emitting QD's tend to aggregate in medium and even if small aggregates are formed, two or three particles, that is enough to increase the size and they would be to big to cross the nuclear membrane (Lóvric *et al*, 2005 a)).

Alberola and co-workers found that coating material can suppress uptake almost completely, and this behaviour could be explained in terms of the electrostatic attraction between the NPs and the surface. Cellular uptake of NPs can be considered as being controlled by a competition between surface attraction and its interaction with cells. They also proved that surface-mediated uptake involves cellular activity.

5. Conclusions

The objectives pursued within this work were accomplished. First a fine suspension culture of *Medicago sativa* was established, and then four main assays of toxicity testing were performed: cell viability and cell growth, ROS production and cell-particle up-take.

M. trucantula due to its highly embryogenic characteristics was used to evaluate differences in cell differentiation at somatic embryogenesis, when cell suspension cultures were exposed to QD's, and no toxicity was found with QD50_MPA QD's at [160 μM].

Assays performed in *M. sativa* cell suspension cultures showed that the presence of QD68_MPA induces variations in cell cycle, namely, the exponential phase is shorter and with a quick increase in biomass, despite the total biomass production is lower than the control. The viability assay confirmed that only the large aggregates of cells were viable.

The evaluation of ROS production allowed to conclude that there is no superoxide anion production, during the assay period (3-78 hours), but from the generalized oxidative stress assay it was assessed that ROS were in fact produced, although the lack of specificity of the probe does not allow to conclude which reactive species is involved.

It seems that for this concentration [40nM], QD's are slightly toxic to cells of *M.sativa* when in contact from 1.30 to 4 hours. But if the exposure of cells to QD's is higher than 24 hours, then some important alterations become visible, namely in cell cycle, viability and in cell morphology, as well as the intensification of ROS production.

Mercaptopropionic acid (MPA) is commonly used for solubilization and several reports stated that MPA coated QD's have shown to be mildly cytotoxic (Lee *et al*, 2009; Jamieson *et al*, 2007). The coatings of QDs are important because they influence stability of QDs, which is reported to be affected by the chain length of the ligand, with longer chain being more stable (Lovric *et al*, 2005) and MPA is known to be one of the smallest ligands among deprotonated thiols, therefore not providing the better stability.

In terms of QD up-take it can be concluded that the cells internalize particles, apparently in a non specific way, and as soon as 30 minutes of exposure QD's attach to the surface of cell wall. Although the extent of internalization, accordingly to literature, depends on particle size and coating, both types of QD's were found in hyaloplasm, and cytoplasmic organelles but never in vacuoles. The internalization is an important factor to be considered in toxicity, since the internalization could damage cells.

This passive internalization of QD's by cells present a main advantage: it does not require the further step for the delivery of QD's in drug delivery or labeling of cells, QD's are simply incubated with the cells

at the appropriate concentration and exposure time and they are subsequently internalized. Nevertheless, the internalization of bioconjugated QD's can be more difficult with molecules that increase the final size of QD's.

Further work is needed to completely access QD toxicity in cell suspension cultures of *M. sativa* and *M. truncatula*, namely to find out which ROS is/are being produced, to elucidate if QD's stay inside cells and for how long, as well as to determine specifically in which organelles do they enter. A full study *in planta* will be also usefull since there are differences in toxicity *in vivo* and *in vitro* systems.

Although CdSe/ZnS MPA coated QD's are not completely innocuous, a safe range for their biological application probably exists. By understanding the parameters that regulate the toxicity of nanoparticles to cells, progress can be made to improve synthesis, processing, and surface-coating strategies, thus minimizing the potential for nanoparticle toxicity in biological applications.

6. References

Alberola A, Rädler J. 2009. The defined presentation of nanoparticles to cells and their surface controlled uptake. *Biomaterials*, 30: 3766–3770.

Alivisatos P, Gu WW, Larabell C. 2005. Quantum dots as cellular probes. *Annual Review of Biomedical Engineering*, 7:55–76.

Alivisatos P. 2004. The use of nanocrystals in biological detection. *Nature biotechnology*, 22: 47-52.

Apel K, Hirt H. 2004. Reactive oxygen species: Metabolism, Oxidative Stress, and Signal Transduction. *Annual Review of Plant Biology*, 55:373–99.

Araújo S, Duque A, Santos D, Fevereiro M. 2004. An efficient transformation method to regenerate a high number of transgenic plants using a new embryogenic line of Medicago truncatula cv. Jemalong. *Plant Cell, Tissue and Organ Culture*, 78: 123–131.

Armstrong J, Whiteman M. 2007. Measurement of Reactive Oxygen Species in Cells and Mitochondria. *Methods in cell biology*, 80: 355-377.

Ashtamker C, Kiss V, Sagi M, Davydov O, Fluhr R. 2007. Diverse Subcellular Locations of Cryptogein-Induced Reactive Oxygen Species Production in Tobacco Bright Yellow-2 Cells. *Plant Physiology*, 143: 1817–1826.

Azzazy H, Mansour M, Kazmierczak S. 2007. From diagnostics to therapy: Prospects of quantum dots. *Clinical Biochemistry*, 40: 917-927.

Batandier C, Fontaine E, Kériel C, Leverve X. 2002. Determination of mitochondrial reactive oxygen species:methodological aspects. *Journal of Cellular and Molecular Medicine*, 6:175-187.

Biju V, Itoh T, Anas A, Sujith A, Ishikawa M. 2008. Semiconductor quantum dots and metal nanoparticles: syntheses, optical properties, and biological applications. *Analytical and Bioanalytical Chemistry*, 391: 2469–2495.

Bolwell G, Wojtaszek P. 1997. Mechanisms for the generation of reactive oxygen species in plant defence ± a broad perspective. *Physiological and Molecular Plant Pathology*, 51: 347-366.

Borovitskaya E, Shur M. 2002. Quantum Dots. Selected Topics in Electronics and Systems - Vol. 25. *World Scientific*.

Brisson L, Tenhaken R, Lamb C. 1994. Function of Oxidative Cross-Linking of Cell Wall Structural Proteins in Plant Disease Resistance. *The Plant Cell*, 6: 1703-1712.

Buzea C, Pacheco I, Robbie K. 2007. Nanomaterials and nanoparticles: Sources and toxicity. *Biointerphases*, 2: MR17-MR71.

Chang E, Thekkek N, Yu W, Colvin V, Drezek R. 2006. Evaluation of Quantum Dot Cytotoxicity Based on Intracellular Uptake. *Small,* 2:1412 – 1417.

References

Chen C, Cheng C, Lai C, Wu P, Wu K, Chou P, Chou Y, Chiu H. 2006. Potassium ion recognition by 15-crown-5 functionalized CdSe/ZnS quantum dots in H2O. *Chemical Communications*, 3:263-265.

Coder D. 1997. Current Protocols in Cytometry. *John Wiley & Sons, Inc.*,

Cordero S, Carson P, Estabrook R, Strouse G, Buratto. 2000. Photo-Activated Luminescence of CdSe Quantum Dot Monolayers. *Journal of Physical Chemistry B.*, 104: 12137 – 12142.

Cook D. 1999. *Medicago truncatula* — a model in the making!. *Current Opinion in Plant Biology*, 2:301–304.

Dabbousi B, Rodriguez-Viejo J, Mikulec F, Heine J, Mattoussi H,Ober R, *et al*. 1997. (CdSe)ZnS Core-Shell Quantum Dots: Synthesis and Characterization of a Size Series of Highly Luminescent Nanocrystallites. *Journal of Physical Chemistry*, 101: 9463-9475.

Delehanty J, Mattoussi H, Medintz I. 2009. Delivering quantum dots into cells: strategies, progress and remaining issues. *Analitical and Bioanalitical Chemistry*, 393:1091–1105.

Derfus A, Chan W, Bhatia S. 2004. Probing the Cytotoxicity of Semiconductor Quantum Dots. *Nano Letters*, 4:11-18.

Etxeberria E, Gonzalez P, Baroja-Fernandez E, Romero J. 2006. Fluid Phase Endocytic Uptake of Artificial Nano-Spheres and Fluorescent Quantum Dots by Sycamore Cultured Cells. *Plant Signaling & Behavior*, 1: 196-200.

Fischer H, Chan W. 2007. Nanotoxicity: the growing need for *in vivo* study. *Current Opinion in Biotechnology*,18: 565–571.

Fryer J, Oxborough K, Mullineaux P, Baker N .2002. Imaging of photo-oxidative stress responses in leaves. *Journal of Experimental Botany*, 53: 1249–1254.

Galian R, de la Guardia M. 2009. The use of quantum dots in organic chemistry. *Trends in Analytical Chemistry*, 28: 279-291.

Gechev T, Breusegem F, Stone J, Denev I, Laloi C. 2006. Reactive oxygen species as signals that modulate plant stress responses and programmed cell death. *BioEssays*, 28:1091–1101.

George E, Hall M, Klerk G. 2008. Plant propagation by tissue culture. 3rd Edition. Volume 1: The background. *Springer*. pp: 14,15.

Gerber I, Dubery I. 2003. Fluorescence microplate assay for the detection of oxidative burst products in tobacco cell suspensions using 2',7'-dichlorofluorescein. *Methods in Cell Science*, 25: 115–122.

Gilbert E, Galgani E, Cadiou Y. 1992. Rapid assessment of metabolic activity in marine microalgae: application in ecotoxicological tests and evaluation of water quality. *Marine Biology*, 112: 199-205.

Gomes A, Fernandes E, Lima J. 2005. Fluorescence probes used for detection of reactive oxygen species. *Journal of Biochemical and Biophysical Methods*, 65: 45–80.

González-Melendi P, Fernández-Pacheco R, Coronado M. J, Corredor E, *et al*. 2007. Nanoparticles as Smart Treatment-delivery Systems in Plants: Assessment of Different Techniques of Microscopy for their Visualization in Plant Tissues. *Annals of Botany*, 101: 187-195.

Green V, Stott D, Diack M. 2006. Assay for fluorescein diacetate hydrolytic activity: Optimization for soil samples. *Soil Biology & Biochemistry*,38: 693–701.

Green M. and Howman E. 2005. Semiconductor quantum dots and free radical induced DNA nicking. *Chemical Communications* (Camb.) 121–123.

Halliwell B. 2007. Biochemistry of oxidative stress. *Biochemical Society Transactions*, 35: 1147-1150

Halliwell B, Whiteman M. 2004. Measuring reactive species and oxidative damage in vivo and in cell culture: how should you do it and what do the results mean?. *British Journal of Pharmacology*, 142: 231–255.

Hardman R. 2006. A toxicologic review of quantum dots: toxicity depends on physicochemical and environmental factors. *Environmental Health Perspectives*, 114:165-172.

Hild W, Breunig M, Goepferich A. 2008. Quantum dots – Nano-sized probes for the exploration of cellular and intracellular targeting. *European Journal of Pharmaceutics and Biopharmaceutics*, 68: 153–168.

Hoek T, Li C, Shao Z, Schumacker P, Becker L. 1997. Significant Levels of Oxidants are Generated by Isolated Cardiomyocytes During Ischemia Prior to Reperfusion. *Journal of Molecular and Cellular Cardiology*, 29: 2571–2583.

Hoet P, Boczkowsky J. 2008. What's new in Nanotoxicology? Brief review of the 2007 literature. *Nanotoxicology*, 2: 171-182.

Hong F S, Zhou J, Liu C, Yang F, Wu C, Zheng L, Yang P. 2005. Effect of nano-TiO2 on photochemical reaction of chloroplasts of spinach**.** *Biological Trace Element Research*, 105: 269-279.

Hoshino A, Fujioka K, Oku T, Suga M, Sasaki Y, *et al.* 2004. Physicochemical properties and cellular toxicity of nanocrystal quantum dots depend on their surface modification. *Nano Letters*, 4: 2163-2169.

Hoch H, Galvani C, Szarowski D, Turner J. 2005. Two new fluorescent dyes applicable for visualization of fungal cell walls. *Mycologia*, 97: 580-588.

Iantcheva A, Vlahova M, Atanassov A, Duque A, Araújo S, Santos D, Fevereiro P. 2006. Cell suspension cultures. Medicago truncatula Handbook.

Ibaraki Y, Kenji K. 2001. Application of image analysis to plant cell suspension cultures. *Computers and electronics in Agriculture*, 30:193-203.

References

Ipe B, Lehnig M, Niemeyer C. 2005. On the Generation of Free Radical Species from Quantum Dots. *Small*, 7: 706 –709.

Jaiswal J, Simon S. 2004. Potentials and pitfalls of fluorescent quantum dots for biological imaging. *Trends in cell biology*, 14: 497- 504.

Jamieson T, Bakhshi R, Petrova D, Pocock R, Imani M, Seifalian A. 2007. Biological applications of quantum dots. *Biomaterials*, 28: 4717–4732.

Jones C, Grainger D. 2009. *In vitro* assessments of nanomaterial toxicity. *Advanced Drug Delivery Reviews*, 61: 438–456.

Joseph T, Morrison M. 2006. Nanotechnology in agriculture and food. www.nanoforum.org

Kirchner C, Liedl T, Kudera S, Pellegrino T, Javier A, Gaub H, Stölzle S, Fertig N, Parak W. 2005. Cytotoxicity of Colloidal CdSe and CdSe/ZnS Nanoparticles. *Nano Letters*, 5: 331-338.

King-Heiden T, Wiecinski P, Mangham A, Metz K, Nesbit D, Pedersen J, Hamers R, Heideman W, Peterson R. 2009. Quantum Dot Nanotoxicity Assessment Using the Zebrafish Embryo*. Enviromental Science &* Technology, 43: 1605–1611.

Klaine S, Alvarez P, Batley G, Fernandes T, Handy R, Lyon D, *et al*. 2008. Root Uptake and Phytotoxicity of ZnO Nanoparticles. *Environmental Science & Technology*, 42: 5580-5585.

Koeneman B, Zhang Y, Hristovski K, Westerhoff P, Chen Y, Crittenden J, Capco D. 2009. Experimental approach for an in vitro toxicity assay with non-aggregated quantum dots. *Toxicology in Vitro*, 23: 955–962.

Lacefield G, Henning J, Rasnake M, Collins M. 1997. Alfalfa: The Queen of Forage Crops. *University of Kentucky, College of Agriculture*. AGR-76.

Lee J. Ji K. , Kim J.Park C. Lim K. Yoon T. Choi K. 2009. Acute Toxicity of Two CdSe/ZnSe Quantum Dots with Different Surface Coating in *Daphnia magna* Under Various Light Conditions. *Environmental toxicology*. Published online in Wiley InterScience.

Li K, Chen J, Bai S, Wen X, Song S, Yu Q, Li J, Wang Y. 2009. Intracellular oxidative stress and cadmium ions release induce cytotoxicity of unmodified cadmium sulfide quantum dots. *Toxicology In Vitro*, 23: 1007-1013.

Lin DH, Xing BS. 2007. Phytotoxicity of nanoparticles: inhibition of seed germination and root elongation. *Environmental Pollution*, 150: 243–250.

Lin DH, Xing BS. 2008. Root Uptake and Phytotoxicity of ZnO Nanoparticles. *Environmental Science & Technology*, 42, 5580–5585.

Loyola-Vargas V. Vázquez-Flota F. 2006. Methods in molecular biology: Plant Cell culture protocols 2nd Edition. *Humana Press*: 52.

References

Lovrić J, Bazzi H, Cuie Y, Fortin G, Winnik F, Maysinger D. 2005 a). Differences in subcellular distribution and toxicity of green and red emitting CdTe quantum dots. *Journal of Molecular Medicine*, 83: 377–385.

Lovrić J, Cho S, Winnik F, Maysinger D. 2005 b). Unmodified Cadmium Telluride Quantum Dots Induce Reactive Oxygen Species Formation Leading to Multiple Organelle Damage and Cell Death. *Chemistry & Biology*, 12: 1227–1234.

Mahendra S, Zhu H, Colvin V, Alvarez P. 2008. Quantum Dot Weathering Results in Microbial Toxicity. *Environ. Sci. Technol.*, 42: 9424–9430.

May G, and Dixon, R. 2004. *Medicago truncatula*. *Current Biology*, 14:R180-R181.

Maysinger D, Behrendt M, Przybytkowski E. 2006. Death by Nanoparticles. *NanoPharmaceuticals Online Journal,*1.

Maysinger D, Lovrić J, Eisenberg A, Savić R. 2007. Fate of micelles and quantum dots in cells. *European Journal of Pharmaceutics and Biopharmaceutics,* 65: 270–281.

Male K, Lachance B, Hrapovic S, Sunahara G, Luong J. 2008. Assessment of Cytotoxicity of Quantum Dots and Gold Nanoparticles Using Cell-Based Impedance Spectroscopy. *Analytical Chemistry*, 80: 5487–5493.

Medintz I, Uyeda H, Goldman E, Mattoussi H. 2005. Quantum dot bioconjugates for imaging, labelling and sensing *Nature Materials*, 4: 435 – 446.

Michalet X, Pinaud F, Bentolila L, Tsay J, Doose S, Li J, Sundaresan G, *et al* 2005. Quantum dots for live cells, *in vivo* imaging, and diagnostics. *Science,* 307: 538-544.

Myhrea O, Andersena J, Aarnesc H, Fonnuma F. 2003. Evaluation of the probes 2',7'-dichlorofluorescin diacetate, luminol, and lucigenin as indicators of reactive species formation. *Biochemical Pharmacology*,65:1575–1582.

Mittler R. 2002. Oxidative stress, antioxidants and stress tolerance. *Trends in Plant Science*, 7: 405-410.

Mujib A. Samaj A. 2005. Plant Cell Monograph (2): Somatic Embryogenesis. *Springer-Verlag*, pp: 299.

Müller F, Houben A, Barker P, Xiao Y, Käs J, Michael Melzer M. 2006. Quantum dots – a versatile tool in plant science? *Journal of Nanobiotechnology*, 4.

Murashige T, Skoog F. 1962. A revised medium for rapid growth and bioassays with tobacco tissue cultures. *Physiol. Plant*. 15: 473–497.

Nel A, Xia T, Mädler L, Li1 N. 2006. Toxic Potential of Materials at the Nanolevel. *Science*, 311: 622-627.

Nelson P, Toussoun T, Cook R (editors). 1985. Fusarium: Diseases, Biology, and Taxonomy. Pennsylvania University Press, University Park, PA.

References

Ortega-Villasante C, Rellán-Álvarez R, Del Campo F, Carpena-Ruiz R, Hernández L. 2005. Cellular damage induced by cadmium and mercury in *Medicago sativa. Journal of Experimental Botany*, 56: 2239–2251.

Pan J, Wang Y, Feng S. 2008. Formulation, Characterization, and *In Vitro* Evaluation of Quantum Dots Loaded in Poly(Lactide)-Vitamin E TPGS Nanoparticles for Cellular and Molecular Imaging. *Biotechnology and Bioengineering*, 101: 622-633.

Parak W, PellegrinoT, Plank C. 2005. Labelling of cells with quantum dots. *Nanotechnology*, 16:R9-R25.

Pfannschmidt T. 2009. Plant Signal Transduction - Methods and Protocols. *Humana Press*, 479:109.

Pollard J. Walker J. 1990. Methods In Molecular Biology. vol 6, Plant Cell and Tissue Culture. *Humana Press*, pp:14,15, 17.

Queval G, Hager J, Gakière B, Noctor G. 2008. Why are literature data for H_2O_2 contents so variable? A discussion of potential difficulties in the quantitative assay of leaf extracts. *Journal of Experimental Botany*, 59: 135–146.

Ravindran S, Kim S, Martin R, Lord E, Ozkan C. 2005. Quantum dots as bio-labels for the localization of a small plant adhesion protein. *Nanotechnology*, 16: 1–4.

Regel R, Ferris J, Ganf G, Brookes J. 2002. Algal esterase activity as a biomeasure of environmental degradation in a freshwater creek. *Aquatic Toxicology*, 59: 209–223.

Rigler R, Vogel H. 2008. Single Molecules and Nanotechnology. *Springer Series in Biophysics 12*, pp: 57,58, 61.

Rio L, Corpas F, Sandalio L, Palma J, Barroso J. 2003. Plant Peroxisomes, Reactive Oxygen Metabolism and Nitric Oxide. *IUBMB Life*, 55:71-81.

Romero-Puertas M, Rodriguez-Serrano M, Corpas F, Gomez M, del Rio L, Sandalio L. 2004. Cadmium-induced subcellular accumulation of $O^{\cdot-}_2$ and H_2O_2 in pea leaves. *Plant, Cell and* Environment, 27: 1122–1134.

Shao H, Chu L, Lu Z, Kang C. 2008. Primary antioxidant free radical scavenging and redox signaling pathways in higher plant cells. *International Journal of Biological Sciences*, 4: 8-14.

Shiohara A, Hoshino A, Hanaki K, Suzuki K, Yamamoto K. 2004. On the cyto-toxicity caused by Quantum Dots. *Microbiol. Immunol.*, 48: 669- 675.

Smirnoff N. 2005. Antioxidants and Reactive Oxygen Species in Plants. *Blackwell Publishing*.

Smith A, Duan H, Mohs A, Nie S.2008. Bioconjugated quantum dots for in vivo molecular and cellular imaging. *Advanced Drug Delivery Reviews*, 60: 1226–1240.

Spence J. 2001. Plant Cell Biology 2nd edition. *Oxford University Press*, pp: 203.

Tarpey M, Fridovich I. 2001. Methods of Detection of Vascular Reactive Species Nitric Oxide, Superoxide, Hydrogen Peroxide, and Peroxynitrite. *Circulation Research*, 89:224-236.

Tenhaken R, Levine A, Brisson L, Dixon R, Lamb C. 1995. Function of the oxidative burst in hypersensitive disease resistance. *Proceedings of the National Academy of Sciences* (*PNAS)*, 92: 4158-4163.

Thordal-Christensen H, Zhang Z, Wei Y, Collinge D. 1997. Subcellular localization of H_2O_2 in plants. H_2O_2 accumulation in papillae and hypersensitive response during the barley-powdery mildew interaction. *The plant journal*, 11: 1187-1194.

Vashist S, Tewari R, Bajpai R, Bharadwaj L, Raiteri R. 2006. Review of Quantum Dot Technologies for Cancer Detection and Treatment. *Azojono*, 2.

Vincelli P, Lacefield G, Henning J. 1997. Managing Diseases of Alfalfa. *University of Kentucky, College of Agriculture*. ID-104.

Wang J, Zhang X, Chen Y, Sommerfeld M, Hu Q. 2008. Toxicity assessment of manufactured nanomaterials using the unicellular green alga *Chlamydomonas reinhardtii*. *Chemosphere*, 73:1121-1128.

Wang H, Joseph J. 1999. Quantifying cellular oxidative stress by dichlorofluorescein assay using microplate reader**.** *Free Radical Biology & Medicine*, 27: 612–616.

Wang Q, Xu Y, Zhao X, Chang Y, Liu Y, Jiang L, Sharma J, Seo D, Yan H. 2007. A Facile One-Step in situ Functionalization of Quantum Dots with Preserved Photoluminescence for Bioconjugation. *Journal of American Chemical Society*, 129: 6380-6381.

Yang F, Hong F S, You W J, Liu C, Gao F Q, Wu C, Yang P. 2006. Influences of nano-anatase TiO2 on the nitrogen metabolism of growing spinach. *Biological Trace Element Research*, 110: 179–190.

Yang L, Watts D. 2005. Particle surface characteristics may play an important role in phytotoxicity of alumina nanoparticles. *Toxicology Letters*, 158: 122–132.

Yang S, Gao M, Xu C, Gao J, Deshpande S, Lin S, Roe B, Zhu H. 2008. Alfalfa benefits from *Medicago truncatula*: The RCT1 gene from *M. truncatula* confers broad-spectrum resistance to anthracnose in alfalfa. *Proceedings of the National Academy of Sciences* (*PNAS)*, 105: 12164-12169

Young N, and Udvardi M. 2009. Translating *Medicago truncatula* genomics to crop legumes. *Current Opinion in Plant Biology*, 12:193-201.

Yu G, Liang J, He Z, Sun M. 2006. Quantum Dot-Mediated Detection of g-Aminobutyric Acid Binding Sites on the Surface of Living Pollen Protoplasts in Tobacco. *Chemistry &* Biology, 13: 723–731.

Zhang F, Zhang H, Wang G, Xub, Shen Z. 2009. Cadmium-induced accumulation of hydrogen peroxide in the leaf apoplast of *Phaseolus aureus* and *Vicia sativa* and the roles of different antioxidant enzymes. *Journal of Hazardous Materials*. (in press)

Zheng L, Hong F, Lu S, Liu C. 2005. Effect of nano-TiO2 on strength of naturally aged seeds and growth of spinach. *Biological Trace Element Research*, 104: 83-91.

Zhu H, Han J, Xiaoa J, Jin Y. 2008. Uptake, translocation, and accumulation of manufactured iron oxide nanoparticles by pumpkin plants. *Journal of Environmental Monitoring*, 10: 713-717.

Zottini M. Barizza E. Bastianelli F. Carimi F. Schiavo F. 2006. Growth and senescence of *Medicago truncatula* cultured cells are associated with characteristic mitochondrial morphology. *New Phytologist*, 172: 239–247.

On-line references:

http://www.fao.org/ag/AGP/AGPC/doc/GBASE/data/Pf000346.HTM

http://www.grainlegumes.com/aep/crops_species/model_legumes/barrel_medic_or_i_medicago_i

http://www.nbtc.cornell.edu/facilities/downloads/Zeta potencial - An introduction in 30 minutes.pdf